# Hydrocarbons in size-fractionated plankton of the Mediterranean Sea (MERITE-HIPPOCAMPE campaign)

Catherine Guigue, Javier Angel Tesán-Onrubia, Léa Guyomarc'H, Daniela Bănaru, François Carlotti, Marc Pagano, Sandrine Chifflet, Deny Malengros, Lassaad Chouba, Jacek Tronczynski, et al.

# Hydrocarbons in size-fractionated plankton of the Mediterranean Sea (MERITE-HIPPOCAMPE campaign)

Catherine Guigue[a]*, Javier Angel Tesán-Onrubia[a], Léa Guyomarc'h[a], Daniela Bănaru[a], François Carlotti[a], Marc Pagano[a], Sandrine Chifflet[a], Deny Malengros[a], Lassaad Chouba[b], Jacek Tronczynski[c], Marc Tedetti[a]

[a] Aix Marseille Univ., Université de Toulon, CNRS, IRD, MIO, Marseille, France

[b] Institut National des Sciences et Technologies de la Mer (INSTM), 28, rue 2 mars 1934, Salammbô 2025, Tunisia

[c] Ifremer, CCEM Contamination Chimique des Ecosystèmes Marins, F-44311 Nantes, France

*Corresponding author; E-mail: catherine.guigue@mio.osupytheas.fr

For submission to Marine Pollution Bulletin – Special issue "*Plankton and Contaminants in the Mediterranean Sea: Biological pump and interactions from regional to global approaches*"

Revised version, 1 August 2023

## Abstract

Aliphatic and polycyclic aromatic hydrocarbons (AHs and PAHs, respectively) were analyzed in the dissolved fraction (< 0.7 µm) of surface water and in various particulate/planktonic size fractions (0.7-60, 60-200, 200-500 and 500-1000 µm) collected at the deep chlorophyll maximum, along a North-South transect in the Mediterranean Sea in spring 2019 (MERITE-HIPPOCAMPE campaign). Suspended particulate matter, biomass, total chlorophyll *a*, particulate organic carbon, C and N isotopic ratios, and lipid biomarkers were also determined to help characterizing the size-fractionated plankton and highlight the potential link with the content in AHs and PAHs in these size fractions. $\Sigma_{28}$AH concentrations ranged 18-489 ng $L^{-1}$ for water, 3.9-72 µg $g^{-1}$ dry weight (dw) for the size fraction 0.7-60 µm, and 3.4-55 µg $g^{-1}$ dw for the fractions 60-200, 200-500 and 500-1000 µm. AH molecular profiles revealed that they were mainly of biogenic origin. $\Sigma_{14}$PAH concentrations were 0.9-16 ng $L^{-1}$ for water, and $\Sigma_{27}$PAH concentrations were 53-220 ng $g^{-1}$ dw for the fraction 0.7-60 µm and 35-255 ng $g^{-1}$ dw for the three higher fractions, phenanthrene being the most abundant compound in planktonic compartment. Two processes were evidenced concerning the PAH patterns, the bioreduction, i.e., the decrease in concentrations from the small size fractions (0.7-60 and 60-200 µm) to the higher ones (200-500 µm and 500-1000 µm), and the biodilution, i.e., the decrease in concentrations in plankton at higher suspended matter or biomass, especially for the 0.7-60 and 60-200-µm size fractions. We estimated the biological pump fluxes of $\Sigma_{27}$PAHs below 100-m depth in the Western Mediterranean Sea at 15 ± 10 ng $m^{-2}$ $day^{-1}$, which is comparable to those previously reported in the South Pacific and Indian Ocean.



**Key words:** Hydrocarbons, PAHs, plankton, size fractions, bioaccumulation, Mediterranean Sea

## 1. Introduction

Hydrocarbons, in particular polycyclic aromatic hydrocarbons (PAHs), are among the most widespread organic pollutants in the marine environment (Hylland, 2006; Duran and Cravo-Laureau, 2016; Ben Othman et al., 2023). PAHs are considered to be almost exclusively of anthropogenic origin, possibly coming from crude oil or its derivatives (petrogenic PAHs) or from the combustion of fossil fuels and biomass (pyrogenic PAHs) (Wang et al., 1999; Yunker et al., 2002; Stogiannidis and Laane, 2015). Aliphatic hydrocarbons (AHs), which also represent an important class of hydrocarbons in the marine environment, can be of anthropogenic (petroleum) and biogenic (terrestrial or marine) origin (Volkman et al., 1992; Bouloubassi and Saliot, 1993; Love et al., 2021). PAHs are listed as priority pollutants by various international organizations (US-EPA, 2012; EU-Directive, 2013) due to their deleterious effects on living organisms (Honda and Suzuki, 2020). Thus, for many years, PAHs, and to a lesser extent AHs, have been studied in different matrices of the marine ecosystems, such as surface sediments (Mille et al., 2007; Zaghden et al., 2017; Mandić et al., 2018), the dissolved phase of water (Guigue et al., 2014; Adhikari et al., 2015; Tong et al., 2019), suspended particles (Bouloubassi et al., 2006; Mzoughi and Chouba, 2011; Rocha and Rocha, 2021), surface microlayer (Stortini et al., 2009; Guitart et al., 2010; Guigue et al., 2011), and biota, especially macro-organisms (Baumard et al., 1998; Tolosa et al., 2005; Pirsaheb et al., 2018).

The incorporation and transfer of PAHs within marine food webs is known to induce major disturbances of ecosystems, and to have negative impacts on the exploitation of marine resources and habitats, socio-economic activities, and human health (Islam and Tanaka, 2004; Balcıoğlu, 2016; Romero et al., 2018). However, even though the concentrations of PAHs in upper food webs has been quite well documented so far, they have been much less

investigated in plankton, i.e., the first trophic levels of pelagic marine ecosystems. Yet, plankton, which includes phytoplankton (mostly unicellular photosynthetic autotrophic organisms), zooplankton (heterotrophic eukaryotes), and bacterioplankton (heterotrophic prokaryotes), is recognized as a key gateway and playing a major role in the transfer of contaminants from water to upper food webs (Berrojalbiz et al., 2011; Tiano et al., 2014; Tao et al., 2018; Chouvelon et al., 2019; Tedetti et al., 2023).

Given their high surface area/volume ratio and the subsequent large areas of exchanges, phytoplankton cells display high bioconcentration capacities (bioconcentration referring to the accumulation of contaminants in a given organism relative to surrounding water by direct absorption from the latter) (Martin and Knauer, 1973; Fan and Reinfelder, 2003; Heimbürger et al., 2010; Chouvelon et al., 2019). Assuming partition equilibrium processes between the cells and the surrounding water (Frouin et al., 2013), the bioconcentration of organic contaminants in phytoplankton may be directly related to their octanol-water partitioning coefficient (Log $K_{OW}$), i.e., their degree of hydrophobicity (the higher the Log $K_{OW}$, the greater the contaminant bioconcentration) (Swackhamer and Skoglund, 1993; Nizzetto et al., 2012; Li et al., 2020), and to the size of the phytoplankton species (the smaller the cell size, the greater the contaminant bioconcentration) (Fan and Reinfelder, 2003). On the other side, bioaccumulation processes in zooplankton (bioaccumulation referring to the accumulation of contaminants in a given organism relative to surrounding water by both direct absorption from water and the consumption of contaminated prey) are made complex by 1) the influence of trophic interactions and transfers between phytoplankton and zooplankton and within zooplanktonic compartment, and 2) the removal processes of contaminants implemented by these organisms, including metabolization, passive release and excretion (Berrojalbiz et al., 2009; Tiano et al., 2014; Alekseenko et al., 2018; Tao et al., 2018; Li et al., 2020). Ultimately, all these processes, which can act concurrently in the same or opposite directions, makes it

difficult to understand and predict the pattern of contaminant concentrations within the planktonic food web (Nizzetto et al., 2012; Strady et al., 2015; Alekseenko et al., 2018; Castro-Jiménez et al., 2021; Li et al., 2021).

Recently, some works have focused on the bioaccumulation of PAHs in the planktonic compartment (here and below the term bioaccumulation includes bioconcentration for simplicity, the latter being a direct form of bioaccumulation) (Berrojalbiz et al., 2009, 2011; Tao et al., 2017a, b, 2018; González-Gaya et al., 2019). These have provided a very interesting insight of the PAH bioaccumulation pattern within the plankton and showed a link between this bioaccumulation and the surrounding biogeochemical parameters. Nevertheless, in these studies, plankton has been generally taken as an entire compartment, without any separation into size fractions. Furthermore, the lipid content was not taken into account, even though, due to their hydrophobic nature, lipids represent a major matrix contributing to the bioaccumulation of the organic contaminants within marine and planktonic organisms (Mackay and Fraser, 2000; Arnot and Gobas, 2006; Lee et al., 2006; Tesán-Onrubia et al., 2023).

In this context, the objectives of the present work were to **1)** determine the contents in hydrocarbons (AHs and PAHs) in the dissolved fraction (< 0.7 µm) of surface water and in various particulate/planktonic size fractions (0.7-60, 60-200, 200-500 and 500-1000 µm) from sampling in the deep chlorophyll maximum (DCM), along a North-South transect in the Mediterranean Sea during the MERITE-HIPPOCAMPE campaign. For these different size fractions, suspended particulate matter (SPM), biomass, total chlorophyll *a* (TChl*a*), particulate organic carbon (POC), C and N isotopic ratios ($\delta^{13}C$, $\delta^{15}N$) and lipid biomarkers were also determined. **2)** Evaluate the spatial variations (between stations) and the distributions within the planktonic size fractions of these parameters (mainly AHs, PAHs, POC, lipids), as well as the correlations between them. **3)** Investigate the concentration

patterns and bioaccumulation of PAHs within plankton according to the size fraction, trophic level, organic carbon partitioning and biomass. **4)** Assess, *via* the estimation of hydrocarbon vertical fluxes, the role of Mediterranean plankton as biological pump for hydrocarbons.

## 2. Material and Methods

### 2.1. Study area

The MERITE-HIPPOCAMPE cruise took place in spring 2019 (from April 13 to May 14), aboard the R/V *Antea*, along a North-South transect in the Mediterranean Sea, from the French coast (La Seyne-sur-Mer, Northwestern Mediterranean) to the Gulf of Gabès in Tunisia (Southeastern Mediterranean). Leg 1 (13-28 April) covered the southward transect, between La Seyne-sur-Mer and Tunis, with sampling of stations St2, St4, St3, St10 and St11. Leg 2 (30 April-14 May) included the end of the southward transect (from Tunis to the Gulf of Gabès), and the return trip back northward to La Seyne-sur-Mer, with sampling of stations St15, St17, St19, St9 and St1 (Fig. 1a, b) (Tedetti and Tronczynski, 2019; Tedetti et al., 2023). The ten stations were chosen according to criteria of physical, biological and biogeochemical conditions and level of anthropogenic pressures, as well as the location of bloom areas and ecoregions of the Mediterranean (see full description in Tedetti et al., 2023).

### 2.2. Sampling, filtration, sieving and conditioning

At each station, a conductivity-temperature-depth probe (CTD; Seabird SBE 911*plus*) equipped with a TChl*a* fluorescence sensor (Chelsea ctg) was deployed over the depth range 0-250 m (or 0-bottom when depth was < 250 m) to identify the DCM. For each station, the sampling depth ranges in the DCM are reported Table S1.

*2.2.1. In situ filtration*. Two McLane *in situ* pumps (WTS6-142LV, 4-8 L $min^{-1}$) were used to collect high amounts of particles/plankton in the DCM. Each pump was mounted with a regular 142-mm filter holder for hosting a pre-combusted (450 °C, 6 h), pre-weighted 142-mm diameter glass fiber (GF/F) filter (Whatman). The holder was covered with a sock-type pre-filter of 60-µm pore size, so as to collect on the filters the size fraction 0.7-60 µm. Both pumps were deployed at the same time by the ship's Moon-Pool on the hydrographic cable to reach the DCM. At the DCM, the pumping lasted 40-60 min, so that ~ 250 L of seawater was passed over each GF/F filter. Back on board, the filters were recovered and dried. One filter was used for the analysis of SPM and hydrocarbons, while the other filter was dedicated to SPM, TChl*a*, POC, and $\delta^{13}C/\delta^{15}N$. Before drying, this second filter was also rinsed with ultra-pure water to remove residues of the seawater salts. Finally, the GF/F filters were placed in glass boxes and stored at -18 °C on board and then in the laboratory before analysis. It should be noted that molecular lipid analyzes were not conducted on these filters/size fraction 0.7-60 µm.

*2.2.2. Plankton sampling*. Multiple Plankton Sampler (Midi type, Hydro-Bios), here referred to as "MultiNet", was used to collect plankton in the DCM. The MultiNet was made of 5 individual opening and closing nets with 0.25-$m^2$ aperture, 60-µm mesh size, and cod ends of 60-µm mesh size, as well as two flowing meters to measure the volume of water filtered by the nets, a CTD sensor and a TChl*a* fluorometer. The MultiNet was deployed horizontally in the DCM from the rear of the ship *via* the electromechanical cable. The Multinet position was maintained stable at the defined depth by means of a V-fin deflector, a helicoidal bucket connector gathering the cod ends, a controlled vessel speed, and real-time control of its position from the on board desk unit. Once the five nets were filled, the MultiNet was brought on board, the cod ends rinsed out with local seawater, and their content

transferred into pre-cleaned 10-L HDPE bottles. The device was then returned to the water as many times as necessary until sufficient quantities of plankton were obtained.

In the on board clean lab container, plankton was then fractionated on a column of five stainless steel sieves (60, 200, 500, 1000 and 2000-µm mesh size) by wet-sieving with GF/F filtered seawater previously retrieved from ASTI pump/in-line filtration system and stored in a stainless steel jerry can (see section 2.2.3). The planktonic size fractions recovered on the stainless-steel sieves (i.e., 60-200, 200-500, 500-1000, 1000-2000 and > 2000 µm) were shared out for the different analyzes. For the analyzes of hydrocarbons, lipids, POC and $\delta^{13}C/\delta^{15}N$, each size fraction was transferred into two pre-combusted 150-mL amber glass flasks. It is worth noting that the quantities obtained for the size fractions 1000-2000 and > 2000 µm were not sufficient enough for PAH analyzes. Hence, only the fractions 60-200, 200-500 and 500-1000 µm are exploited in the present work. The glass flasks were stored at -18 °C on board and then in the laboratory before analysis.

*2.2.3. Water sampling and in-line filtration.* Seawater was sampled at ~ 5-20-m depth, depending on the stations, with a pneumatically-operated Teflon ASTI pump (model PFD2) set up on board, connected to Teflon tubing, which was weighted down and immersed with the hydrology gallows. The pump was connected to a clean dry air supply. The seawater brought on board in the Teflon tubing was then filtered in-line onto a pre-combusted GF/F 142-mm filter using a Teflon filtration holder. The seawater filtered through GF/F was stored in two stainless steel jerry cans of 20 L each. The seawater of the first jerry can was used exclusively for sieving the plankton collected with the MultiNet. The seawater of the second jerry can was amended with 50 mL of dichloromethane ($CH_2Cl_2$) for subsequent analyzes of dissolved (< 0.7 µm) AHs and PAHs. This jerry can was stored at ~ 20 °C on board and then in the laboratory before analysis. Before filling the jerry cans, several liters of filtered seawater were thrown away.

## 2.3. Analysis

*2.3.1. SPM, Biomass*. SPM was measured on the size fraction 0.7-60 µm by weighing, with a precision balance, the tare, the entire (142-mm GF/F) filters before filtration, and the entire filters, wet and dry (freeze dried), after filtration, taking into account the volumes of water filtered with the McLane pumps (Tesán-Onrubia et al., 2023). Dry-weight biomasses of the size fractions 60-200, 200-500 and 500-1000 µm were determined after drying samples on pre-weighed GF/F filters (60 °C, 24 h) and then re-weighed with a precision balance, taking into consideration the volumes of water filtered by the MultiNet (Fierro-González et al., 2023). The contributions of zooplankton, phytoplankton and detritus components to the total weighted biomass were estimated according to Fierro-González et al. (2023). SPM is expressed in mg $L^{-1}$, and biomass concentrations in µg (or mg) dry weight (dw) $L^{-1}$.

*2.3.2. TChla, POC, $\delta^{13}C$, $\delta^{15}N$*. The determination of TChl*a* concentration on the size fraction 0.7-60 µm was performed on a 22-mm diameter aliquot of the 142-mm GF/F filter by fluorescence method after methanol (MeOH) extraction according to Welschmeyer (1994) and Raimbault et al. (2004). TChl*a* concentration is expressed in µg $L^{-1}$. POC concentration and $\delta^{13}C/\delta^{15}N$ were determined on the size fractions 0.7-60 to 500-1000 µm. POC samples, i.e., 22-mm diameter aliquots of the freeze dried 142-mm GF/F filters (0.7-60 µm) and ~ 1 mg of the freeze dried plankton material (60-200 to 500-1000 µm), were analyzed using the persulfate wet-oxidation procedure according to Raimbault et al. (1999). For the fraction 0.7-60 µm, POC concentration is expressed either in mg $L^{-1}$ or in mg $g^{-1}$ dw (when normalized by SPM). For the fractions 60-200 to 500-1000 µm, POC concentration is expressed in mg $g^{-1}$ dw. Concerning $\delta^{13}C/\delta^{15}N$ samples, the SPM collected on the GF/F filters were scraped off with a scalpel, whereas plankton fractions were ground to fine powder.

225 Samples were then acidified (for $\delta^{13}C$) or not (for $\delta^{15}N$) and analyzed using an elemental
226 analyzer (Flash EA 2000, Thermo Scientific®) coupled with a continuous flow isotope ratio
227 mass spectrometer (Delta V Plus, Thermo Scientific®) (see details in Tesán-Onrubia et al.,
228 2023). Isotope compositions are expressed in ‰ as deviations from the standard reference
229 materials ($N_2$ in air for $\delta^{15}N$ and Vienna Pee Dee Belemnite for $\delta^{13}C$).
230 *2.3.3. Lipid biomarkers*. Lipid biomarkers were determined on the size fractions 60-
231 200 to 500-1000 µm. For each fraction, ~ 10 mg of freeze dried plankton were mixed with 15
232 mL MeOH and reduced with excess sodium borohydride ($NaBH_4$). This process was
233 conducted to reduce any hydroperoxides in samples (Galeron et al., 2015), which are known
234 to induce autoxidative damage of some lipids during the hot saponification step.
235 Saponification was carried out on each reduced sample. After $NaBH_4$ reduction, water and
236 potassium hydroxide (KOH) were added and the mixture directly saponified by refluxing.
237 After cooling, the contents of the flask were acidified with hydrochloric acid (HCl) to pH 1,
238 and extracted 3 times with 30-mL $CH_2Cl_2$. The combined $CH_2Cl_2$ extracts were dried over
239 anhydrous sodium sulfate ($Na_2SO_4$), filtered and concentrated to give the total lipid extract.
240 These latter were derivatized by dissolution in 300 µL
241 pyridine/bis(trimethylsilyl)trifluoroacetamide (BSTFA, Supelco) (2:1, v/v) and silylated.
242 After evaporation to dryness under a stream of $N_2$, the derivatized residue was dissolved in
243 hexane/BSTFA (2:1, v/v) to avoid desilylation and analyzed using gas chromatography-
244 electron ionization quadrupole time of flight mass spectrometry (GC-QTOF). Individual fatty
245 acids, fatty alcohols and sterols were identified and quantified using an Agilent 7890B/7200
246 GC-QTOF System (Agilent Technologies, France) according to Rontani et al. (2017). It
247 should be noticed that the polyunsaturated fatty acid concentrations must be regarded as
248 minimal values because they might have been affected by oxidative losses occurring during

249 the 2-year storage of samples at -18 °C before analysis. Concentrations of individual and total
250 lipid biomarkers (fatty acids, fatty alcohols and sterols) are expressed in mg $g^{-1}$ dw.
251 *2.3.4. Hydrocarbons.* Twenty-eight AHs, i.e., a series of *n*-alkanes from *n*-$C_{15}$ to *n*-$C_{40}$
252 and two isoprenoids, pristane (Pr) and phytane (Phy), were determined in this study.
253 Unresolved complex mixture (UCM) was not detected or negligible in our samples. For
254 PAHs, we determined the concentrations of 17 parent PAHs, namely naphthalene (Nap),
255 acenaphthylene (Acy), acenaphtene (Ace), fluorene (Flu), dibenzothiophene (DBT),
256 phenanthrene (Phe), anthracene (Ant), fluoranthene (Flt), pyrene (Pyr), benz[*a*]anthracene
257 (BaA), chrysene (Chr), benzo[*b*]fluoranthene (BbF), benzo[*k*]fluoranthene (BkF),
258 benzo[*a*]pyrene (BaP), dibenz[*a,h*]anthracene (DahA), benzo[*g,h,i*]perylene (BP),
259 indeno[1,2,3-*cd*]pyrene (IndP), as well as the concentrations of methylated derivatives
260 (methyl- = C1-, dimethyl- = C2-, trimethyl- = C3-) of the five compounds Nap (C1, C2, C3),
261 Flu (C1, C2), DBT (C1, C2), Phe/Ant (C1, C2) and Flt/Pyr (C1), which lead to a total of 27
262 PAHs (or groups of PAHs). AHs and PAHs were determined on the dissolved fraction (< 0.7
263 µm) of seawater, as well as on the size fractions 0.7-60, 60-200, 200-500 and 500-1000 µm.
264 For the fractions > 0.7 µm, samples (entire GF/F filters and plankton) were freeze dried for
265 24-96 h, then spiked with a multi-standard mixture containing surrogate standards for AHs
266 ($C_{16}$-$d_{34}$, $C_{24}$-$d_{50}$ and $C_{36}$-$d_{74}$) and PAHs (Nap-$d_8$, Flu-$d_{10}$, Phe-$d_{10}$, Flt-$d_{10}$ and BaP-$d_{12}$), and
267 extracted with $CH_2Cl_2$ using accelerated solvent extraction (ASE 350, Dionex, Thermo
268 Scientific) with the following procedure: 150 °C, 110 bars, 3 cycles of 10 min, 100% of
269 rinsing and purging for 60 s (Guigue et al., 2017; Fourati et al., 2018a). For the fraction < 0.7
270 µm, samples, i.e., 20 L of filtered seawater with 50 mL of $CH_2Cl_2$, were spiked with the
271 multi-standard mixture and extracted by liquid-liquid extraction with $CH_2Cl_2$ (3 × 60 mL per
272 liter) according to Guigue et al. (2014) and Fourati et al. (2018b). All $CH_2Cl_2$ extracts were
273 concentrated and solvent was exchanged by *n*-hexane. Extracts were reduced to ~ 1 mL, and

cleaned with a silica-alumina column (10 mm i.d., made of glass) packed from bottom to top with 1-3 g deactivated alumina (by 3% ultra-pure water w/w), 1-3 g activated silica, and 1 g dehydrated $Na_2SO_4$, depending on the quantity of extracted matter. First, the sorbents were conditioned with 20 mL *n*-hexane, then the extract was deposited on the top of the column and both AHs and PAHs were eluted with 50-mL *n*-hexane:$CH_2Cl_2$ (9:1 v/v). This was followed by solvent reduction to 200-500 µL, and deuterated mixtures for AHs ($C_{19}$-$d_{40}$ and $C_{30}$-$d_{62}$) and PAHs (Ace-$d_{10}$, Ant-$d_{10}$, Pyr-$d_{10}$, Chr-$d_{12}$ and Per-$d_{12}$) were spiked as internal standards before analysis.

AHs and PAHs were analyzed separately by gas chromatography (Trace ISQ, Thermo Electron) equipped with a mass spectrometry (MS) detector operating at an ionization energy of 70 eV, with hydrogen (1.2 mL $min^{-1}$) as carry gas. The capillary column (HP-5MS, Agilent Technologies, USA) was 30 m in length with an internal diameter of 0.25 mm and a film thickness of 0.25 µm. The injector (used in splitless mode) and detector temperatures were 250 and 320 °C, respectively. The column temperature was initially held at 70 °C for 3 min, increased to 150 °C at 15 °C $min^{-1}$, then increased to 320 °C at 7 °C $min^{-1}$ and finally held for 10 min. AHs and PAHs were identified and quantified in full scan and selected ion monitoring (SIM) modes simultaneously using two distinct methods (Guigue et al., 2011, 2014, 2017). All solvents and chemicals used were of high purity grade. Σ AHs and Σ PAHs represented the sum of the targeted AH and PAH compounds, respectively. Concentrations of dissolved AHs and PAHs are expressed in ng $L^{-1}$. Concentrations of AHs and PAHs for the fractions > 0.7 µm are expressed in µg $g^{-1}$ dw and ng $g^{-1}$ dw, respectively.

The quality control procedures were strictly followed throughout the whole sampling and laboratory treatments. They included control/validation of GC-MS calibration and tuning, laboratory and field blanks, method limit of detection/quantification (LODs/LOQs), as well as surrogate recoveries. Field and laboratory blanks were prepared, processed and analyzed in

299 the same manner as the real samples. LOQs ranged from 30 to 100 pg $L^{-1}$ and from 10 to 50
300 pg $L^{-1}$ in water for AHs and PAHs, respectively. They ranged from 0.3 to 1 ng $g^{-1}$ and from
301 0.1 to 0.5 ng $g^{-1}$ in plankton for AHs and PAHs, respectively. Blank values were below LODs
302 or LOQs and surrogate recoveries were > 75 and > 70% for AHs and PAHs, respectively. All
303 the concentrations reported here were not neither blank- nor recovery-corrected.
304
305 **2.4. Data handling**
306 To fully compare our PAH concentrations in the planktonic size fractions with those in
307 literature, we estimated the concentrations of individual PAHs (and of POC) in the entire size
308 fraction 60-1000 µm by summing the concentrations of individual PAHs (and of POC) in the
309 fractions 60-200, 200-500 and 500-1000 µm, each of these concentrations being weighted
310 (multiplied) by the contribution of the biomass of the given fraction to the total biomass of the
311 fraction 60-1000 µm ($f_{Biomass}$ = biomass of the given fraction / biomass 60-1000 µm).
312 According to González-Gaya et al. (2019), we estimated the biological pump fluxes of
313 PAHs, i.e., the vertical fluxes of PAHs exported in depth through the biological pump process
314 (in ng $m^{-2}$ $day^{-1}$), for the Western basin of the Mediterranean Sea. For this, we normalized the
315 PAH concentrations in the size fraction 60-1000 µm at each station (in ng $g^{-1}$ dw) by the
316 corresponding organic carbon (OC) content (in g C $g^{-1}$ dw). Then, we averaged these OC-
317 normalized PAH concentrations (in ng $g^{-1}$ C dw), and multiplied this obtained mean
318 concentration by the vertical settling flux of POC (in g C $m^{-2}$ $day^{-1}$) below 100-m depth for
319 the Western Mediterranean Sea estimated by Guyennon et al. (2015), where POC is defined
320 as being fueled by the natural mortality of the largest organisms (mesozooplankton, diatoms
321 and ciliates) and by the excretion of fecal pellets and sloppy feeding by mesozooplankton.
322 This calculation was performed for total PAHs (sum of our 27 parent and alkylated

compounds; $\Sigma_{27}$PAHs) but also for Phe alone, which was the dominant PAH in the planktonic fractions.

The partition coefficient between particulate matter and water ($K_D$ in L $kg^{-1}$) was calculated for seven individual PAHs (the ones present both in water and particulate/planktonic phases, namely Nap, Flu, Phe, Flt, Pyr, BaA and Chr) in each size fraction (0.7-60, 60-200, 200-500, 500-1000 and 60-1000 µm) as ($C_P$ / $C_W$) × 1000 where $C_P$ is the concentration of the given PAH in the given size fraction in ng $g^{-1}$ dw, and $C_W$ is the concentration of the PAH in the dissolved phase (size fraction < 0.7 µm) in ng $L^{-1}$. The partition coefficient between organic carbon and water ($K_{OC}$ in L $kg^{-1}$) was then determined for the seven individual PAHs in each size fraction as $K_D$ / $f_{OC}$ where $f_{OC}$ is the contribution of the OC mass (in g) to the total matter mass (in g) for a given size fraction ($f_{OC}$ = POC in mg $g^{-1}$ dw / 1000).

According to the previous works by Berrojalbiz et al. (2011) and González-Gaya et al. (2019), we assume that the relationships between SPM or biomass concentration in a given size fraction and the concentration of individual PAHs in this size fraction can be approximated by a power function of the form: $C_P = aSPM^{-m}$ or $aBiomass^{-m}$ where a is the constant and m the slope of the regression. In the present study, the Log $K_{OC}$ and slope (m) values were exploited to highlight the influence of plankton on the PAH bioaccumulation.

### 2.5. Statistics

Statistical analyzes were performed using XLSTAT software (version 2021.1.1). Student's parametric test (t-test) was used to determine significant differences between the means of two groups, i.e., the mean concentrations in two size fractions over the 10 stations.

## 3. Results and Discussion

### 3.1. TChla, POC and SPM/biomass

In the size fraction 0.7-60 µm sampled from the DCM, TChl*a*, POC and SPM concentrations followed substantially the same spatial distribution (Fig. 2a; Table S1), and were thus significantly positively correlated with each other ($r = 0.70\text{-}0.93$, $n = 10$, $p < 0.05$). The lowest concentrations were found at two southern coastal stations, St17 and St15. Low values were also recorded at St3 and St11. The highest concentrations were observed at the offshore station St9. High values were also found at two coastal stations, St19 and St1 (Fig. 2a; Table S1).

These results are in accordance with the observations by Tedetti et al. (2023) who highlighted that St9 displayed the highest contents in silicates [$Si(OH)_4$] and nitrates ($NO_3^-$), and the highest concentrations in POC and TChl*a* in the size fraction > 0.7 µm in the DCM compared to the other stations. The high levels of TChl*a* in St9 during the sampling period were also confirmed from satellite data (Tedetti et al., 2023). Indeed, St9, situated at the boundary of the Ligurian consensus region (Ayata et al., 2018) in the deep convection area, benefited from a relatively intense phytoplankton bloom in late March 2019 (still visible in May), consecutive to a pronounced winter convection process (Margirier et al., 2020; Bosse et al., 2022). In line with our results, Tedetti et al. (2023) also reported high concentrations in $Si(OH)_4$ and phosphates ($PO_4^{3-}$), as well as TChl*a* and POC in the fraction > 0.7 µm at St19. This enrichment could be related to nutrient inputs and the subsequent stimulation of phytoplankton activity from Saharan dust deposition event that occurred in the south of the Gulf of Gabès during sampling. Such Saharan dust deposition events have been already reported and recognized to provide nutrients in this area (Béjaoui et al., 2019). Apart from St9 and St19, the fraction 0.7-60 µm exhibited higher TChl*a*, POC and SPM contents for the northern stations (St1-St4) than for the offshore and southern stations (St10-St17) (Fig. 2a),

373 which is consistent with their positioning in terms of bloom-condition areas and consensus
374 regions defined by D'Ortenzio and d'Alcalà (2009) and Ayata et al. (2018).

375 The highest biomasses of the size fractions 60-200 to 500-1000 µm recovered from the
376 DCM sampling were determined at the southern (St17, St19) and northern (St4, St1) coastal
377 stations. The lowest ones were recorded at St3 and St10 (Fig. 2b; Table S1). The fractions 60-
378 200 and 200-500 µm contributed the most to the total biomass (37 and 41% on average,
379 respectively), while the contribution of the fraction 500-1000 µm was smaller (22% on
380 average) (Fig. 2b; Table S1).

381 The spatial distribution pattern of the biomasses of the size fractions 60-200 to 500-
382 1000 µm (Fig. 2b) did not really correspond to that of the SPM of the fraction 0.7-60 µm (Fig.
383 2a). According to Fierro-González et al. (2023) and Tesán-Onrubia et al. (2023), the biomass
384 of the fractions 60-200 and 200-500 µm was dominated by detritus and phytoplankton, which
385 represented on average 68.8% (fraction 60-200 µm) and 59.2% (fraction 200-500 µm) of the
386 total biomass (against 31.2 and 40.8% for zooplankton, respectively). An inverse pattern was
387 found for the fraction 500-1000 µm whose biomass was dominated by zooplankton (69.8% on
388 average). Zooplankton was mainly composed of copepods, which accounted for 48.9, 91.9
389 and 69.7% of total zooplankton in the fractions 60-200, 200-500 and 500-1000 µm,
390 respectively (Fierro-González et al., 2023; Tesán-Onrubia et al., 2023). Compared to the other
391 stations, the fraction 60-200 µm at St4 was enriched in phytoplankton, while the fractions 60-
392 200 and 200-500 µm at St17 were enriched in detritus.

393 The POC concentrations in the fractions 60-200 to 500-1000 µm were the highest in the
394 three offshore stations (St9-St11) and at the coastal station St1. They were the lowest at the
395 coastal stations St17, St4 and St3 (Fig. 2c; Table S1). The low POC levels at St17 could be
396 related to the high proportion of detritus within the biomass at this site. The POC
397 concentrations were generally the highest for the fraction 200-500 µm, and the lowest for the

60-200 µm. The POC concentrations of the three size fractions were quite well correlated with each other (r = 0.87-0.91, n = 9-10, $p < 0.05$). However, the latter were not at all correlated with the those of the 0.7-60-µm fraction, as seen from Fig. 2a, c.

### 3.2. Lipids

Concentrations of total lipid biomarkers in the planktonic fractions 60-200 to 500-1000 µm from the DCM are shown in Fig. 3. Concentrations of individual compounds are also presented in Table S2. Concentration of total ($\Sigma_{39}$) lipids (= concentrations of $\Sigma_{25}$fatty acids + $\Sigma_{8}$fatty alcohols + $\Sigma_{6}$sterols) ranged from 3.5 mg $g^{-1}$ dw (equivalent to 0.35%) at St2, fraction 500-1000 µm to 35.6 mg $g^{-1}$ dw (equivalent to 3.6%) at St9, fraction 200-500 µm (Fig. 3a). The highest $\Sigma_{39}$lipid concentrations were recorded in the three offshore stations St9-St11, as well as in the southern coastal stations St15 and St19, while the lowest ones were found at St17 and St3 (Fig. 3a). $\Sigma_{39}$lipid concentrations in the three fractions were significantly positively correlated with each other (r = 0.79-0.86, n = 9-10, $p < 0.05$) and no significant difference was detected between the mean concentrations of the three fractions over the 10 stations (t-test, $p > 0.05$). The distribution of $\Sigma_{39}$lipid concentrations throughout stations and fractions was very close to that of POC (Fig. 2c). Logically, a significant positive relationship appeared between $\Sigma_{39}$lipid and POC concentrations when considering the fractions 60-200 to 500-1000 µm (r = 0.69, n = 29, $p < 0.05$) (Fig. S1a). This underlines the strong link between the lipid and POC contents in the planktonic compartment. Interestingly, our $\Sigma_{39}$lipid concentrations (determined by GC-MS) were compared to those obtained by colorimetric method by Tesán-Onrubia et al. (2023) on the same samples. Both were rather well correlated (r = 0.75, n = 29, $p < 0.05$) albeit the colorimetric method gave slightly higher concentrations (Fig. S1b).

The $\Sigma_{39}$lipid concentrations we measured here in the three fractions (0.35-3.6%) were quite low compared to works by Båmstedt (1986) who found up to 61% lipid in some copepod species from temperate areas. However, they were of the same order of magnitude as a previous study conducted in the Mediterranean waters (3.0 ± 2.8%; Tiano et al., 2014). According to Lee et al. (2006), the plankton that has a year-round low-level supply of food available do not accumulate lipid reserves. This is in agreement with the oligotrophic character of the Mediterranean waters along with poor seasonality of food supply for plankton. In addition, even though zooplankton is known to have a higher content in lipids than phytoplankton, the occurrence of phytoplankton and detritus in addition to zooplankton species (mainly copepods) in each of our size fractions tended to lower their lipid content (Tesán-Onrubia et al., 2023), as for St17 where the high proportion of detritus was accompanied by a very low lipid content.

Concentrations of $\Sigma_{25}$fatty acids, $\Sigma_{8}$fatty alcohols and $\Sigma_{6}$sterols represented 80 ± 7.9%, 15 ± 8.6% and 5.0 ± 2.5% of the $\Sigma_{39}$lipid concentration, respectively (Fig. 3b-d). The distribution of $\Sigma_{25}$fatty acid concentrations throughout stations and fractions (Fig. 3b) was very similar to that of $\Sigma_{39}$lipid concentrations. While the distribution of $\Sigma_{6}$sterol concentrations (Fig. 3d) followed also quite well those of $\Sigma_{39}$lipids and $\Sigma_{25}$fatty acids, the distribution of $\Sigma_{8}$fatty alcohol concentrations (Fig. 3c) was rather different from the three others. Overall, as for $\Sigma_{39}$lipids and $\Sigma_{25}$fatty acids, the highest $\Sigma_{8}$fatty alcohol and $\Sigma_{6}$sterol concentrations were measured in St9-St11, followed by St15, St19 and St1 (Fig. 3c, d).

The prevalence of 16:0, 14:0, 18:1w9, 18:0 and 16:1w7 compounds for fatty acids, and of 16:0 and 14:0 compounds for fatty alcohols (Table S2) reflected the overall dominance of the carnivorous/omnivorous zooplankton (Lee et al., 2006). Nevertheless, some indicators allowed us to point out substantial differences between stations. Indeed, some phytoplankton (organisms or detrital matter) biomarkers, such as 16:1w7/18:1w9 and 16:1w7/16:0 fatty acid

447 ratios and the relative abundance of phytol among the fatty alcohols, were abundant at St4 and
448 St17 (Fig. S2a-c). This could be related to the much higher contributions of phytoplankton
449 and detritus found within the total biomass for the fractions 60-200 to 500-1000 µm at these
450 two stations (Fierro-González et al., 2023; Tesán-Onrubia et al., 2023). These phytoplankton
451 biomarkers revealed more pronounced signatures of diatoms and/or organisms feeding on
452 phytoplankton residues (Falk-Petersen et al., 1981, 1982; Sargent and Falk-Petersen, 1981;
453 Tolosa et al., 2004). Zooplankton biomarkers were also used: the relative abundance of 22:1,
454 20:5 and 22:6 fatty acids. The latter were higher in offshore stations, especially at St11 in the
455 fraction 500-1000 µm, and St15 (Fig. S3a-c). They could highlight together the presence of
456 herbivorous zooplankton feeding on diatoms (Kates and Volcani, 1966; Harrington et al.,
457 1970; Graeve 1993; Lee et al., 2006). Indeed, according to Fierro-González et al. (2023),
458 there was a high % (in biomass) of large crustaceans which could be euphausiids, actually
459 potential consumers of diatoms, in the fractions 500-100 and 1000-2000 µm at St11 and St15.
460 Moreover, according to the taxonomy results (M. Pagano personal communication), the % (in
461 number) of herbivorous filter feeders (large calanides of the Calanus type) over the entire
462 water column was the highest at these two stations, especially St11.
463 Among sterols, cholesterol (Cholest-5-en-3ß-ol) was the dominant compound (63.5 ±
464 6.5%) followed by Cholesta-5,22*E*-dien-3ß-ol (14.4 ± 6.5%) (Table S2). These % are in
465 agreement with previous values found in crustaceans from the Northern Adriatic Sea
466 (Serrazanetti et al., 1989). The concentrations of cholesterol were low, in accordance with the
467 overall low lipid content. This may be due not only to the composition of the zooplankton
468 diet, but also to the absence in these organisms of biochemical mechanisms capable of
469 converting into cholesterol some of the most diffused sterols in the marine environment
470 (Serrazanetti et al., 1989).
471

## 3.3. Hydrocarbons

### *3.3.1. AH distribution*

In seawater, dissolved $\Sigma_{28}$AH concentrations varied from 18 ng $L^{-1}$ (St10) to 489 ng $L^{-1}$ (St1) (Fig. S4a; Table S3). The highest values were recorded at St1, St9, St11, and at the Tunisian coasts (St15-St19), and were associated with monomodal molecular profiles in the range *n*-$C_{22}$-*n*-$C_{36}$ without predominance of odd over even carbon numbered *n*-alkanes, which reflected anthropogenic inputs from uncombusted oil-derived products (Fig. S4b) (Bouloubassi and Saliot, 1993; Wang et al., 1997). The lower concentrations recorded at St2-St4 and St10 were associated with bimodal molecular profiles exhibiting, in the range *n*-$C_{24}$-*n*-$C_{36}$, anthropogenic input residues, and in the range *n*-$C_{15}$-*n*-$C_{24}$, the peculiar abundance of *n*-$C_{16}$ and *n*-$C_{18}$ linked to microorganism contribution (bacteria, fungi, yeast) and their action on algal detritus (Fig. S4c) (Elias et al., 1997). These molecular profiles have been already observed in the dissolved phase of variably anthropogenic-stressed marine coastal areas (Guigue et al., 2014).

In the fraction 0.7-60 µm, $\Sigma_{28}$AH concentrations varied from 3.9 µg $g^{-1}$ dw (St9) to 104 µg $g^{-1}$ dw (St11) (Fig. 4a; Table S4). The molecular profiles were dominated by *n*-$C_{15}$ and *n*-$C_{17}$ (Fig. 4b), indicative of phytoplanktonic contribution linked to high primary production (Blumer et al., 1971; Goutx and Saliot, 1980). Despite these predominant biological fingerprints, no correlation was found between *n*-$C_{15}$ or *n*-$C_{17}$ and TChl*a* concentrations ($r$ = -0.12 to 0.23, n = 19, $p > 0.05$). *n*-pentadecane (*n*-$C_{15}$) has been shown to be produced by cyanobacteria, mainly in the lower euphotic zone, and rapidly consumed by heterotrophic prokaryotes in the ocean (Love et al., 2021). This could explain the absence of correlation between *n*-$C_{15}$ and TChl*a* concentrations.

In the fractions 60-200 to 500-1000 µm, $\Sigma_{28}$AH concentrations ranged from 3.4 µg $g^{-1}$ dw (St17, 60-200 µm) to 55 µg $g^{-1}$ dw (St11, 500-1000 µm) (Fig. 4c; Table S4). While $\Sigma_{28}$AH

concentrations in these three fractions were significantly positively correlated with each other (r = 0.62-0.88, n = 9-10, $p < 0.05$), they were all weakly correlated with that of the fraction 0.7-60 µm (r = 0.24-0.64, n = 9-10, $p < 0.05$ or $> 0.05$). No significant difference was detected between the mean concentrations of the four fractions over the 10 stations (t-test, $p > 0.05$). Interestingly, $\Sigma_{28}$AH concentration was significantly positively correlated to $\Sigma_{39}$lipid and POC concentrations only in the fraction 60-200 µm (r = 0.62-0.65, n = 10, $p < 0.05$).

Pristane was one of the main compounds within the low molecular weight range (< *n*-$C_{22}$) (Fig. 4d; Table S4), which is in line with the presence of zooplankton, especially the dominance of copepods (Blumer et al., 1963). Indeed, the high values of pristane in the fractions 200-500 and 500-1000 µm at St11 (Table S4) coincided with very high proportions of zooplankton (Fierro-González et al., 2023). Also, the abundance of *n*-$C_{15}$ and *n*-$C_{17}$ revealed the presence of phytoplanktonic residues (Fig. 4d), although no significant correlation was observed with these two latter biomarkers and the 16:1w7 diatom biomarker (r = -0.28 to 0.16, n = 29, $p > 0.05$) (Blumer at al., 1971). The high molecular weight compounds (> *n*-$C_{22}$) displayed the predominance of odd over even carbon numbered compounds (*n*-$C_{27}$, *n*-$C_{29}$, *n*-$C_{31}$, *n*-$C_{33}$) (Fig. 4d; Table S4), illustrating the presence of terrigenous higher plant debris in the samples (Douglas and Eglinton, 1966). It is unlikely that these debris were ingested by the organisms. It seems more likely that they were part of some allochthonous detritus collected along with zooplankton as observed by imagery analyzes (Fierro-González et al., 2023). Moreover, a background series of *n*-alkanes with no predominance of odd over even compounds was visible and may originate from anthropogenic inputs with minor occurrence. These results (AH concentrations and their molecular profiles in plankton) are in good agreement with previous studies from neighboring areas (Serrazanetti et al., 1989, 1991; Salas et al., 2006).

521 This class of compounds is very useful to better assess the sources of hydrocarbons in
522 planktonic organisms. Nevertheless, the dominance of biogenic signatures observed here
523 makes AH biomarkers not very explanatory in the study of the bioaccumulation of
524 hydrocarbons.
525
526 ***3.3.2 PAH distribution***
527 In seawater, the dissolved $\Sigma_{14}$PAH concentrations ranged from 0.9 ng $L^{-1}$ (St11) to 16
528 ng $L^{-1}$ (St4) (Fig. S5a; Table S5). The concentrations were quite low (< 5 ng $L^{-1}$) and the
529 methylated derivatives were not really identifiable, except at St4 (Fig. S5b, c). At this station,
530 the concentration reached 16 ng $L^{-1}$ due to significant inputs of C1-, C2- and C3-Nap (Fig.
531 S5c). The 2-3 ring PAHs were the major compounds representing 71 ± 16% of the total
532 PAHs, which is in accordance with their lower hydrophobicity (Fig. S5b, c; Table S5). The
533 quite low levels of concentrations along with the highly altered methylated derivatives at
534 almost all sites reflected remote or aged (weathered/photo- and bio-degraded) inputs, except
535 at St4, where local and recent moderate petrogenic inputs were suspected (Wang and Fingas,
536 1995; Chifflet et al., 2023).
537 In the fraction 0.7-60 µm, the $\Sigma_{27}$PAH concentrations ranged from 53 ng $g^{-1}$ dw (St9) to
538 ~ 220 ng $g^{-1}$ dw (St3 and St11) (Fig. 5a; Table S6). The PAH profiles in the fraction 0.7-60
539 µm (Fig. 5b) were different from those found in water (Fig. S5b, c), the 2-3 ring PAHs being
540 less abundant (49 ± 9% of total PAHs) and the 4-6 ring PAHs more abundant (Fig. 5b), which
541 is consistent with previous studies on particles in the Mediterranean Sea (Dachs et al., 1997;
542 Marti et al., 2001). However, as for PAHs in water (Fig. S5b, c), the methylated derivatives
543 were not well visible in this fraction and suspected to be highly degraded. Hence, the PAH
544 profiles in the fraction 0.7-60 µm might be explained by a high microbial degradation which
545 rather affected LMW PAHs, especially methylated derivatives (Lipiatou et al., 1993; Dachs et

546 al., 1997). Another explanation could be inputs of atmospheric aerosols or from sediments
547 (Chifflet et al., 2023), which are important sources of pyrogenic PAHs (HMW PAHs with a
548 low proportion of methylated derivatives) (Lipiatou et al., 1997), but the lack of 5-6 ring
549 compounds suggests that these inputs were minor.

550 In the fractions 60-200 to 500-1000 µm, the $\Sigma_{27}$PAH concentrations ranged from 35 ng
551 $g^{-1}$ dw (St19, 200-500 µm) to 255 ng $g^{-1}$ dw (St1, 60-200 µm) (Fig. 5c; Table S6). The lowest
552 $\Sigma_{27}$PAH concentrations were found at St9, St17 and St19 (Fig. 5c). Two of them, St9 and
553 St19, showed the highest TChl*a* concentrations. These two stations displayed a particular
554 biogeochemical context with regard to the other stations, as explained in section 3.1. $\Sigma_{27}$PAH
555 concentrations in these three fractions were rather well positively correlated with each other (r
556 = 0.50-0.73, n = 9-10, $p < 0.05$ or $> 0.05$), but not significantly correlated with that in the
557 fraction 0.7-60 µm (r = 0.14-0.55, n = 9-10, $p > 0.05$). The mean $\Sigma_{27}$PAH concentration of the
558 fraction 60-200 µm was significantly higher than those of the fractions 200-500 and 500-1000
559 µm (Fig. 5c) (t-test, $p < 0.05$). $\Sigma_{27}$PAH concentration was significantly positively correlated to
560 $\Sigma_{28}$AH concentration only in the fraction 0.7-60 µm (r = 0.84, n = 10, $p < 0.05$), while
561 $\Sigma_{27}$PAH concentrations were not correlated with $\Sigma_{39}$lipid and POC concentrations whatever
562 the size fraction. The PAH molecular profiles in the three fractions, i.e., dominance (80 ±
563 12%) of the 2-3 ring compounds (parents and methylated), especially Phe, and very low
564 abundance of the 4-6 ring compounds (Fig. 5d), were in agreement with those reported by
565 Salas et al. (2006) and Berrojalbiz et al. (2011).

566

567 **3.4. Comparison of plankton PAH concentrations and biological pump**
568 **fluxes of PAHs**

569 It is important to note that comparisons of our concentrations/fluxes of PAHs and
570 individual Phe (the dominant PAH in our study and also in most of previously works) with

571 those reported in the literature should be taken with caution since the methodologies for
572 sampling/separations of planktonic fractions, the planktonic size fractions, analyzes of PAHs
573 and the number of PAHs analyzed are not the same. Despite these limitations, these
574 comparisons still allow us to situate our data in relation to those obtained formerly.
575 The $\Sigma_{27}$PAH and Phe concentrations in plankton we determined here in the Western
576 Mediterranean Sea were globally lower than those measured in the Western and Eastern
577 Mediterranean Sea (Berrojalbiz et al., 2011), and in the Atlantic, Pacific and Indian Oceans
578 (González-Gaya et al., 2019), when taking into account maximal and mean values (see data in
579 Table 1). Salas et al. (2006) also found higher concentrations in the Galician coast (NW
580 Spain) after the Prestige oil spill (353-2035 ng $g^{-1}$ dw; not reported in Table 1). However,
581 when considering minimal and median values, our $\Sigma_{27}$PAH concentrations were very close to
582 those of other oceanic areas, and our Phe concentrations were even slightly higher (Table 1).
583 From the vertical settling flux of POC (in Table 1) and OC-normalized PAH
584 concentrations (not in Table 1), we estimated the biological pump fluxes of $\Sigma_{27}$PAHs and Phe
585 below 100-m depth in the Western Mediterranean Sea at 15 ± 10 and 4 ± 2 ng $m^{-2}$ $day^{-1}$,
586 respectively (Table 1). González-Gaya et al. (2019) found mean biological pump fluxes of
587 $\Sigma_{64}$PAHs and Phe below the surface mixed layer depth of 172 and 23 ng $m^{-2}$ $day^{-1}$ in the North
588 Atlantic, 91 and 6 ng $m^{-2}$ $day^{-1}$ in the South Atlantic, 55 and 7 ng $m^{-2}$ $day^{-1}$ in the North
589 Pacific, 14 and 1 ng $m^{-2}$ $day^{-1}$ in the South Pacific, and 22 and 2 ng $m^{-2}$ $day^{-1}$ in the Indian
590 Ocean (Table 1). Therefore, our biological pump fluxes were lower than those in the Atlantic
591 and North Pacific but comparable to those in the South Pacific and Indian Ocean. From our
592 results, the annual biological pump flux of $\Sigma_{27}$PAHs for the whole Western Mediterranean Sea
593 would be of 5274 ± 3467 kg $yr^{-1}$.
594
595 **3.5. Concentration patterns and bioaccumulation of PAHs within plankton**

596 It is important to note that only seven parent PAHs (Nap, Flu, Phe, Flt, Pyr, BaA and
597 Chr) were found both in water and all particulate/planktonic size fractions (Table S7). They
598 were thus selected to investigate the concentration patterns and bioaccumulation of PAHs
599 within plankton (see below).

600 ***3.5.1. Concentration pattern with the size fraction and trophic level***

601 The concentrations of $\Sigma_7$PAHs and $\Sigma_6$PAHs (without Phe) significantly decreased from
602 the fractions 0.7-60 or 60-200 µm to the fractions 200-500 or 500-1000 µm (t-test, $p < 0.05$)
603 (Fig. 6a, b), highlighting the bioreduction process of PAHs within the planktonic food web,
604 i.e., decreasing concentration with increasing organism size/trophic level. The fact that the
605 highest concentrations were found in the smallest fraction (0.7-60 µm) is in agreement with
606 recent observations (Berroralbiz et al., 2011; Tao et al., 2018; González-Gaya et al., 2019)
607 and related to the strong capacity of small cells to bioaccumulate contaminants due to their
608 high surface/volume ratio (Fan and Reinfelder, 2003; Heimbürger et al., 2010; Chouvelon et
609 al., 2019). Fig. 7 shows the concentrations in relation with the trophic levels, given by $\delta^{13}C$
610 and $\delta^{15}N$. It appears that the fraction 0.7-60 µm was trophically decoupled from the three
611 other ones. In other words, the bioaccumulation of PAHs in the upper 60-200-µm fraction
612 would not take place by trophic transfer from the 0.7-60-µm fraction but rather by water.
613 Then, considering the trophic proximity between the fractions 60-200, 200-500 and 500-1000
614 µm, it is possible that besides transfer from water, the PAHs were also transferred by
615 ingestion/diet between these three fractions (Fig. 7a, b). The overall bioreduction observed
616 along the planktonic food web would be due to the fact that when going up in the trophic
617 levels, even if there was trophic transfer of PAHs, the processes of absorption directly by the
618 water would have been less and less effective and the removal processes of PAHs (such as
619 depuration or metabolization) likely more effective, which ultimately would have led to this
620 decrease of PAH concentrations within the planktonic food web.

Phe presented a different pattern from the other compounds, with the highest concentrations mainly found in the fraction 60-200 µm (Fig. 6c; Fig. 7c). Phe was the most abundant compound representing for all sites 14, 51, 48 and 41% of $\Sigma_7$PAHs in the fractions 0.7-60, 60-200, 200-500 and 500-1000 µm, respectively. Berrojalbiz et al. (2011) also reported Phe (and alkylated homologues) as dominant compound in particles and plankton along a West-East transect in the Mediterranean Sea. In the present work, the peculiar Phe bioaccumulation in the fraction 60-200 µm, systematically observed at all stations (see Table S6), is intriguing. It could originate from a biogenic production within the collected plankton, as already suggested by Nizzetto et al. (2008). However, since there were no correlations between Phe concentrations, neither with POC, TChl*a*, nor lipids (in both fractions 0.7-60 and 60-200 µm) ($r = -0.33$ to $-0.04$, $n = 20$, $p > 0.05$), this suggests that even if this process had occurred, it would have been minor and hidden within the complex dynamics of Phe in plankton. Another explanation for the Phe bioaccumulation in the 60-200-µm fraction could be that this compound was less subjected to depuration/metabolization processes than the other compounds and than in the other fractions.

### *3.5.2. Water-OC partitioning and influence of biomass*

For each fraction at each station, the water-particulate matter coefficients ($K_D$ in L $kg^{-1}$), then the water-organic carbon partition coefficients ($K_{OC}$ in L $kg^{-1}$) were calculated for the 7 targeted PAHs (Tables S7-S9). It should be noticed that $K_D$ and $K_{OC}$ values were determined using dissolved PAH concentrations measured in surface waters (at ~ 5-20-m depth depending on stations) and particulate/plankton PAH concentrations measured in the DCM (at ~ 20-60 depth depending on the stations). Despite these depth discrepancies, and the possible differences in the dissolved PAH concentrations between surface waters and the DCM, the use of $K_{OC}$ as determined here remains very likely more suitable and reflects the PAH

biogeochemistry much better than the use of $K_{OW}$ that are theoretical values provided under partition equilibrium conditions (these equilibrium conditions certainly did not prevail in the water at the time of sampling). Consistent with the concentration patterns, Log $K_{OC}$ values clearly decreased with the size fractions, which confirms the higher PAH bioaccumulation in the smaller size fractions (Fig. 8a). Moreover, for each individual compound and each station, the PAH concentrations in size fractions (ng $g^{-1}$ dw) were plotted against the plankton biomass concentrations (mg dw $L^{-1}$). For most of PAHs and size fractions (except 500-1000 µm), the concentrations decreased with biomass, following a power function equation $[PAH] = a[Biomass]^{-m}$ (Fig. 8b; Table S10), reinforcing the results presented above (Fig. 6, 7). This highlights the biodilution process, which reflects the decrease in PAH concentrations with plankton biomass (Berrojalbiz et al., 2011; Nizzetto et al., 2012; Everaert et al., 2015; Morales et al., 2015; Ding et al., 2021).

The -m slope values originating from the power function equations were further examined because they are indicative of the influence level of the SPM or biomass load on the PAH concentration (Berrojalbiz et al., 2011). As for Log $K_{OC}$, the -m values noticeably decreased with the size fraction (Fig. 8b), which illustrates once again the more important role of the smaller fractions in the bioaccumulation of PAH, as well as the biodilution process. These m values were then plotted against Log $K_{OC}$. Finally, a positive significant relationship was found between "-m" and the Log $K_{OC}$ for the 7 PAHs and the different size fractions (0.7-60 to 500-1000 µm, as well as 60-1000 µm) (Fig. S6; Table S11). Such a linear relationship highlighted the strong link between the PAH bioaccumulation and the impact of the planktonic biomass on the PAH concentrations in plankton, implying also the biological pump process for the PAHs. González-Gaya et al. (2019) observed the same type of relationship between -m slope and Log $K_{OW}$. Tao et al. (2018) also reported a decrease in the PAH concentration along with phyto- and zooplankton biomass, but without any obvious

linear relationship between Log $K_{OW}$ et -m. The present results show that through the bioaccumulation process, the plankton, and in particular its smallest fractions, plays a key role in the PAH cycling in the Mediterranean Sea. Besides, biotransformation/degradation is another essential fate for PAHs in the ocean. This biological reworking has already been reported by González-Gaya et al. (2019), who observed a linear negative relationship between Log $K_{ow}$ and -m for some LMW PAHs. In our study, the biological removal was very likely present, especially in the fraction 60-200 µm, for which we also found a negative linear relationship between Log $K_{OC}$ et -m for the LMW HAPs, as well as the low abundance of methylated derivatives.

## 4. Conclusion

In this study, we determined the hydrocarbon (AH and PAH) content in water and size-fractionated plankton to help characterizing the bioaccumulation of these compounds at the water-plankton interface in the Western Mediterranean Sea. Zooplankton was mainly composed of copepods and its low lipid content was in accordance with the oligotrophic character of the Mediterranean waters, along with poor seasonality of food supply for plankton. Concerning AHs, anthropogenic inputs were recorded in water at all sites, even though these inputs were masked in plankton by major biogenic signatures. Regarding PAHs, profiles in water and in the 0.7-60-µm size fraction were quite similar but distinct from those in zooplankton, highlighting differences in the bioaccumulation processes. The peculiar bioaccumulation of Phe in the 60-200 µm is intriguing and could be related to reduced metabolization/depuration processes. We also demonstrate the strong PAH bioaccumulation in the 0.7-60-µm fraction (relative to water), followed by a limited transfer to higher size fractions, ultimately underscoring a bioreduction process along the planktonic food web.

Furthermore, the biodilution process (the decrease in concentration at higher SPM/biomass) was evidenced for the fractions 0.7-60 and 60-200 µm. Finally, our results point out the key role of the smallest size fractions of plankton in the PAH cycling in the Mediterranean Sea.

## Data availability

All data from this paper is stored in the MISTRALS-SEDOO database (https://mistrals.sedoo.fr/MERITE/) and will be made publicly accessible once all the articles related to the MERITE-HIPPOCAMPE cruise are published. In the meantime, data can be obtained upon request from the corresponding author.

## Author contribution statement

All the authors participated in the MERITE-HIPPOCAMPE project and design of the manuscript.

***Conception and design of study:*** C.G., J.A.T.-O., D.B., F.C., M.P., S.C., J.T., M.T.

***Acquisition of data:*** C.G., J.A.T.-O., L.G., D.B., F.C., M.P., S.C., D.M., L.C., M.T.

***Analysis and/or interpretation of data:*** C.G., J.A.T.-O., L.G., D.B., F.C., M.P., S.C., D.M., L.C., J.T., M.T.

***Drafting the manuscript:*** C.G., M.T.

***Revising/editing the manuscript:*** C.G., J.A.T.-O., L.G., D.B., F.C., M.P., S.C., D.M., L.C., J.T., M.T.

***Project administration and funding acquisition:*** F.C., M.P., J.T., M.T.

## Acknowledgments

The MERITE-HIPPOCAMPE project was initiated and funded by the cross-disciplinary *Pollution & Contaminants* axis of the CNRS-INSU MISTRALS program (joint action of the

721 MERMEX-MERITE and CHARMEX subprograms). The project also received financial
722 support from the IRD French-Tunisian International Joint Laboratory (LMI) COSYS-Med.
723 The MERITE-HIPPOCAMPE cruise was organized and supported by the French
724 Oceanographic Fleet (FOF), CNRS/INSU, IFREMER, IRD, the Tunisian Ministry of
725 Agriculture, Water Resources and Fisheries, and the Tunisian Ministry of Higher Education
726 and Scientific Research. The project also benefited from additional funding by IFREMER, by
727 the MIO Action Sud and Transverse Axis programs (CONTAM Transverse Axis), by the IRD
728 Ocean Department, and by the CONTAMPUMP project (ANR JCJC #19-CE34-0001-01). We
729 are grateful to the captains and crew of the R/V *Antea* for their help and assistance during the
730 cruise. Various MIO platforms also provided valuable support: the Service Atmosphère-Mer
731 (SAM), the Plateforme Analytique de Chimie des Environnements Marins (PACEM platform)
732 and the Platforme Microscopie et Imagerie (MIM platform). We warmly thank J.-F. Rontani
733 for his expertise on lipid biomarkers. Finally, we acknowledge two Reviewers for their
734 relevant and helpful comments.
735

## 736 Supplementary information

737 Supplementary material related to this article is available online at: xxx
738
739

## 740 References

741 Adhikari, P.L., Maiti, K., Overton, E.B., 2015. Vertical fluxes of polycyclic aromatic
742 hydrocarbons in the northern Gulf of Mexico. Marine Chemistry, 168, 60–68.
743 https://doi.org/10.1016/j.marchem.2014.11.001
744 Alekseenko, E., Thouvenin, B., Tronczyński, J., Carlotti, F., Garreau, P., Tixier, C., Baklouti,
745 M., 2018. Modeling of PCB trophic transfer in the Gulf of Lions; 3D coupled model

746 application. Marine Pollution Bulletin, 128, 140–155.
747 https://doi.org/10.1016/j.marpolbul.2018.01.008.
748 Arnot, J.A., Gobas, F.A.P.C., 2006. A Review of Bioconcentration Factor (BCF) and
749 Bioaccumulation Factor (BAF) Assessments for Organic Chemicals in Aquatic
750 Organisms. Environmental Reviews, 14, 257–297. https://doi.org/10.1139/A06-005
751 Ayata, S.D., Irisson, J.O., Aubert, A., Berline, L., Dutay, J.C., Mayot, N., Nieblas, A.E.,
752 D'Ortenzio, F., Palmieri, J., Reygondeau, G., Rossi, V., Guieu, C., 2018. Regionalisation
753 of the Mediterranean basin, a MERMEX synthesis. Progress in Oceanography, 163, 7–20.
754 https://doi.org/10.1016/j.pocean.2017.09.016
755 Balcıoğlu, E.B., 2016. Potential effects of polycyclic aromatic hydrocarbons (PAHs) in
756 marine foods on human health: a critical review. Toxin Reviews, 35, 98–105.
757 https://doi.org/10.1080/15569543.2016.1201513
758 Båmstedt, U., 1986. Chemical composition and energy content. In: Corner, E.D.S., O'Hara, S.
759 C.M. (eds.), The biological chemistry of marine copepods. Oxford University Press, New
760 York, pp. 1–58.
761 Bănaru, D., Diaz, F., Verley, P., Campbell, R., Navarro, J., Yohia, C., Oliveros-Ramos, R.,
762 Mellon-Duval, C., Shin, Y.-J., 2019. Implementation of an end-to-end model of the Gulf
763 of Lions ecosystem (NW Mediterranean Sea). I. Parameterization, calibration and
764 evaluation. Ecological Modelling, 401, 1–19.
765 https://doi.org/10.1016/j.ecolmodel.2019.03.005
766 Baumard, P., Budzinski, H., Garrigues, P., 1998. Polycyclic aromatic hydrocarbons in
767 sediments and mussels of the western Mediterranean Sea. Environmental Toxicology and
768 Chemistry, 17, 765–776. https://doi.org/10.1002/etc.5620170501
769 Béjaoui, B., Ben Ismail, S., Othmani, A., Ben Abdallah-Ben Hadj Hamida, O., Chevalier, C.,
770 Feki-Sahnoun, W., Harzallah, A., Ben Hadj Hamida, N., Bouaziz, R., Dahech, S., Diaz, F.,

771 Tounsi, K., Sammari, C., Pagano, M., Bel Hassen, M., 2019. Synthesis review of the Gulf
772 of Gabes (eastern Mediterranean Sea, Tunisia): morphological, climatic, physical
773 oceanographic, biogeochemical and fisheries features. Estuarine, Coastal and Shelf
774 Science, 219, 395–408. https://doi.org/10.1016/j.ecss.2019.01.006
775 Ben Othman, H., Pick, F.R., Sakka Hlaili, A., Leboulanger, C., 2023. Effects of polycyclic
776 aromatic hydrocarbons on marine and freshwater microalgae – A review. Journal of
777 Hazardous Materials, 441, 129869. https://doi.org/10.1016/j.jhazmat.2022.129869
778 Berrojalbiz, N., Dachs, J., Ojeda, M.J., Valle, M.C., Castro-Jimenez, J., Wollgast, J., Ghiani,
779 M., Hanke, G., Zaldivar, J.M., 2011. Biogeochemical and physical controls on
780 concentrations of polycyclic aromatic hydrocarbons in water and plankton of the
781 Mediterranean and Black Seas. Global Biogeochemical Cycles, 25, GB4003.
782 https://doi.org/10.1029/2010GB003775
783 Berrojalbiz, N., S. Lacorte, A. Calbet, E. Saiz, C. Barata, J. Dachs, 2009. Accumulation and
784 cycling of polycyclic aromatic hydrocarbons in zooplankton, Environmental Science and
785 Technology, 43, 2295–2301. https://doi.org/10.1021/es8018226
786 Blumer, M., Guillard, R.R.L., Chase, T., 1971. Hydrocarbons of marine phytoplankton.
787 Marine Biology, 8, 183. https://doi.org/10.1007/BF00355214
788 Blumer, M., Mullin, M.M., Thomas, D.W., 1963. Pristane in Zooplankton. Science, 140, 974–
789 974. https://doi.org/10.1126/science.140.3570.974
790 Bosse, A., Testor, P., Coppola L., Bretel, P., Dausse, D., Durrieu de Madron, X., Houpert, L.,
791 Labaste, M., Legoff, H., Mortier, L., D'Ortenzio, F., 2022. LION observatory data.
792 SEANOE. https://doi.org/10.17882/44411
793 Boudriga, I., Thyssen, M., Zouari, A., Garcia, N., Tedetti, M., Bel Hassen, M., 2022.
794 Ultraphytoplankton community structure in subsurface waters along a North-South

795 Mediterranean transect. Marine Pollution Bulletin, 182, 113977.
796 https://doi.org/10.1016/j.marpolbul.2022.113977
797 Bouloubassi, I., Méjanelle, L., Pete, R., Fillaux, J., Lorre, A., Point, V., 2006. PAH transport
798 by sinking particles in the open Mediterranean Sea: A 1 year sediment trap study. Marine
799 Pollution Bulletin, 52, 560–571. https://doi.org/10.1016/j.marpolbul.2005.10.003
800 Bouloubassi, I., Saliot, A., 1993. Investigation of anthropogenic and natural organic inputs in
801 estuarine sediments using hydrocarbon markers (NAH, LAB, PAH). Oceanologica Acta
802 16, 145–161.
803 Castro-Jiménez, J., Bănaru, D., Chen, C.-T., Jiménez, B., Muñoz-Arnanz, J., Deviller, G.,
804 Sempéré, R., 2021. Persistent organic pollutants burden, trophic magnification and risk in
805 a pelagic food web from coastal NW Mediterranean Sea. Environmental Science and
806 Technology, 55, 9557–9568. https://doi.org/10.1021/acs.est.1c00904
807 Chen, C.-T., Carlotti, F., Harmelin-Vivien, M., Lebreton, B., Guillou, G., Vassallo, L., Le
808 Bihan, M., Bănaru, D., 2022. Diet and trophic interactions of Mediterranean
809 planktivorous fishes. Marine Biology, 169, 119. https://doi.org/10.1007/s00227-022-
810 04103-1
811 Chifflet, S., Briant, N., Tesán-Onrubia, J.A., Zaaboub, N., Amri, S., Radakovitch, O., Bãnaru,
812 D., Tedetti, M., 2023. Distribution and accumulation of metals and metalloids in
813 planktonic food webs of the Mediterranean Sea (MERITE-HIPPOCAMPE campaign).
814 Marine Pollution Bulletin, 186, 114384. https://doi.org/10.1016/j.marpolbul.2022.114384
815 Chouvelon, T., Strady, E., Harmelin-Vivien, M., Radakovitch, O., Brach-Papa, C., Crochet,
816 S., Knoery, J., Rozuel, E., Thomas, B., Tronczynski, J., Chiffoleau, J.F., 2019. Patterns of
817 trace metal bioaccumulation and trophic transfer in a phytoplankton-zooplankton-small
818 pelagic fish marine food web, Marine Pollution Bulletin, 146, 1013–1030.
819 https://doi.org/10.1016/j.marpolbul.2019.07.047

820 Dachs, J., Bayona, J.M., Raoux, C., Albaigés, J., 1997. Spatial, Vertical Distribution and
821 Budget of Polycyclic Aromatic Hydrocarbons in the Western Mediterranean Seawater.
822 Environmental Science and Technology, 31, 682–688. https://doi.org/10.1021/es960233j
823 Ding, Q., Gong, X., Jin, M., Yao, X., Zhang, L., Zhao, Z., 2021. The biological pump effects
824 of phytoplankton on the occurrence and benthic bioaccumulation of hydrophobic organic
825 contaminants (HOCs) in a hypereutrophic lake. Ecotoxicoly and Environmental Safety,
826 213, 112017. https://doi.org/10.1016/j.ecoenv.2021.112017
827 D'Ortenzio, F., d'Alcalà, M.R., 2009. On the trophic regimes of the Mediterranean Sea: a
828 satellite analysis. Biogeosciences, 6, 139–148. https://doi.org/10.5194/bg-6-139-2009
829 Douglas, G., Eglinton, G., 1966. Distribution of Alkanes, in Comparative Phytochemistry.
830 Academic Press, New York, 57–77.
831 Duran, R., Cravo-Laureau, C., 2016. Role of environmental factors and microorganisms in
832 determining the fate of polycyclic aromatic hydrocarbons in the marine environment.
833 FEMS Microbiological Reviews, 40, 814–830. https://doi.org/10.1093/femsre/fuw031
834 Elias, V.O., Simoneit, B.R.T., Cardoso, J.N., 1997. Even n-alkanes on the Amazon shelf and a
835 northeast Pacific hydrothermal system. Naturwissenschaften, 84, 415.
836 https://doi.org/10.1007/s001140050421
837 EU-Directive, 2013. Directive 2013/39/EU of the European Parliament and of the Council of
838 12 August 2013 amending directives 2000/60/EC and 2008/105/EC as regards priority
839 substances in the field of water policy. Official Journal of the European Union 1–17.
840 Everaert, G., De Laender, F., Goethals, P.L.M., Janssen, C.R., 2015. Multidecadal field data
841 support intimate links between phytoplankton dynamics and PCB concentrations in
842 marine sediments and biota. Environmental Science and Technology, 49, 8704–8711.
843 https://doi.org/10.1021/acs.est.5b01159

844 Fan, C.-W., Reinfelder, J.R., 2003. Phenanthrene Accumulation Kinetics in Marine Diatoms.
845 Environmental Science and Technology, 37, 3405−3412.
846 https://doi.org/10.1021/es026367g
847 Falk-Petersen, S., Gatten, R.R., Sargent, J.R., Hopkins, C.C.E., 1981. Ecological investigation
848 on the zooplankton community in Balsfjorden, northern Norway: Seasonal changes in the
849 lipid class composition of Meganyctiphanes norvegia (M. Sars), Thysanoessa raschii (M
850 Sars), T. inermis (Krøyer). Journal of Experimental Marine Biology and Ecology, 54,
851 209–224.
852 Falk-Petersen, S., Sargent, J.R., Hopkins, C.C.E., Vaja, B., 1982. Ecological investigations on
853 the zooplankton community of Balsfjorden, northern Norway: lipids in the euphausiids
854 Thysanoessa raschii and T. inermis during the spring. Marine Biology, 68, 97–102.
855 Fierro-González, P., Pagano, M., Guilloux, L., Makhlouf Belkahia, N., Tedetti, M., Carlotti,
856 F., 2023. Zooplankton biomass, size structure, and associated metabolic fluxes with focus
857 on its roles at the chlorophyll maximum layer during the plankton-contaminant MERITE-
858 HIPPOCAMPE cruise. Marine Pollution Bulletin, 193, 115056.
859 https://doi.org/10.1016/j.marpolbul.2023.115056
860 Fourati, R., Tedetti, M., Guigue, C., Goutx, M., Garcia, N., Zaghden, H., Sayadi, S., Elleuch,
861 B., 2018a. Sources and spatial distribution of dissolved aliphatic and polycyclic aromatic
862 hydrocarbons in surface coastal waters from the Gulf of Gabès (Tunisia, Southern
863 Mediterranean Sea). Progress in Oceanography, 163, 232–247.
864 http://dx.doi.org/10.1016/j.pocean.2017.02.001
865 Fourati, R., Tedetti, M., Guigue, C., Goutx, M., Zaghden, H., Sayadi, S., Elleuch, B., 2018b.
866 Natural and anthropogenic particulate-bound aliphatic and polycyclic aromatic
867 hydrocarbons in surface waters of the Gulf of Gabès (Tunisia, Southern Mediterranean

Sea). Environmental Science and Pollution Research, 25, 2476–2494. https://link.springer.com/article/10.1007/s11356-017-0641-7

Frouin, H., Dangerfield, N., Macdonald, R.W., Galbraith, M., Crewe, N., Shaw, P., Mackas, D., Ross, P.S., 2013. Partitioning and bioaccumulation of PCBs and PBDEs in marine plankton from the Strait of Georgia, British Columbia, Canada. Progress in Oceanography, 115, 65–75. http://dx.doi.org/10.1016/j.pocean.2013.05.023

Galeron, M.-A., Amiraux, R., Charriere, B., Radakovitch, O., Raimbault, P., Garcia, N., Lagadec, V., Vaultier, F., Rontani, J.-F., 2015. Seasonal survey of the composition and degradation state of particulate organic matter in the Rhône River using lipid tracers. Biogeosciences, 12, 1431–1446. https://doi.org/10.5194/bg-12-1431-2015

González-Gaya, B., Martínez-Varela, A., Vila-Costa, M., Casal, P., Cerro-Gálvez, E., Berrojalbiz, N., Lundin, D., Vidal, M., Mompean, C., Bode, A., Jiménez, B., Dachs, J., 2019. Biodegradation as an important sink of aromatic hydrocarbons in the oceans. Nature Geosciences, 12, 119–125. https://doi.org/10.1038/s41561-018-0285-3

Goutx, M., Saliot, A., 1980. Relationship between dissolved and particulate fatty acids and hydrocarbons, chlorophyll-a and zooplankton biomass in Villefranche Bay, Mediterranean Sea. Marine Chemistry, 8, 299. http://doi.org/10.1016/0304-4203(80)90019-5

Graeve, M., 1993. Umsatz und Verteilung von Lipiden in arktischen marinen Organismen unter besonderer Berücksichtigung unterer trophischer Stufen. Reports on Polar Research, 124, 1–141.

Guigue, C., Tedetti, M., Dang, D.H., Mullot, J.-U., Garnier, C., Goutx, M., 2017. Remobilization of polycyclic aromatic hydrocarbons and organic matter in seawater during sediment resuspension experiments from a polluted coastal environment: insights

892 from Toulon Bay (France). Environmental Pollution, 229, 627–638.
893 https://doi.org/10.1016/j.envpol.2017.06.090
894 Guigue, C., Tedetti, M., Ferretto, N., Garcia, N., Méjanelle, L., Goutx, M., 2014. Spatial and
895 seasonal variabilities of dissolved hydrocarbons in surface waters from the Northwestern
896 Mediterranean Sea: Results from one-year intensive sampling. Science of the Total
897 Environment, 466–467, 650–662. https://doi.org/10.1016/j.scitotenv.2013.07.082
898 Guigue, C., Tedetti, M., Giorgi, S., Goutx, M., 2011. Occurrence and distribution of
899 hydrocarbons in the surface microlayer and subsurface water from the urban coastal
900 marine area off Marseilles, Northwestern Mediterranean Sea. Marine Pollution Bulletin,
901 62, 2741–2752. http://dx.doi.org/10.1016/j.marpolbul.2011.09.013
902 Guitart, C., García-Flor, N., Miquel, J. C., Fowler, S. W., Albaigés, J., 2010. Effect of the
903 accumulation of polycyclic aromatic hydrocarbons in the sea surface microlayer on their
904 coastal air-sea exchanges. Journal of Marine Systems, 79, 210–217.
905 https://doi.org/10.1016/j.jmarsys.2009.09.003
906 Guyennon, A., Baklouti, M., Diaz, F., Palmieri, J., Beuvier, J., Lebaupin-Brossier, C.,
907 Arsouze, T., Béranger, K., Dutay, J.-C., and Moutin, T., 2015. New insights into the
908 organic carbon export in the Mediterranean Sea from 3-D modeling. Biogeosciences, 12,
909 7025–7046. https://doi.org/10.5194/bg-12-7025-2015
910 Harrington, G.W., Beach, D.H., Dunham, J.E., Holz, G.G., 1970. The polyunsaturated fatty
911 acids of dinoflagellates. Journal of Protozoology, 17, 213–219.
912 Heimbürger, L.E., Cossa, D., Marty, J.C., Migon, C., Averty, B., Dufour, A., Ras, J., 2010.
913 Methylmercury distributions in relation to the presence of nano and picophytoplankton in
914 an oceanic water column (Ligurian Sea, North-western Mediterranean). Geochimica
915 Cosmochimica Acta, 74, 5549–5559. https://doi.org/10.1016/j.gca.2010.06.036

916 Honda, M., Suzuki, N., 2020. Toxicities of polycyclic aromatic hydrocarbons for aquatic
917 animals. International Journal of Environmental Research and Public Health, 17, 1363.
918 https://doi.org/10.3390%2Fijerph17041363
919 Hylland, K., 2006. Polycyclic Aromatic Hydrocarbon (PAH) ecotoxicology in marine
920 ecosystems. Journal of Toxicology and Environmental Health Part A, 69, 109–123.
921 https://doi.org/10.1080/15287390500259327.
922 Islam, Md. S., Tanaka, M., 2004. Impacts of pollution on coastal and marine ecosystems
923 including coastal and marine fisheries and approach for management: a review and
924 synthesis. Marine Pollution Bulletin, 48, 624–649.
925 https://doi.org/10.1016/j.marpolbul.2003.12.004
926 Jónasdóttir, S.H., 2019. Fatty Acid Profiles and Production in Marine Phytoplankton. Marine
927 Drugs, 17, 151. https://doi.org/10.3390/md17030151
928 Kates, K., Volcani, B.E., 1966. Lipid components of diatoms. Biochemical and Biophysical
929 Acta, 116, 264–278.
930 Lee, R.F., Hagen, W., Kattner, G., 2006. Lipid storage in marine zooplankton. Marine
931 Ecology Progress Series, 307, 273–306. http://dx.doi.org/10.3354/meps307273
932 Li, H., Duan, D., Beckingham, B., Yang, Y., Ran, Y., Grathwohl, P., 2020. Impact of trophic
933 levels on partitioning and bioaccumulation of polycyclic aromatic hydrocarbons in
934 particulate organic matter and plankton. Marine Pollution Bulletin, 160, 111527.
935 https://doi.org/10.1016/j.marpolbul.2020.111527
936 Li, Z., Chi, J., Wu, Z., Zhang, Y., Liu, Y., Huang, L., Lu, Y., Uddin, M., Zhang, W., Wand,
937 X., Lin, Y., Tong, Y., 2021. Characteristics of plankton Hg bioaccumulations based on a
938 global data set and the implications for aquatic systems with aggravating nutrient
939 imbalance. Frontiers of Environmental Science & Engineering, 16, 37.
940 https://doi.org/10.1007/s11783-021-1471-x

941 Lipiatou, E., Marty, J.-C., Saliot, A., 1993. Sediment trap fluxes of polycyclic aromatic
942 hydrocarbons in the Mediterranean Sea. Marine Chemistry, 44, 43–54.
943 https://doi.org/10.1016/0304-4203(93)90005-9
944 Lipiatou, E., Tolosa, I., Simó, R., Bouloubassi, I., Dachs, J., Marti, S., Sicre, M.A., Bayona,
945 J.M., Grimalt, J.O., Saliot, A., Albaigés, J., 1997. Mass budget and dynamics of
946 polycyclic aromatic hydrocarbons in the Mediterranean Sea. Deep-Sea Research II, 44,
947 881–905. https://doi.org/10.1016/S0967-0645(96)00093-8
948 Love, C.R., Arrington, E.C., Gosselin, K.M., Reddy, C.M., Van Mooy, B.A.S., Nelson, R.K.,
949 Valentine, D.L., 2021. Nature Microbiology, 6, 489–498. https://doi.org/10.1038/s41564-
950 020-00859-8
951 Mackay, D., Fraser, A., 2000. Bioaccumulation of Persistent Organic Chemicals: Mechanisms
952 and Models. Environmental Pollution, 110, 375-391. http://dx.doi.org/10.1016/S0269-
953 7491(00)00162-7
954 Mandić, J., Tronczyński, J., Kušpilić, G., 2018. Polycyclic aromatic hydrocarbons in surface
955 sediments of the mid-Adriatic and along the Croatian coast: Levels, distributions and
956 sources. Environmental Pollution, 242, 519–527.
957 https://doi.org/10.1016/J.ENVPOL.2018.06.095
958 Margirier, F., Testor, P., Heslop, E., Mallil, K., Bosse, A., Houpert, L., Mortier, L., Bouin,
959 M.-N., Coppola, L., D'Ortenzio, F., Durrieu de Madron, X., Mourre, B., Prieur, L.,
960 Raimbault, P., Taillandier, V., 2020. Abrupt warming and salinification of intermediate
961 waters interplays with decline of deep convection in the Northwestern Mediterranean Sea.
962 Scientific Reports, 10, 20923. https://doi.org/10.1038/s41598-020-77859-5.
963 Martí, S., Bayona, J.M., Méjanelle, L., Saliot, A., Albaigés, J., 2001. Biogeochemical
964 evolution of the outflow of the Mediterranean deep-lying particulate organic matter into
965 the northeasterne Atlantic. Marine Chemistry, 76, 211–231.

https://doi.org/10.1016/S0304-4203(01)00064-0

Martin, J.H., Knauer, G.A., 1973. The elemental composition of plankton. Geochimica Cosmochimica Acta, 37, 1639–1653. https://doi.org/10.1016/0016-7037(73)90154-3.

Mille, G., Asia, L., Guiliano, M., Malleret, L., Doumenq, P., 2007. Hydrocarbons in coastal sediments from the Mediterranean Sea (Gulf of Fos area, France). Marine Pollution Bulletin, 54, 566–575. https://doi.org/10.1016/j.marpolbul.2006.12.009

Morales, L., Dachs, J., Fernández-Pinos, M.C., Berrojalbiz, N., Mompean, C., González-Gaya, B., Jiménez, B., Bode, A., Abalos, M., Abad, E., 2015. Oceanic sink and biogeochemical controls on the accumulation of polychlorinated dibenzo-pdioxins, dibenzofurans, and biphenyls in plankton. Environmental Science and Technology, 49, 13853–13861. https://doi.org/10.1021/acs.est.5b01360

Mzoughi, N., Chouba, L., 2011. Distribution and partitioning of aliphatic hydrocarbons and polycyclic aromatic hydrocarbons between water, suspended particulate matter, and sediment in harbours of the West coastal of the Gulf of Tunis (Tunisia). Journal of Environmental Monitoring, 13, 689–698. https://doi.org/10.1039/C0EM00616E

Nizzetto, L., Gioia, R., Li, J., Borga, K., Pomati, F., Bettinetti, R., Dachs, J., Jones, K.C., 2012. Biological pump control of the fate and distribution of hydrophobic organic pollutants in water and plankton. Environmental Science and Technology, 46, 3204–3211. http://dx.doi.org/10.1021/es204176q

Nizzetto, L., Lohmann, R., Gioia, R., Jahnke, A., Temme, C., Dachs, J., Herckes, P., Di Guardo, A., Jones, K.C., 2008. PAHs in air and seawater along north-south Atlantic transect: trends, processes and possible sources. Environmental Science and Technology, 42, 1580. https://doi.org/10.1021/ES0717414

989 Pirsaheb, M., Irandost, M., Asadi, F., Fakhri, Y., Asadi, A., 2018. Evaluation of polycyclic
990 aromatic hydrocarbons (PAHs) in fish: a review and meta-analysis. Toxin Reviews, 39,
991 205–213. https://doi.org/10.1080/15569543.2018.1522643
992 Raimbault, P., Pouvesle, W., Sempéré, R., 1999. Wet-oxidation and automated colorimetry
993 for simultaneous determination of organic carbon, nitrogen and phosphorus dissolved in
994 seawater. Marine Chemistry, 66, 161–169. https://doi.org/10.1016/S0304-
995 4203%2899%2900038-9
996 Raimbault, P., Lantoine, F., Neveux, J., 2004. Dosage rapide de la chlorophylle a et des
997 phéopigments a par fluorimétrie après extraction au méthanol. Comparaison avec la
998 méthode classique d'extraction à l'acétone. Océanis, 30, 189–205.
999 Rocha, M.J., Rocha, E., 2021. Concentrations, sources and risks of PAHs in dissolved and
1000 suspended material particulate fractions from the Northwest Atlantic Coast of the Iberian
1001 Peninsula. Marine Pollution Bulletin, 165, 112–143.
1002 https://doi.org/10.1016/j.marpolbul.2021.112143
1003 Romero, I.C., Sutton, T., Carr, B., Quintana-Rizzo, E., Ross, S.W., Hollander, D.J., Torres,
1004 J.J., 2018. Decadal Assessment of Polycyclic Aromatic Hydrocarbons in Mesopelagic
1005 Fishes from the Gulf of Mexico Reveals Exposure to Oil-Derived Sources.
1006 Environmental Science and Technology, 52, 10985–10996.
1007 https://doi.org/10.1021/acs.est.8b02243
1008 Rontani, J.-F., Galeron, M.-A., Amiraux, R., Artigue, L., Belt, S.T., 2017. Identification of di-
1009 and triterpenoid lipid tracers confirms the significant role of autoxidation in the
1010 degradation of terrestrial vascular plant material in the Canadian Arctic. Organic
1011 Geochemistry, 108, 43–50. https://doi.org/10.1016/j.orggeochem.2017.03.011
1012 Salas, N., Ortiz L., Gilcoto, M., Varela, M., Bayona J.M., Groom, S., Álvarez-Salgado, X.A.,
1013 Albaigés J., 2006. Fingerprinting petroleum hydrocarbons in plankton and surface

1014 sediments during the spring and early summer blooms in the Galician coast (NW Spain)
1015 after the Prestige oil spill. Marine Environmental Research, 62, 388–413.
1016 https://doi.org/10.1016/j.marenvres.2006.06.004
1017 Sargent, J.R., Falk-Petersen, S.F., 1981. Ecological investigations on the zooplankton
1018 community in Balsfjorden, northern Norway: Lipids and fatty acids in Meganyctiphanes
1019 norvegia, Thysanoessa raschi, and T. inermis during midwinter. Marine Biology, 62,
1020 131–137.
1021 Schäfer, S., Buchmeier, G., Claus, E., Duester, L., Heininger, P., Körner, A., Mayer, P.,
1022 Paschke, A., Rauert, C., Reifferscheid, G., Rüdel, H., Schlechtriem, C., Schröter-
1023 Kermani, C., Schudoma, D., Smedes, F., Steffen, D., Vietoris, F., 2015. Bioaccumulation
1024 in aquatic systems: methodological approaches, monitoring and assessment.
1025 Environmental Sciences Europe, 27, 5. https://doi.org/10.1186%2Fs12302-014-0036-z
1026 Serrazanetti, G.P., Conte, L.S., Carpené, E., Bergami, C., Fonda-Umani, S., 1991.
1027 DISTRIBUTION OF ALIPHATIC HYDROCARBONS IN PLANKTON OF
1028 ADRIATIC SEA OPEN WATERS. Chemosphere, 23, 925–938.
1029 https://doi.org/10.1016/0045-6535(91)90097-W
1030 Serrazanetti, G.P., Conte, L.S., Cattani, O., 1989. ALIPHATIC HYDROCARBON AND
1031 STEROL CONTENT OF ZOOPLANKTON OF THE EMILIA-ROMAGNA COAST
1032 (NORTHERN ADRIATIC). Comparative Biochemistry and Physiology, 94B, 143–148.
1033 https://doi.org/10.1016/0305-0491(89)90025-4
1034 Siegel, D.A., Buesseler, K.O., Doney, S.C., Sailley, S.F., Behrenfeld, M.J., Boyd, P.W., 2014.
1035 Global assessment of ocean carbon export by combining satellite observations and food-
1036 web models. Global Biogeochemical Cycles, 28, 181–196, doi:10.1002/2013GB004743.
1037 Stogiannidis, E., Laane, R., 2015. Source characterization of polycyclic aromatic
1038 hydrocarbons by using their molecular indices: an overview of possibilities. Reviews of

Environmental Contamination and Toxicology, 234, 49–133. https://doi.org/10.1007/978-3-319-10638-0_2

Stortini, A.M., Martellini, T., Del Bubba, M., Lepri, L., Capodaglio, G., Cincinelli, A., 2009. n-Alkanes, PAHs and surfactants in the sea surface microlayer and sea water samples of the Gerlache Inlet sea (Antartica). Microchemical Journal, 92, 37–43. https://doi.org/10.1016/j.microc.2008.11.005

Strady, E., Harmelin-Vivien, M., Chiffoleau, J.F., Veron, A., Tronczynski, J., Radakovitch, O., 2015. $^{210}$Po and $^{210}$Pb trophic transfer within the phytoplankton–zooplankton–anchovy/sardine food web: a case study from the Gulf of Lion (NW Mediterranean Sea. Journal of Environmental Radioactivity, 143, 141–151. http://dx.doi.org/10.1016/j.jenvrad.2015.02.019

Swackhamer, D.L., Skoglund, R.S., 1993. Bioaccumulation of PCBs by algae: kinetics versus equilibrium. Environmental Toxicology and Chemistry, 12, 831–838. https://doi.org/10.1002/etc.5620120506

Tao, Y., Xue, B., Lei, G., Liu, F., Wang, Z., 2017a. Effects of climate change on bioaccumulation and biomagnification of polycyclic aromatic hydrocarbons in the planktonic food web of a subtropical shallow eutrophic lake in China. Environmental Pollution, 223, 624–634. https://doi.org/10.1016/j.envpol.2017.01.068

Tao, Y., Yu, J., Liu, X., Xue, B., Wang, S., 2018. Factors affecting annual occurrence, bioaccumulation, and biomagnification of polycyclic aromatic hydrocarbons in plankton food webs of subtropical eutrophic lakes. Water Research, 132, 1–11. https://doi.org/10.1016/j.watres.2017.12.053

Tao, Y., Yu, J., Xue, B., Yao, S., Wang, S., 2017b. Precipitation and temperature drive seasonal variation in bioaccumulation of polycyclic aromatic hydrocarbons in the

planktonic food webs of a subtropical shallow eutrophic lake in China. Science of the Total Environment, 583, 447–457. http://dx.doi.org/10.1016/j.scitotenv.2017.01.100

Tedetti, M., Tronczynski, J., 2019. HIPPOCAMPE cruise, RV Antea. https://doi.org/10.17600/18000900

Tedetti, M., Tronczynski, J., Carlotti, F., Pagano, M., Sammari, C., Bel Hassen, M., Ben Ismail, S., Desboeufs, K., Poindron, C., Chifflet, S., Abdennadher, M., Amri, S., Bănaru, D., Ben Abdallah, L., Bhairy, N., Boudriga, I., Bourin, A., Brach-Papa, C., Briant, N., Cabrol, L., Chevalier, C., Chouba, L., Coudray, S., Daly Yahia, M.N., de Garidel-Thoron, T., Dufour, A., Dutay, J.-C., Espinasse, B., Fierro-González, P., Fornier, M., Garcia, N., Giner, F., Guigue, C., Guilloux, L., Hamza, A., Heimbürger-Boavida, L.-E., Jacquet, S., Knoery, J., Lajnef, R., Makhlouf Belkahia, N., Malengros, D., Martinot, P.L., Bosse, A., Mazur, J.-C., Meddeb, M., Misson, B., Pringault, O., Quéméneur, M., Radakovitch, O., Raimbault, P., Ravel, C., Rossi, V., Rwawi, C., Sakka Hlaili, A., Tesán Onrubia, J.A., Thomas, B., Thyssen, M., Zaaboub, N., Zouari, A., Garnier, C., 2023. Contamination of planktonic food webs in the Mediterranean Sea: Setting the frame for the MERITE-HIPPOCAMPE oceanographic cruise (spring 2019). Marine Pollution Bulletin, 189, 114765. https://doi.org/10.1016/j.marpolbul.2023.114765

Tesán-Onrubia, J.A., Tedetti, M., Carlotti, F., Tenaille, M., Guilloux, L., Pagano, M., Lebreton, B., Guillou, G., Fierro-González, P., Guigue, C., Chifflet, S., Garcia, T., Boudriga, I., Belhassen, M., Bellaaj-Zouari, M., Bănaru, D., 2023. Spatial variations of biochemical content and stable isotope ratios of size-fractionated plankton in the Mediterranean Sea (MERITE-HIPPOCAMPE campaign). Marine Pollution Bulletin, 189, 114787. https://doi.org/10.1016/j.marpolbul.2023.114787

Tiano, M., Tronczyński, J., Harmelin-Vivien, M., Tixier, C., Carlotti, F., 2014. PCB concentrations in plankton size classes, a temporal study in Marseille Bay, Western

Mediterranean Sea. Marine Pollution Bulletin, 89, 331–339. https://doi.org/10.1016/j.marpolbul.2014.09.040

Tolosa, I., J. de Mora, S., Fowler, S.W., Villeneuve, J.-P., Bartocci, J., Cattini, C., 2005. Aliphatic and aromatic hydrocarbons in marine biota and coastal sediments from the Gulf and the Gulf of Oman, Marine Pollution Bulletin, 50, 1619-1633. https://doi.org/10.1016/j.marpolbul.2005.06.029

Tolosa, I., Vescovalib, I., LeBlond, N., Marty, J.C., de Moraa, S., Prieur, L., 2004. Distribution of pigments and fatty acid biomarkers in particulate matter from the frontal structure of the Alboran Sea (SW Mediterranean Sea). Marine Chemistry, 88, 103– 125. https://doi.org/10.1016/j.marchem.2004.03.005

Tong, Y., Chen, L., Liu, Y., Wang, Y., Tian, S., 2019. Distribution, sources an ecological risk assessment of PAHs in surface seawater from coastal Bohai Bay, China. Marine Pollution Bulletin, 142, 520–524. https://doi.org/10.1016/j.marpolbul.2019.04.004

US-EPA, 2012. US Environmental Protection Agency. Appendix A to 40 CFR, Part 423–126, Priority Pollutants.

Volkman, J.K., Holdsworth, D.G., Neill, G.P., Bavor, H.J., 1992. Identification of natural, anthropogenic and petroleum hydrocarbons in aquatic sediments. Science of The Total Environment, 112, 203–219. https://doi.org/10.1016/0048-9697(92)90188-X

Wang, Z., Fingas, M., 1995. Differentiation of the source of spilled oil and monitoring of the oil weathering process using gas chromatography–mass spectrometry. Journal of Chromatography A, 712, 321–43. https://doi.org/10.1016/0021-9673(95)00546-Y

Wang, Z., Fingas, M., Landriault, M., Sigouin, L., Feng, Y., Mullin, J., 1997. Using systematic and comparative analytical data to identify the source of an unknown oil on contaminated birds. Journal of Chromatography A, 775, 251–265.

Wang, Z., Fingas, M., Page, D.S., 1999. Oil spill identification. Journal of Chromatography A, 843, 369–411. http://dx.doi.org/10.1016/S0021-9673(99)00120-X

Welschmeyer, N.A., 1994. Fluorometric analysis of chlorophyll a in the presence of chlorophyll b and pheopigments. Limnology and Oceanography, 39, 1985–1992. https://doi.org/10.4319/LO.1994.39.8.1985

Yunker, M.B., Macdonald, R.W., Vingarzan, R., Mitchell, R.H., Goyette, D., Sylvestre, S., 2002. PAHs in the Fraser River basin: A critical appraisal of PAH ratios as indicators of PAH source and composition. Organic Geochemistry, 33, 489–515. https://doi.org/10.1016/S0146-6380(02)00002-5

Zaghden, H., Tedetti, M., Sayadi, S., Serbaji, M.M., Elleuch, B., Saliot, A., 2017. Origin and distribution of hydrocarbons and organic matter in the surficial sediments of the Sfax-Kerkennah channel (Tunisia, Southern Mediterranean Sea). Marine Pollution Bulletin, 117, 414–428. https://doi.org/10.1016/j.marpolbul.2017.02.007

## Figure caption

**Figure 1. a)** Location of the ten stations (black circles) investigated during the MERITE-HIPPOCAMPE cruise (13 April-14 May 2019) along a North-South transect in the Mediterranean Sea on board the R/V *Antea*, and **b)** cruise track with the position of the stations. St2, St4, St3, St10 and St11 were sampled during leg 1 (13-28 April; from La Seyne-sur-Mer to Tunis), whereas St15, St17, St19, St9 and St1 were sampled during leg 2 (30 April-14 May; from Tunis to Gulf of Gabès, and then return to La Seyne-sur-Mer). See the detailed description of stations in Tedetti et al. (2023).

**Figure 2. a)** Concentrations of total chlorophyll *a* (TChl*a*, in µg $L^{-1}$), suspended particulate matter (SPM, in mg $L^{-1}$) and particulate organic carbon (POC, in mg $L^{-1}$) in the size fraction 0.7-60 µm, **b)** total biomass (in µg dw $L^{-1}$) (see Fierro-González et al., 2023, this cumulates phytoplankton, zooplankton and detritus biomasses), and **c)** concentration of POC (in mg $g^{-1}$ dw) in the planktonic size fractions 60-200, 200-500 and 500-1000 µm, sampled at the deep chlorophyll maximum (DCM). All measurements are presented for the 10 stations. For POC, sample St17 500-1000 µm is not available.

**Figure 3.** Concentrations of total lipid biomarkers (in mg $g^{-1}$ dw) in the planktonic size fractions 60-200, 200-500 and 500-1000 µm recovered from the deep chlorophyll maximum (DCM) at the 10 stations: **a)** $\Sigma_{39}$lipids (= $\Sigma_{25}$fatty acids + $\Sigma_{8}$fatty alcohols + $\Sigma_{6}$sterols), **b)** $\Sigma_{25}$fatty acids, **c)** $\Sigma_{8}$fatty alcohols and **d)** $\Sigma_{6}$sterols. Sample St17 500-1000 µm is not available.

**Figure 4.** Concentrations of total aliphatic hydrocarbons ($\Sigma_{28}$AHs, in µg $g^{-1}$ dw) in the particulate/planktonic size fractions **a)** 0.7-60 µm and **c)** 60-200, 200-500 and 500-1000 µm, recovered from the deep chlorophyll maximum (DCM) at the 10 stations, and mean relative abundances of individual AHs (in %) for the 10 stations in the fractions **b)** 0.7-60 µm and **d)** 60-200, 200-500 and 500-1000 µm. $\Sigma_{28}$AHs = Σ *n*-$C_{15}$–*n*-$C_{40}$, Pr, Phy (28 compounds).

**Figure 5.** Concentrations of total polycyclic aromatic hydrocarbons ($\Sigma_{27}$PAHs, in ng $g^{-1}$ dw) in the particulate/planktonic size fractions **a)** 0.7-60 µm and **c)** 60-200, 200-500 and 500-1000 µm, recovered from the deep chlorophyll maximum (DCM) at the 10 stations, and mean relative abundances of individual PAHs (in %) for the 10 stations in the fractions **b)** 0.7-60 µm and **d)** 60-200, 200-500 and 500-1000 µm. $\Sigma_{27}$PAHs = Σ Nap–BP (27 compounds).

**Figure 6.** Concentrations (in ng $g^{-1}$ dw) of **a)** $\Sigma_7$PAHs (= Nap + Flu + Phe + Flt + Pyr + BaA + Chr), **b)** $\Sigma_6$PAHs (= Nap + Flu + Flt + Pyr + BaA + Chr), and **c)** Phe, for all 10 stations in the particulate/planktonic size fractions 0.7-60, 60-200, 200-500 and 500-1000 µm recovered from the deep chlorophyll maximum (DCM). Letters ***a)*** and ***b)*** indicate significant differences between the means of the distributions (t-test; $p < 0.05$).

**Figure 7.** Concentrations (in ng $g^{-1}$ dw) of **a)** $\Sigma_7$PAHs (= Nap + Flu + Phe + Flt + Pyr + BaA + Chr), **b)** $\Sigma_6$PAHs (= Nap + Flu + Flt + Pyr + BaA + Chr), and **c)** Phe, with regard to the C and N isotopic ratios ($\delta^{13}C$ and $\delta^{15}N$, in ‰) for all 10 stations in the particulate/planktonic size fractions 0.7-60, 60-200, 200-500 and 500-1000 µm recovered from the deep chlorophyll maximum (DCM).

**Figure 8.** Distribution of **a)** Log $K_{OC}$ and **b)** slope value (-m) in the particulate/planktonic size fractions 0.7-60, 60-200, 200-500 and 500-1000 µm recovered from the deep chlorophyll maximum (DCM). The letters ***a)***, ***b)*** and ***c)*** indicate significant differences between the means of the distributions (t-test; $p < 0.05$). Log $K_{OC}$ and -m were determined in each fraction, at the 10 stations, for each of the 7 PAHs (Nap, Flu, Phe, Flt, Pyr, BaA, Chr). For each size fraction, the value m is the slope of the regression (power function) between the SPM/biomass concentration (in mg $L^{-1}$ dw) and the concentration of the given PAH (in ng $g^{-1}$ dw) for the 10 stations. Examples of SPM/biomass *versus* PAH power relationships and associated -m values are presented for Phe for each size fraction. The detailed regression parameters of the power functions for the 7 PAHs, including m values, are found in Table S10.

**Table 1.** Comparison of plankton PAH concentrations and biological pump fluxes of PAHs determined here for the Western Mediterranean Sea (over our ten stations) with those reported previously in the same and other oceanic areas. We present the data for total PAHs (sum of individual compounds) and individual phenanthrene.

| | | This study[a, b] | Berrojalbiz et al. (2011)[c, d] | González-Gaya et al. (2019)[d, e] | | | | |
|---|---|---|---|---|---|---|---|---|
| | | **Western Med. Sea** | **Western and Eastern Med. Sea** | **North Atlantic** | **South Atlantic** | **North Pacific** | **South Pacific** | **Indian Ocean** |
| Plankton total PAH concentration (ng $g^{-1}$ dw) | Min | 40 | 57 | 18 | 13 | 11 | 40 | 15 |
| | Max | 163 | 1903 | 790 | 1300 | 7700 | 360 | 440 |
| | Median | 102 | *na* | 180 | 88 | 37 | 110 | 45 |
| | Mean ± SD | 96 ± 41 | *na* | 250 ± 230 | 280 ± 350 | 590 ± 2000 | 140 ± 120 | 130 ± 130 |
| Plankton Phe concentration (ng $g^{-1}$ dw) | Min | 12 | 9 | 2 | 1 | 1 | 5 | 2 |
| | Max | 39 | 235 | 120 | 120 | 1035 | 33 | 59 |
| | Median | 26 | *na* | 8 | 7 | 4 | 8 | 6 |
| | Mean ± SD | 25 ± 10 | 77 ± *na* | 30 ± 39 | 18 ± 28 | 78 ± 280 | 11 ± 11 | 13 ± 15 |
| POC vertical flux (mg C $m^{-2}$ $day^{-1}$) | Mean | 27[f] | *na* | 39[g] | 37[g] | 57[g] | 58[g] | 46[g] |
| Biological pump flux of total PAHs (ng $m^{-2}$ $day^{-1}$) | Min | 5 | *na* | *na* | *na* | *na* | *na* | *na* |
| | Max | 39 | *na* | *na* | *na* | *na* | *na* | *na* |
| | Median | 15 | *na* | *na* | *na* | *na* | *na* | *na* |
| | Mean ± SD | 15 ± 10 | *na* | 172 ± *na* | 91 ± *na* | 55 ± *na* | 14 ± *na* | 22 ± *na* |
| Biological pump flux of Phe (ng $m^{-2}$ $day^{-1}$) | Min | 1 | *na* | *na* | *na* | *na* | *na* | *na* |
| | Max | 7 | *na* | *na* | *na* | *na* | *na* | *na* |
| | Median | 4 | *na* | *na* | *na* | *na* | *na* | *na* |
| | Mean ± SD | 4 ± 2 | *na* | 23 ± *na* | 6 ± *na* | 7 ± *na* | 1 ± *na* | 2 ± *na* |

*na*: not available; Phe: phenanthrene; POC: particulate organic carbon; [a] Total PAHs = sum of 27 compounds ($\Sigma_{27}$PAHs); [b] The plankton fraction corresponds to the size fraction 60-1000 µm; [c] Total PAHs = sum of 19 compounds ($\Sigma_{19}$PAHs); [d] The plankton fraction corresponds to the size fraction > 50 µm; [e] Total PAHs = sum of 64 compounds ($\Sigma_{64}$PAHs); [f] Vertical settling flux of POC below 100-m depth for the western Mediterranean Sea estimated by Guyennon et al. (2015), where POC is defined as being fueled by the natural mortality of the largest organisms (mesozooplankton, diatoms and ciliates) and by the excretion of fecal pellets and sloppy feeding by mesozooplankton; [g] Vertical settling flux of POC from the surface mixed layer due to phytoplankton and to zooplankton-associated pellets estimated from Siegel et al. (2014)'s global climatology.

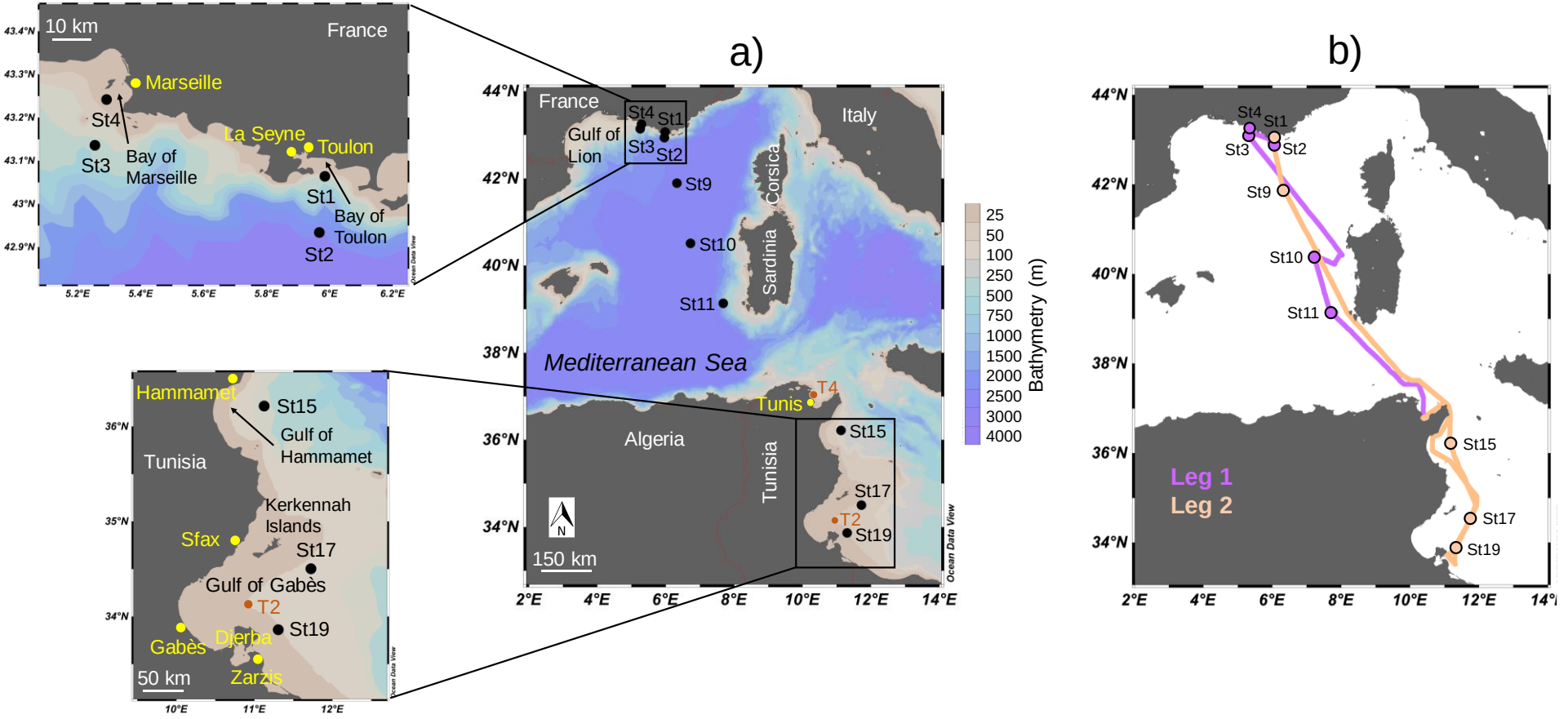
a)
b)
10 km
France
Marseille
St4
St3
Bay of Marseille
La Seyne
Toulon
St1
Bay of Toulon
St2
Hammamet
St15
Gulf of Hammamet
Tunisia
Kerkennah Islands
Sfax
St17
Gulf of Gabès
T2
St19
Gabès
Djerba
Zarzis
50 km
Italy
Gulf of Lion
St9
Corsica
St10
Sardinia
St11
Mediterranean Sea
T4
Tunis
Algeria
150 km
Bathymetry (m)
25
50
100
250
500
750
1000
1500
2000
2500
3000
4000
Leg 1
Leg 2

Figure 1

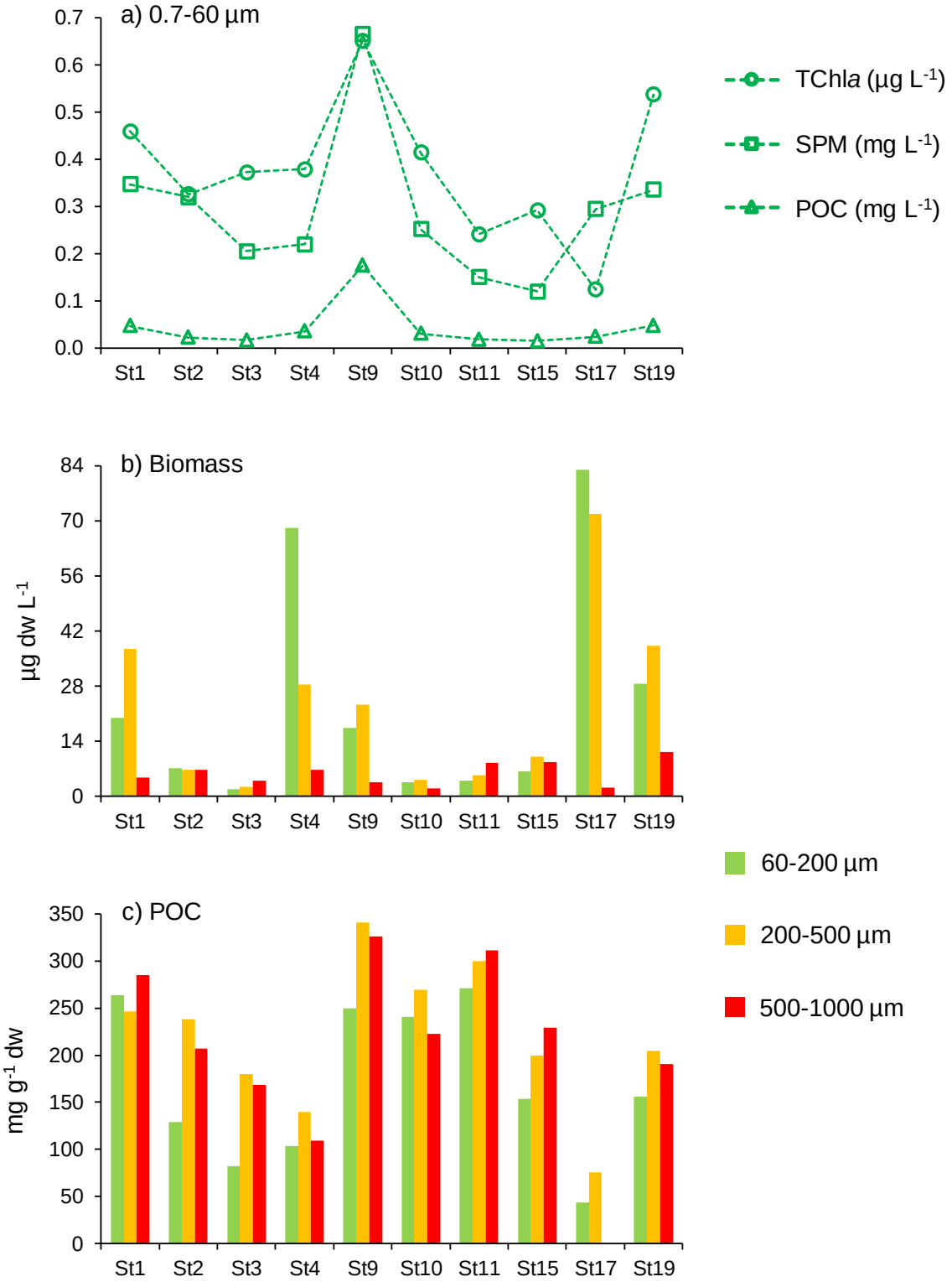
a) 0.7-60 µm
0.7
0.6
0.5
0.4
0.3
0.2
0.1
0.0
St1 St2 St3 St4 St9 St10 St11 St15 St17 St19
TChla (µg L-1)
SPM (mg L-1)
POC (mg L-1)
b) Biomass
µg dw L-1
84
70
56
42
28
14
0
St1 St2 St3 St4 St9 St10 St11 St15 St17 St19
60-200 µm
200-500 µm
500-1000 µm
c) POC
mg g-1 dw
350
300
250
200
150
100
50
0
St1 St2 St3 St4 St9 St10 St11 St15 St17 St19

Figure 2

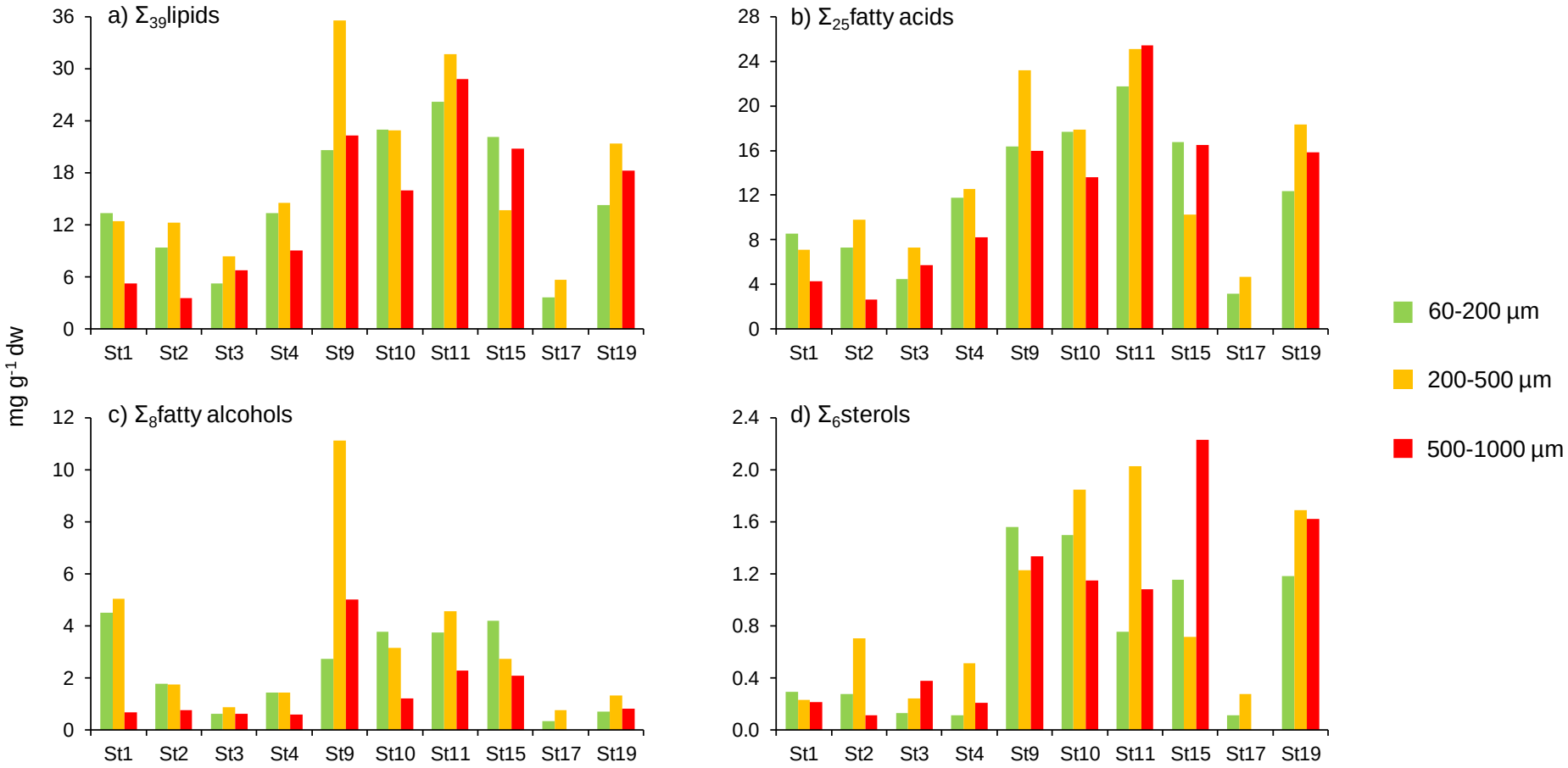
a) Σ39lipids
b) Σ25fatty acids
c) Σ8fatty alcohols
d) Σ6sterols
mg g-1 dw
St1
St2
St3
St4
St9
St10
St11
St15
St17
St19
60-200 µm
200-500 µm
500-1000 µm

Figure 3

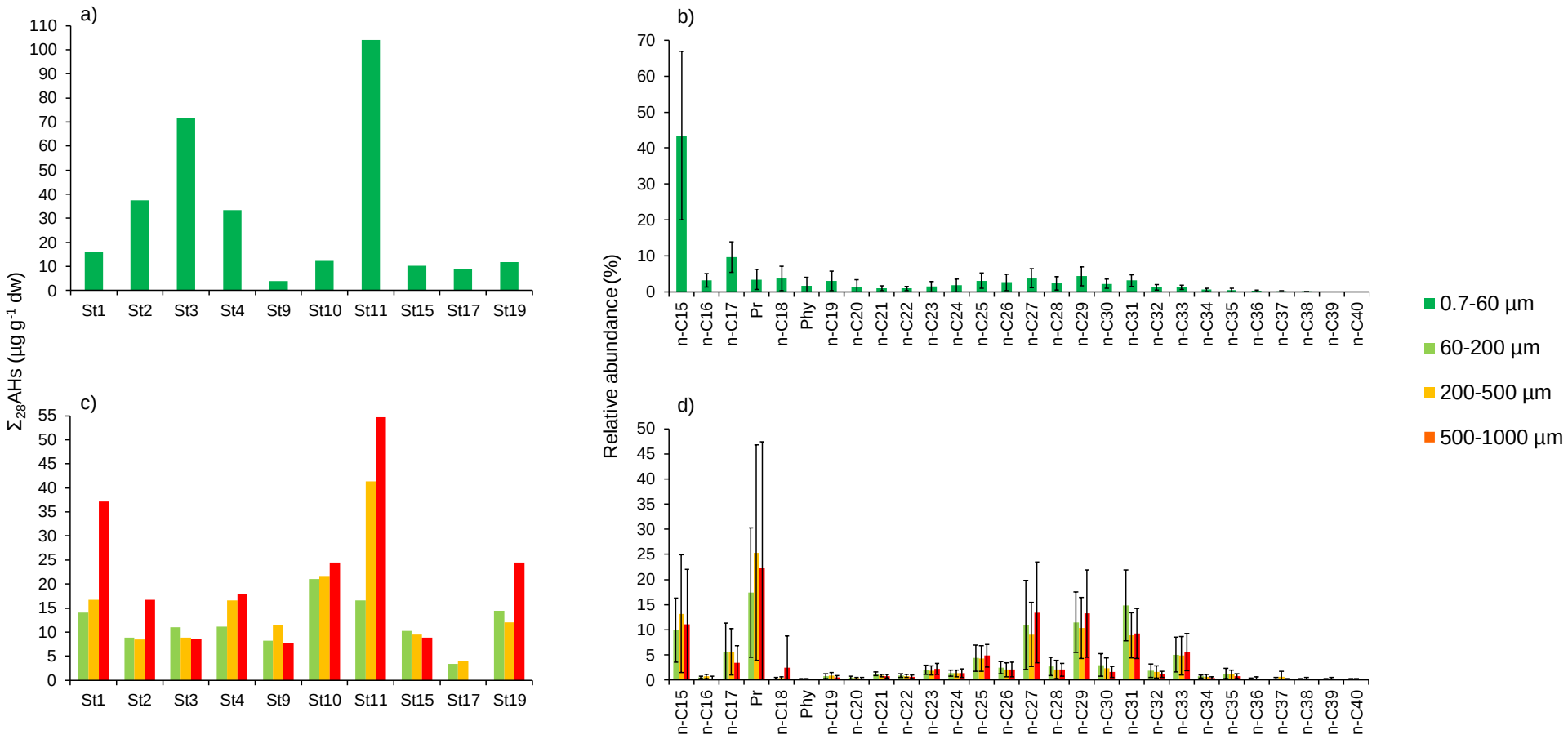
a)
b)
c)
d)
$\Sigma_{28}$AHs (µg g$^{-1}$ dw)
Relative abundance (%)
St1
St2
St3
St4
St9
St10
St11
St15
St17
St19
n-C15
n-C16
n-C17
Pr
n-C18
Phy
n-C19
n-C20
n-C21
n-C22
n-C23
n-C24
n-C25
n-C26
n-C27
n-C28
n-C29
n-C30
n-C31
n-C32
n-C33
n-C34
n-C35
n-C36
n-C37
n-C38
n-C39
n-C40
0.7-60 µm
60-200 µm
200-500 µm
500-1000 µm

Figure 4

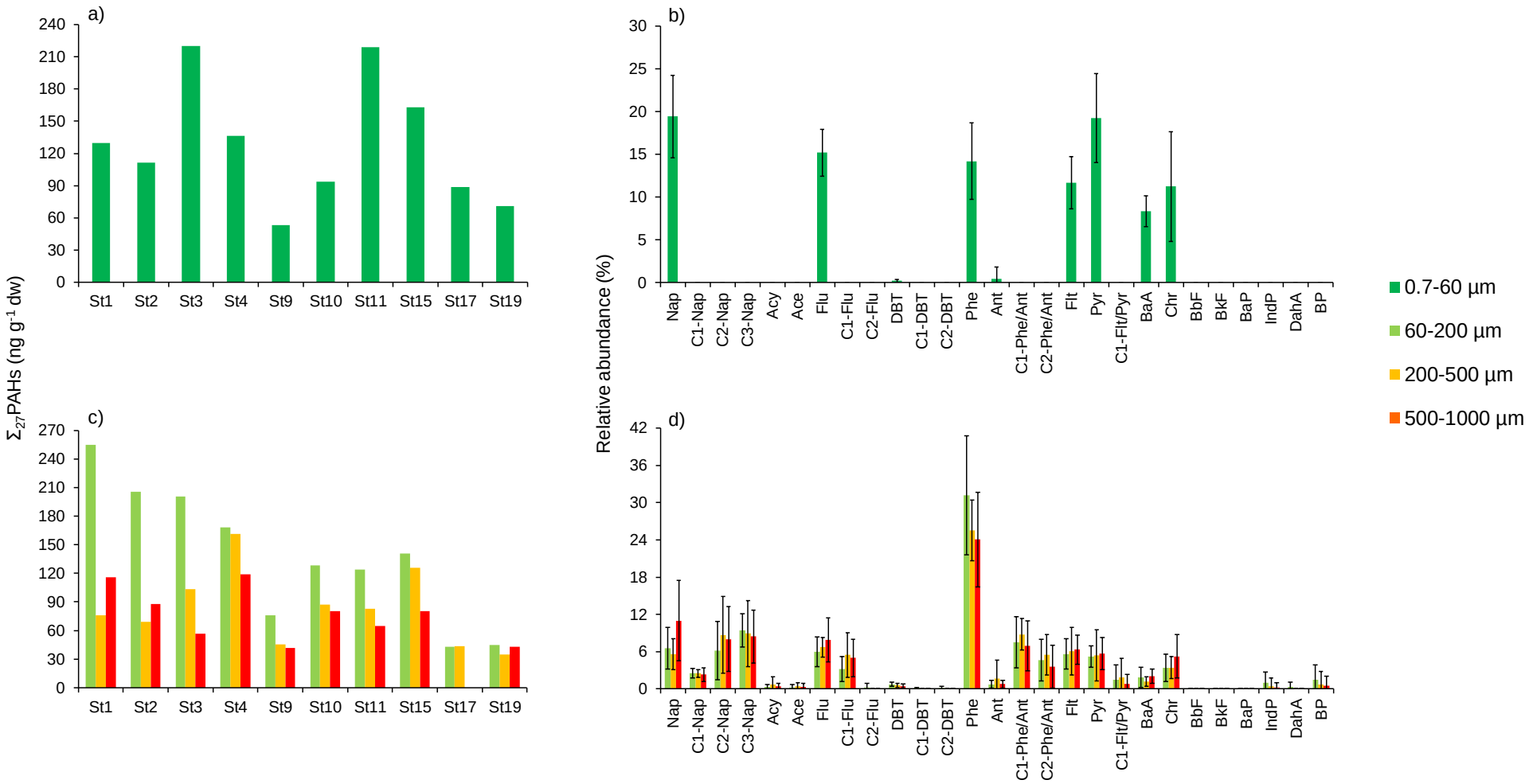
a)
b)
c)
d)
Σ27PAHs (ng g-1 dw)
Relative abundance (%)
St1
St2
St3
St4
St9
St10
St11
St15
St17
St19
Nap
C1-Nap
C2-Nap
C3-Nap
Acy
Ace
Flu
C1-Flu
C2-Flu
DBT
C1-DBT
C2-DBT
Phe
Ant
C1-Phe/Ant
C2-Phe/Ant
Flt
Pyr
C1-Flt/Pyr
BaA
Chr
BbF
BkF
BaP
IndP
DahA
BP
0.7-60 µm
60-200 µm
200-500 µm
500-1000 µm

Figure 5

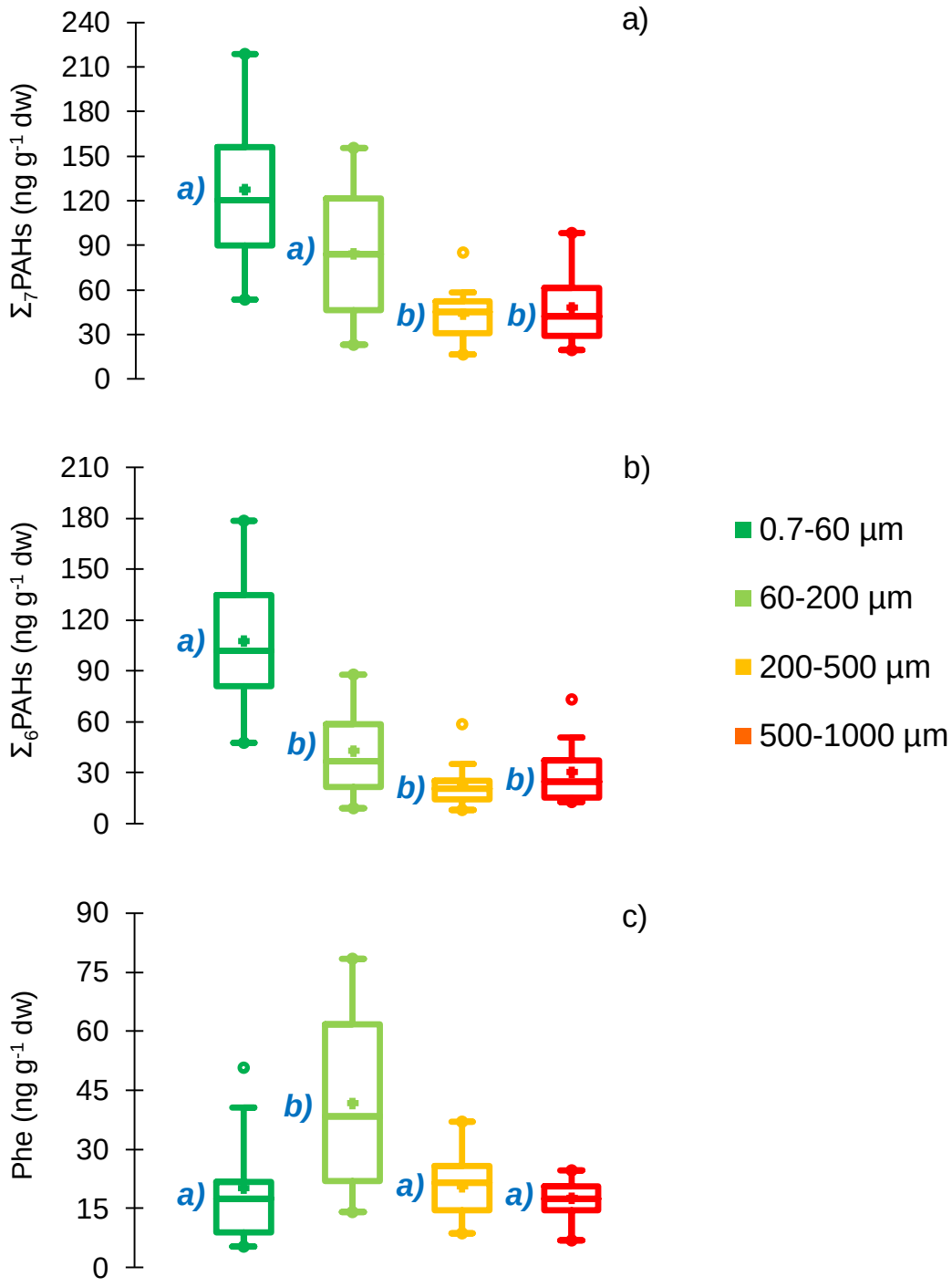
a)
240
210
180
150
120
90
60
30
0
Σ7PAHs (ng g-1 dw)
a)
a)
b)
b)
b)
210
180
150
120
90
60
30
0
Σ6PAHs (ng g-1 dw)
a)
b)
b)
b)
0.7-60 µm
60-200 µm
200-500 µm
500-1000 µm
c)
90
75
60
45
30
15
0
Phe (ng g-1 dw)
a)
b)
a)
a)

Figure 6

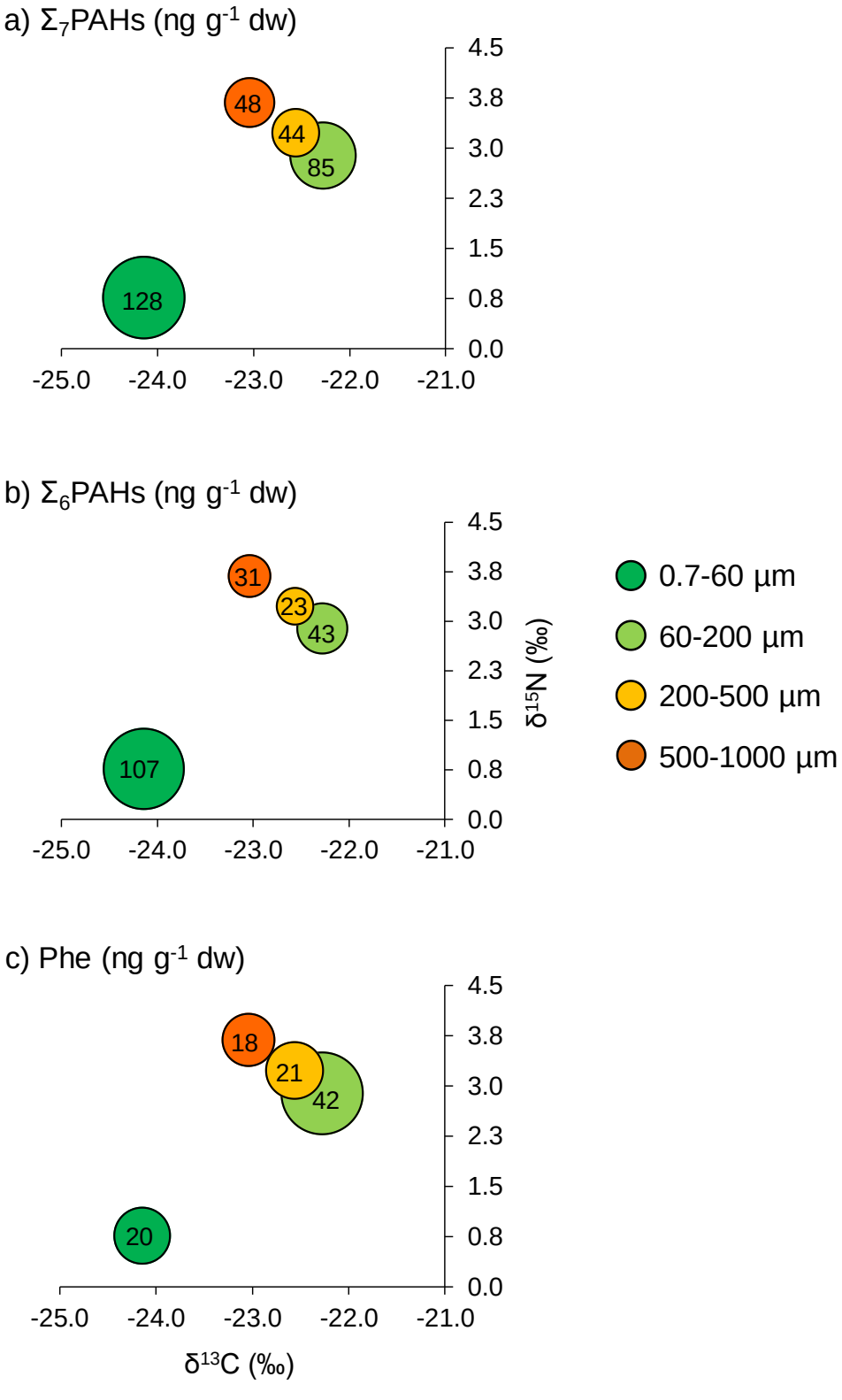
a) Σ7PAHs (ng g-1 dw)
48
44
85
128
4.5
3.8
3.0
2.3
1.5
0.8
0.0
-25.0
-24.0
-23.0
-22.0
-21.0
b) Σ6PAHs (ng g-1 dw)
31
23
43
107
δ15N (‰)
0.7-60 µm
60-200 µm
200-500 µm
500-1000 µm
c) Phe (ng g-1 dw)
18
21
42
20
δ13C (‰)

Figure 7

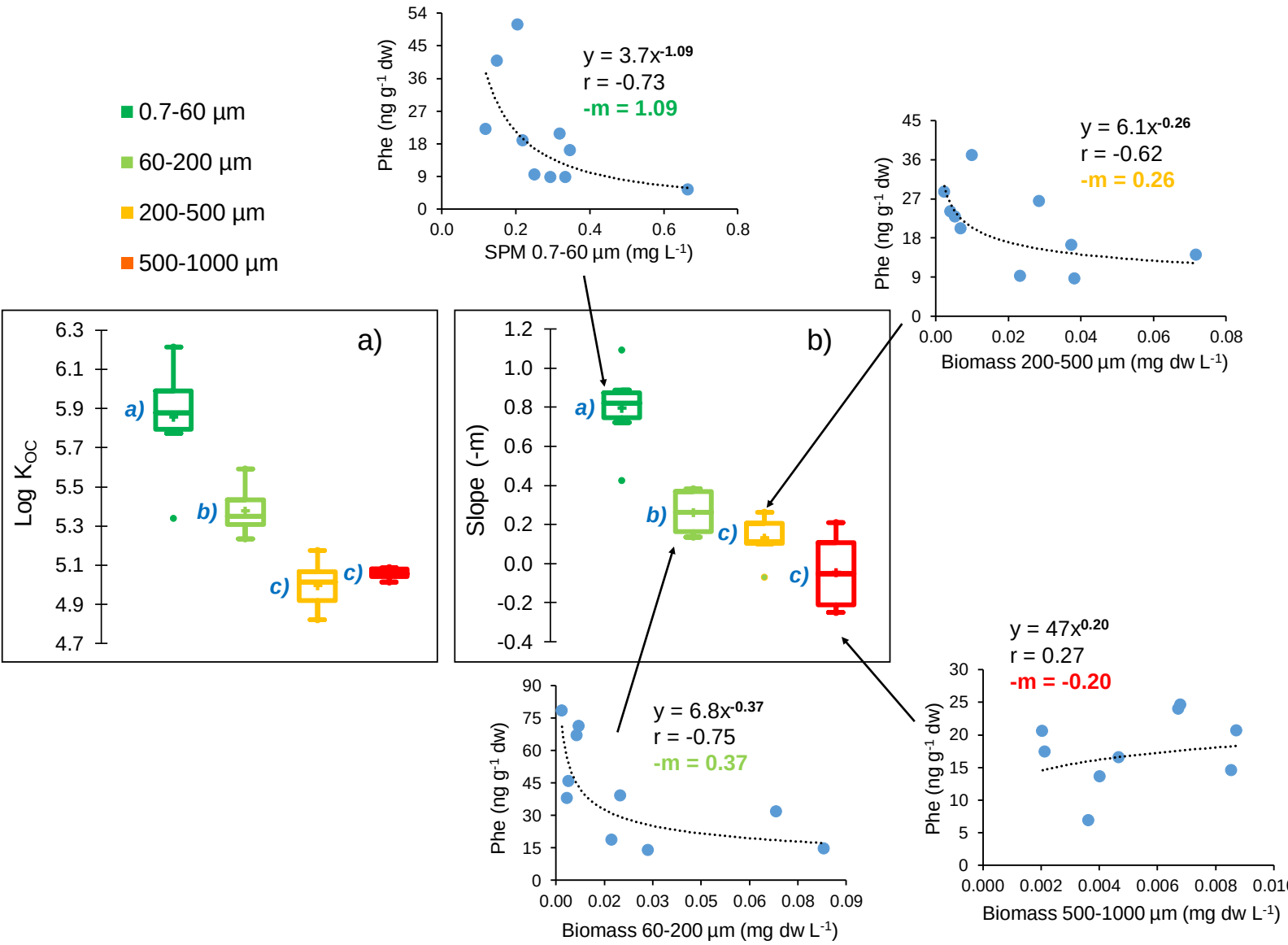
0.7-60 µm
60-200 µm
200-500 µm
500-1000 µm
Phe (ng g-1 dw)
y = 3.7x-1.09
r = -0.73
-m = 1.09
SPM 0.7-60 µm (mg L-1)
Phe (ng g-1 dw)
y = 6.1x-0.26
r = -0.62
-m = 0.26
Biomass 200-500 µm (mg dw L-1)
a)
Log KOC
b)
Slope (-m)
Phe (ng g-1 dw)
y = 6.8x-0.37
r = -0.75
-m = 0.37
Biomass 60-200 µm (mg dw L-1)
Phe (ng g-1 dw)
y = 47x0.20
r = 0.27
-m = -0.20
Biomass 500-1000 µm (mg dw L-1)

Figure 8

# Hydrocarbons in size-fractionated plankton of the Mediterranean Sea (MERITE-HIPPOCAMPE campaign)

Catherine Guigue[a]*, Javier Angel Tesán-Onrubia[a], Léa Guyomarc'h[a], Daniela Bănaru[a], François Carlotti[a], Marc Pagano[a], Sandrine Chifflet[a], Deny Malengros[a], Lassaad Chouba[b], Jacek Tronczynski[c], Marc Tedetti[a]

[a] Aix Marseille Univ., Université de Toulon, CNRS, IRD, MIO, Marseille, France

[b] Institut National des Sciences et Technologies de la Mer (INSTM), 28, rue 2 mars 1934, Salammbô 2025, Tunisia

[c] Ifremer, CCEM Contamination Chimique des Ecosystèmes Marins, F-44311 Nantes, France

*Corresponding author; E-mail: catherine.guigue@mio.osupytheas.fr

## Supplementary Material

The supplementary material contains 26 pages, and includes 11 tables and 6 figures.

**Table S1.** Biogeochemical parameters measured in the different particulate/planktonic size fractions (0.7-60, 60-200, 200-500 and 500-1000 µm) recovered from the deep chlorophyll maximum (DCM) at the 10 stations.

| | | | **St1** | **St2** | **St3** | **St4** | **St9** | **St10** | **St11** | **St15** | **St17** | **St19** |
|---|---|---|---|---|---|---|---|---|---|---|---|---|
| Sampling depth range in the DCM (m) | | | 20-24 | 25-53 | 53-58 | 13-35 | 20 | 40-60 | 30-58 | 60-68 | 37-46 | 30-46 |
| Parameter | Unit | Size fraction (µm) | | | | | | | | | | |
| **TChl*a*** | µg $L^{-1}$ | 0.7-60 | 0.46 | 0.33 | 0.37 | 0.38 | 0.65 | 0.41 | 0.24 | 0.29 | 0.12 | 0.54 |
| **SPM** | mg $L^{-1}$ | 0.7-60 | 0.35 | 0.32 | 0.21 | 0.22 | 0.67 | 0.25 | 0.15 | 0.12 | 0.29 | 0.34 |
| **Biomass** | µg dw $L^{-1}$ | 60-200 | 20.0 | 7.1 | 1.9 | 68.3 | 17.3 | 3.5 | 3.9 | 6.4 | 83.1 | 28.5 |
| | | 200-500 | 37.4 | 6.8 | 2.3 | 28.5 | 23.3 | 4.1 | 5.4 | 10.0 | 71.8 | 38.2 |
| | | 500-1000 | 4.7 | 6.7 | 4.0 | 6.8 | 3.6 | 2.0 | 8.6 | 8.7 | 2.1 | 11.2 |
| | | Tot 60-1000 | 62.1 | 20.6 | 8.2 | 103.5 | 44.2 | 9.6 | 17.9 | 25.2 | 157.0 | 77.9 |
| **POC** | mg $L^{-1}$ | 0.7-60 | 0.047 | 0.022 | 0.016 | 0.035 | 0.175 | 0.030 | 0.018 | 0.014 | 0.024 | 0.048 |
| | mg $g^{-1}$ dw | 0.7-60 | 134.5 | 67.3 | 78.3 | 159.5 | 261.8 | 118.6 | 121.7 | 120.6 | 80.9 | 141.9 |
| | | 60-200 | 263.4 | 129.4 | 81.9 | 103.5 | 249.8 | 240.3 | 271.5 | 153.7 | 43.5 | 156.0 |
| | | 200-500 | 246.4 | 238.0 | 179.6 | 139.4 | 341.0 | 269.8 | 299.9 | 199.6 | 75.9 | 204.7 |
| | | 500-1000 | 284.9 | 207.1 | 168.5 | 109.7 | 326.2 | 222.8 | 311.4 | 228.9 | *na* | 190.5 |
| | % | 0.7-60 | 13.5 | 6.7 | 7.8 | 15.9 | 26.2 | 11.9 | 12.2 | 12.1 | 8.1 | 14.2 |
| | | 60-200 | 26.3 | 12.9 | 8.2 | 10.4 | 25.0 | 24.0 | 27.1 | 15.4 | 4.4 | 15.6 |
| | | 200-500 | 24.6 | 23.8 | 18.0 | 13.9 | 34.1 | 27.0 | 30.0 | 20.0 | 7.6 | 20.5 |
| | | 500-1000 | 28.5 | 20.7 | 16.9 | 11.0 | 32.6 | 22.3 | 31.1 | 22.9 | *na* | 19.1 |
| **$\delta^{13}C$** | ‰ | 0.7-60 | -24.5 | -24.8 | -23.6 | -23.2 | -24.2 | -24.6 | -24.1 | -25.1 | -23.7 | -23.6 |
| | | 60-200 | -22.8 | -22.7 | -21.7 | -20.5 | -22.7 | -22.8 | -22.9 | -22.8 | -21.8 | -22.3 |
| | | 200-500 | -23.9 | -23.9 | -23.0 | -21.5 | -23.2 | -23.7 | -24.0 | -23.4 | -17.4 | -21.8 |
| | | 500-1000 | -23.4 | -23.8 | -22.7 | -22.2 | -22.9 | -23.3 | -23.4 | -22.7 | *na* | -23.1 |
| **$\delta^{15}N$** | | 0.7-60 | 1.8 | 0.9 | 0.1 | 2.1 | -1.3 | 0.4 | 0.9 | 1.6 | 0.8 | 0.3 |
| | | 60-200 | 3.2 | 3.1 | 2.9 | 3.6 | 2.0 | 3.6 | 3.5 | 3.6 | 1.9 | 1.5 |
| | | 200-500 | 3.7 | 3.3 | 3.4 | 3.6 | 2.7 | 3.9 | 3.8 | 3.9 | 2.4 | 1.6 |
| | | 500-1000 | 4.4 | 3.5 | 3.4 | 3.5 | 3.9 | 4.5 | 4.2 | 3.3 | *na* | 2.5 |

*na*: not available; TChl*a*: total chlorophyll *a*; SPM: suspended particulate matter; Biomass: total biomass including the biomasses of zooplankton, phytoplankton and detritus (see Fierro-González et al., 2023); POC: particulate organic carbon; $\delta^{13}C$ and $\delta^{15}N$: C and N stable isotopic ratios.

**Table S2.** Concentrations (in mg $g^{-1}$ dw) of individual and total lipid biomarkers (fatty acids, fatty alcohols and sterols) in the planktonic size fractions 60-200, 200-500 and 500-1000 µm recovered from the DCM at the 10 stations.

| | **St1** | | | **St2** | | | **St3** | | | **St4** | | | **St9** | | |
|---|---|---|---|---|---|---|---|---|---|---|---|---|---|---|---|
| Size fraction (µm) | 60-200 | 200-500 | 500-1000 | 60-200 | 200-500 | 500-1000 | 60-200 | 200-500 | 500-1000 | 60-200 | 200-500 | 500-1000 | 60-200 | 200-500 | 500-1000 |
| **$\Sigma_{39}$lipids (mg $g^{-1}$ dw)** | 13.4 | 12.4 | 5.21 | 9.36 | 12.3 | 3.53 | 5.22 | 8.37 | 6.72 | 13.3 | 14.5 | 9.01 | 20.7 | 35.6 | 22.3 |
| **$\Sigma_{25}$fatty acids (mg $g^{-1}$ dw)** | 8.58 | 7.13 | 4.30 | 7.32 | 9.80 | 2.65 | 4.46 | 7.27 | 5.74 | 11.8 | 12.6 | 8.21 | 16.4 | 23.2 | 16.0 |
| 14:0 | 1.61 | 1.12 | 0.76 | 1.07 | 1.08 | 0.51 | 0.58 | 0.86 | 0.81 | 4.28 | 3.73 | 2.24 | 1.99 | 1.86 | 1.58 |
| i15:0 | 0.07 | 0.05 | 0.03 | 0.05 | 0.06 | 0.02 | 0.05 | 0.06 | 0.06 | 0.05 | 0.07 | 0.04 | 0.10 | 0.14 | 0.12 |
| a15:0 | 0.04 | 0.03 | 0.02 | 0.03 | 0.04 | 0.01 | 0.02 | 0.03 | 0.03 | 0.03 | 0.04 | 0.03 | 0.06 | 0.07 | 0.05 |
| 15:0 | 0.16 | 0.14 | 0.12 | 0.15 | 0.21 | 0.07 | 0.11 | 0.17 | 0.16 | 0.18 | 0.21 | 0.15 | 0.26 | 0.31 | 0.35 |
| 16:0 | 4.53 | 3.60 | 2.23 | 3.95 | 4.92 | 1.31 | 2.15 | 3.83 | 3.03 | 3.50 | 4.46 | 2.90 | 8.21 | 10.2 | 8.18 |
| 16:1ω7 | 0.32 | 0.30 | 0.16 | 0.25 | 0.55 | 0.15 | 0.13 | 0.23 | 0.18 | 1.77 | 1.54 | 1.06 | 0.48 | 0.53 | 0.37 |
| 16:1ω11 | 0.08 | 0.07 | 0.03 | 0.05 | 0.05 | 0.02 | 0.02 | 0.03 | 0.02 | 0.09 | 0.09 | 0.06 | 0.17 | 0.14 | 0.08 |
| br17:0 | *nd* | *nd* | *nd* | *nd* | *nd* | *nd* | *nd* | *nd* | *nd* | *nd* | *nd* | *nd* | *nd* | *nd* | *nd* |
| i17:0 | *nd* | *nd* | 0.01 | *nd* | 0.02 | *nd* | 0.02 | 0.02 | 0.02 | 0.02 | 0.02 | 0.02 | 0.03 | 0.04 | 0.03 |
| a17:0 | *nd* | *nd* | *nd* | *nd* | 0.03 | *nd* | 0.02 | 0.02 | 0.02 | 0.02 | 0.02 | 0.01 | *nd* | 0.06 | *nd* |
| 17:0 | 0.02 | 0.14 | 0.08 | 0.14 | 0.22 | 0.05 | 0.07 | 0.17 | 0.13 | 0.08 | 0.13 | 0.07 | 0.41 | 0.51 | 0.46 |
| 18:0 | 0.51 | 0.44 | 0.24 | 0.59 | 0.88 | 0.16 | 0.45 | 0.80 | 0.60 | 0.58 | 0.79 | 0.54 | 1.28 | 2.12 | 1.43 |
| 18:1ω9 | 0.90 | 0.95 | 0.41 | 0.75 | 1.19 | 0.23 | 0.59 | 0.64 | 0.35 | 0.54 | 0.71 | 0.42 | 1.67 | 5.31 | 2.04 |
| 18:1ω7 | 0.15 | 0.16 | 0.11 | 0.13 | 0.24 | 0.08 | 0.09 | 0.15 | 0.11 | 0.29 | 0.32 | 0.26 | 0.37 | 0.45 | 0.34 |
| 18:2 | 0.05 | 0.07 | 0.06 | 0.04 | 0.11 | 0.01 | 0.04 | 0.05 | 0.04 | 0.07 | 0.08 | 0.06 | 0.20 | 0.17 | 0.12 |
| 18:4 | *nd* | *nd* | 0.01 | *nd* | *nd* | *nd* | 0.00 | 0.00 | *nd* | 0.01 | *nd* | *nd* | 0.14 | 0.13 | 0.07 |
| 20:0 | *nd* | *nd* | *nd* | 0.01 | 0.04 | *nd* | 0.03 | 0.03 | 0.03 | 0.03 | 0.05 | 0.03 | 0.08 | 0.14 | 0.04 |
| 20:1 | *nd* | *nd* | *nd* | 0.02 | 0.04 | *nd* | 0.03 | 0.04 | 0.04 | 0.04 | 0.07 | 0.03 | 0.07 | 0.12 | 0.10 |
| 20:5 | *nd* | *nd* | *nd* | *nd* | *nd* | *nd* | 0.01 | 0.02 | 0.02 | 0.08 | 0.06 | 0.07 | 0.11 | 0.12 | 0.09 |
| 22:0 | *nd* | *nd* | *nd* | *nd* | *nd* | *nd* | *nd* | 0.01 | 0.01 | 0.03 | 0.05 | 0.02 | 0.05 | 0.07 | 0.03 |
| 22:1 | *nd* | *nd* | *nd* | *nd* | *nd* | *nd* | *nd* | 0.00 | *nd* | *nd* | *nd* | *nd* | *nd* | *nd* | 0.01 |
| 22:6 | *nd* | *nd* | *nd* | *nd* | *nd* | *nd* | 0.01 | 0.02 | 0.02 | 0.02 | 0.02 | 0.04 | 0.19 | 0.22 | 0.13 |
| 24:1 | *nd* | *nd* | *nd* | *nd* | 0.07 | *nd* | *nd* | 0.01 | 0.02 | *nd* | 0.02 | 0.01 | 0.13 | 0.28 | 0.22 |
| Phytanic acid | 0.13 | 0.07 | 0.03 | 0.08 | 0.06 | 0.02 | 0.04 | 0.06 | 0.05 | 0.07 | 0.11 | 0.08 | 0.23 | 0.12 | 0.08 |

| | | | | | | | | | | | | | | | |
|---|---|---|---|---|---|---|---|---|---|---|---|---|---|---|---|
| Isomeric dihydroxy 16:0 | *nd* | 0.00 | *nd* | *nd* | 0.00 | *nd* | *nd* | 0.00 | *nd* | *nd* | *nd* | 0.05 | 0.14 | 0.10 | 0.03 |
| **$\Sigma_8$fatty alcohols (mg g$^{-1}$ dw)** | 4.52 | 5.04 | 0.69 | 1.77 | 1.75 | 0.76 | 0.62 | 0.86 | 0.61 | 1.43 | 1.44 | 0.59 | 2.73 | 11.1 | 5.01 |
| 14:0 | 0.77 | 0.13 | 0.03 | 0.27 | 0.04 | 0.03 | 0.09 | 0.04 | 0.05 | 0.22 | 0.15 | 0.04 | 0.28 | 0.15 | 0.09 |
| 16:0 | 3.48 | 4.64 | 0.54 | 1.33 | 1.56 | 0.47 | 0.37 | 0.70 | 0.41 | 0.62 | 0.77 | 0.25 | 2.17 | 10.1 | 4.28 |
| 16:1 | 0.01 | 0.00 | *nd* | *nd* | *nd* | *nd* | 0.01 | *nd* | 0.01 | 0.02 | 0.03 | 0.01 | *nd* | 0.01 | *nd* |
| 18:0 | 0.21 | 0.19 | 0.04 | 0.10 | 0.08 | 0.03 | 0.05 | 0.06 | 0.03 | 0.11 | 0.12 | 0.07 | 0.16 | 0.63 | 0.28 |
| 18:1 | 0.01 | 0.08 | 0.02 | 0.05 | 0.05 | 0.04 | 0.03 | 0.03 | 0.03 | 0.04 | 0.05 | 0.03 | 0.08 | 0.24 | 0.13 |
| 20:1 | *nd* | *nd* | 0.02 | *nd* | *nd* | 0.09 | 0.03 | 0.00 | 0.03 | *nd* | *nd* | *nd* | *nd* | *nd* | 0.08 |
| 22:1 | *nd* | *nd* | 0.02 | *nd* | *nd* | 0.09 | 0.03 | 0.02 | 0.03 | *nd* | 0.04 | 0.01 | nd | 0.06 | 0.14 |
| Phytol | 0.03 | 0.01 | 0.01 | 0.02 | 0.01 | 0.01 | 0.02 | 0.01 | 0.02 | 0.41 | 0.28 | 0.18 | 0.04 | *nd* | *nd* |
| | | | | | | | | | | | | | | | |
| **$\Sigma_6$sterols (mg g$^{-1}$ dw)** | 0.30 | 0.23 | 0.22 | 0.28 | 0.71 | 0.11 | 0.13 | 0.24 | 0.38 | 0.12 | 0.52 | 0.21 | 1.56 | 1.23 | 1.34 |
| 24-Norcholesta-5,22E-dien-3β-ol | 0.01 | *nd* | *nd* | 0.02 | 0.03 | *nd* | 0.01 | 0.01 | 0.02 | *nd* | 0.02 | 0.01 | 0.06 | 0.05 | 0.03 |
| 5α-Cholestan-3β-ol | 0.03 | 0.01 | 0.01 | 0.02 | 0.04 | 0.01 | 0.02 | 0.02 | 0.04 | 0.01 | 0.04 | 0.01 | 0.12 | 0.08 | 0.06 |
| Cholesta-5,22E-dien-3β-ol | 0.05 | 0.04 | 0.02 | 0.04 | 0.10 | 0.02 | 0.02 | 0.03 | 0.06 | 0.04 | 0.12 | 0.05 | 0.17 | 0.13 | 0.12 |
| Cholest-5-en-3β-ol | 0.18 | 0.16 | 0.16 | 0.17 | 0.45 | 0.08 | 0.07 | 0.15 | 0.21 | 0.06 | 0.29 | 0.13 | 0.99 | 0.82 | 1.01 |
| Cholesta-5,24-dien-3β-ol | 0.02 | 0.01 | 0.01 | 0.01 | 0.03 | *nd* | *nd* | 0.01 | 0.01 | *nd* | 0.02 | 0.01 | 0.17 | 0.12 | 0.09 |
| 24-Methylcholesta-5,22E-dien-3β-ol | 0.01 | 0.01 | 0.01 | 0.01 | 0.05 | 0.01 | 0.01 | 0.02 | 0.04 | *nd* | 0.03 | 0.01 | 0.06 | 0.03 | 0.03 |
| | | | | | | | | | | | | | | | |
| | **St10** | | | **St11** | | | **St15** | | | **St17** | | | **St19** | | |
| Size fraction (µm) | 60-200 | 200-500 | 500-1000 | 60-200 | 200-500 | 500-1000 | 60-200 | 200-500 | 500-1000 | 60-200 | 200-500 | 500-1000 | 60-200 | 200-500 | 500-1000 |
| | | | | | | | | | | | | | | | |
| **$\Sigma_{39}$lipids (mg g$^{-1}$ dw)** | 23.0 | 22.9 | 16.0 | 26.2 | 31.7 | 28.8 | 22.1 | 13.7 | 20.8 | 3.60 | 5.69 | *na* | 14.3 | 21.4 | 18.3 |
| | | | | | | | | | | | | | | | |
| **$\Sigma_{25}$fatty acids (mg g$^{-1}$ dw)** | 17.7 | 17.9 | 13.6 | 21.7 | 25.1 | 25.5 | 16.7 | 10.3 | 16.5 | 3.14 | 4.66 | *na* | 12.4 | 18.3 | 15.8 |
| 14:0 | 2.08 | 2.14 | 1.44 | 2.76 | 3.13 | 2.01 | 2.38 | 1.38 | 1.73 | 0.74 | 1.13 | *na* | 1.38 | 2.80 | 2.01 |
| i15:0 | 0.16 | 0.17 | 0.12 | 0.20 | 0.20 | 0.16 | 0.14 | 0.08 | 0.10 | 0.02 | 0.04 | *na* | 0.16 | 0.20 | 0.16 |
| a15:0 | 0.08 | 0.09 | 0.08 | 0.10 | 0.10 | 0.08 | 0.09 | 0.03 | 0.05 | 0.02 | 0.02 | *na* | 0.04 | 0.09 | 0.05 |
| 15:0 | 0.31 | 0.36 | 0.32 | 0.42 | 0.42 | 0.45 | 0.37 | 0.21 | 0.32 | 0.07 | 0.11 | *na* | 0.26 | 0.43 | 0.41 |
| 16:0 | 7.32 | 8.07 | 6.35 | 9.28 | 10.1 | 9.51 | 7.05 | 4.35 | 7.61 | 1.18 | 1.80 | *na* | 6.58 | 9.26 | 8.20 |
| 16:1ω7 | 0.59 | 0.59 | 0.59 | 0.77 | 0.77 | 0.88 | 1.19 | 0.61 | 1.09 | 0.47 | 0.55 | *na* | 0.47 | 0.60 | 0.57 |
| 16:1ω11 | 0.08 | 0.09 | 0.08 | 0.14 | 0.13 | 0.11 | 0.10 | 0.05 | 0.07 | 0.03 | 0.03 | *na* | 0.06 | 0.12 | 0.11 |
| br17:0 | 0.02 | 0.04 | 0.02 | 0.04 | 0.04 | 0.05 | 0.03 | 0.03 | 0.04 | 0.00 | *nd* | *na* | *nd* | *nd* | *nd* |
| i17:0 | 0.04 | 0.06 | 0.05 | 0.06 | 0.08 | 0.09 | 0.05 | 0.04 | 0.09 | 0.02 | 0.02 | *na* | 0.06 | 0.07 | 0.06 |
| a17:0 | 0.07 | 0.07 | 0.06 | 0.06 | 0.07 | 0.05 | 0.05 | 0.04 | 0.05 | 0.01 | 0.01 | *na* | 0.04 | 0.05 | 0.04 |

| | | | | | | | | | | | | | | | |
|---|---|---|---|---|---|---|---|---|---|---|---|---|---|---|---|
| 17:0 | 0.38 | 0.47 | 0.31 | 0.45 | 0.48 | 0.51 | 0.32 | 0.22 | 0.37 | 0.05 | 0.08 | *na* | 0.35 | 0.06 | 0.44 |
| 18:0 | 1.37 | 1.77 | 1.18 | 1.65 | 1.91 | 1.75 | 1.07 | 0.79 | 1.25 | 0.22 | 0.35 | *na* | 1.48 | 2.61 | 1.98 |
| 18:1ω9 | 3.67 | 2.44 | 1.62 | 3.18 | 5.16 | 5.12 | 2.30 | 1.55 | 1.87 | 0.14 | 0.25 | *na* | 0.53 | 0.85 | 0.68 |
| 18:1ω7 | 0.33 | 0.40 | 0.30 | 0.42 | 0.46 | 0.47 | 0.47 | 0.30 | 0.60 | 0.07 | 0.08 | *na* | 0.25 | 0.28 | 0.27 |
| 18:2 | 0.14 | 0.13 | 0.09 | 0.36 | 0.31 | 0.51 | 0.19 | 0.08 | 0.18 | 0.03 | 0.03 | *na* | 0.11 | 0.10 | 0.10 |
| 18:4 | 0.10 | 0.10 | 0.07 | 0.16 | 0.13 | 0.13 | 0.09 | 0.05 | 0.09 | *nd* | *nd* | *na* | 0.05 | 0.06 | 0.05 |
| 20:0 | 0.11 | 0.11 | 0.07 | 0.10 | 0.12 | 0.20 | 0.08 | 0.07 | 0.10 | *nd* | 0.02 | *na* | 0.07 | 0.15 | 0.12 |
| 20:1 | 0.09 | 0.10 | 0.10 | 0.16 | 0.27 | 0.16 | 0.13 | 0.08 | 0.15 | *nd* | 0.02 | *na* | 0.06 | 0.09 | 0.05 |
| 20:5 | 0.07 | 0.10 | 0.07 | 0.29 | 0.17 | 0.73 | 0.09 | 0.05 | 0.21 | 0.01 | 0.02 | *na* | 0.03 | 0.08 | 0.05 |
| 22:0 | 0.05 | 0.04 | 0.07 | 0.08 | 0.09 | 0.12 | 0.05 | 0.03 | 0.08 | 0.02 | 0.02 | *na* | 0.05 | 0.11 | 0.06 |
| 22:1 | *nd* | *nd* | 0.08 | 0.09 | 0.13 | 0.66 | 0.11 | 0.05 | 0.09 | *nd* | *nd* | *na* | *nd* | *nd* | *nd* |
| 22:6 | 0.13 | 0.13 | 0.14 | 0.47 | 0.29 | 1.18 | 0.16 | 0.06 | 0.18 | 0.01 | 0.02 | *na* | 0.06 | 0.10 | 0.05 |
| 24:1 | 0.16 | 0.19 | 0.15 | 0.20 | 0.37 | 0.26 | 0.08 | 0.06 | 0.08 | 0.00 | *nd* | *na* | 0.07 | 0.12 | 0.11 |
| Phytanic acid | 0.12 | 0.11 | 0.08 | 0.19 | 0.15 | 0.15 | 0.11 | 0.06 | 0.10 | 0.04 | 0.04 | *na* | 0.05 | 0.07 | 0.06 |
| Isomeric dihydroxy 16:0 | 0.24 | 0.12 | 0.16 | 0.10 | 0.06 | 0.11 | 0.05 | *nd* | *nd* | *nd* | *nd* | *na* | 0.14 | 0.04 | 0.20 |
| | | | | | | | | | | | | | | | |
| **$\Sigma_8$fatty alcohols (mg g$^{-1}$ dw)** | 3.78 | 3.15 | 1.20 | 3.75 | 4.58 | 2.29 | 4.20 | 2.72 | 2.08 | 0.35 | 0.76 | *na* | 0.72 | 1.31 | 0.82 |
| 14:0 | 1.12 | 0.34 | 0.09 | 1.68 | 0.38 | 0.26 | 1.50 | 0.47 | 0.17 | 0.04 | 0.07 | *na* | 0.09 | 0.23 | 0.09 |
| 16:0 | 2.06 | 2.44 | 0.75 | 1.71 | 3.83 | 1.67 | 2.03 | 1.85 | 0.94 | 0.20 | 0.54 | *na* | 0.44 | 0.83 | 0.49 |
| 16:1 | 0.02 | 0.01 | 0.02 | 0.02 | 0.01 | 0.01 | 0.05 | 0.02 | 0.04 | 0.01 | 0.01 | *na* | 0.03 | 0.03 | 0.03 |
| 18:0 | 0.23 | 0.17 | 0.07 | 0.14 | 0.23 | 0.13 | 0.19 | 0.15 | 0.13 | 0.06 | 0.07 | *na* | 0.12 | 0.16 | 0.12 |
| 18:1 | 0.24 | 0.13 | 0.10 | 0.11 | 0.13 | 0.15 | 0.15 | 0.12 | 0.12 | 0.01 | 0.02 | *na* | 0.04 | 0.07 | 0.10 |
| 20:1 | *nd* | *nd* | 0.03 | *nd* | *nd* | *nd* | *nd* | *nd* | 0.17 | *nd* | *nd* | *na* | *nd* | *nd* | *nd* |
| 22:1 | *nd* | *nd* | 0.05 | *nd* | *nd* | 0.07 | 0.04 | *nd* | 0.39 | *nd* | *nd* | *na* | *nd* | *nd* | *nd* |
| Phytol | 0.12 | 0.06 | 0.10 | 0.09 | *nd* | *nd* | 0.23 | 0.12 | 0.12 | 0.03 | 0.03 | *na* | *nd* | *nd* | *nd* |
| | | | | | | | | | | | | | | | |
| **$\Sigma_6$sterols (mg g$^{-1}$ dw)** | 1.50 | 1.85 | 1.15 | 0.75 | 2.03 | 1.08 | 1.16 | 0.72 | 2.23 | 0.11 | 0.28 | *na* | 1.18 | 1.69 | 1.62 |
| 24-Norcholesta-5,22E-dien-3β-ol | 0.06 | 0.04 | 0.04 | 0.03 | 0.08 | 0.03 | 0.04 | 0.04 | 0.11 | 0.00 | 0.01 | *na* | 0.04 | 0.00 | 0.05 |
| 5α-Cholestan-3β-ol | 0.14 | 0.11 | 0.10 | 0.09 | 0.16 | 0.08 | 0.09 | 0.05 | 0.07 | 0.02 | 0.04 | *na* | 0.09 | 0.10 | 0.07 |
| Cholesta-5,22E-dien-3β-ol | 0.20 | 0.22 | 0.16 | 0.10 | 0.25 | 0.13 | 0.18 | 0.11 | 0.21 | 0.02 | 0.04 | *na* | 0.12 | 0.15 | 0.14 |
| Cholest-5-en-3β-ol | 0.95 | 1.31 | 0.70 | 0.42 | 1.30 | 0.70 | 0.67 | 0.42 | 1.67 | 0.06 | 0.16 | *na* | 0.75 | 1.18 | 1.20 |
| Cholesta-5,24-dien-3β-ol | 0.06 | 0.08 | 0.04 | 0.07 | 0.11 | 0.07 | 0.08 | 0.03 | 0.06 | 0.01 | 0.01 | *na* | 0.07 | 0.11 | 0.06 |
| 24-Methylcholesta-5,22E-dien-3β-ol | 0.09 | 0.09 | 0.10 | 0.03 | 0.13 | 0.07 | 0.10 | 0.07 | 0.11 | 0.01 | 0.02 | *na* | 0.12 | 0.15 | 0.10 |

*na*: not available; *nd*: not detected; $\Sigma_{39}$lipids = $\Sigma_{25}$fatty acids + $\Sigma_8$fatty alcohols + $\Sigma_6$sterols; $\Sigma_{25}$fatty acids = Σ 14:0–isomeric dihydroxy 16:0 (25 compounds); $\Sigma_8$fatty alcohols = Σ 14:0–phytol (8 compounds); $\Sigma_6$sterols = Σ 24-Norcholesta-5,22E-dien-3β-ol–24-Methylcholesta-5,22E-dien-3β-ol (6 compounds).

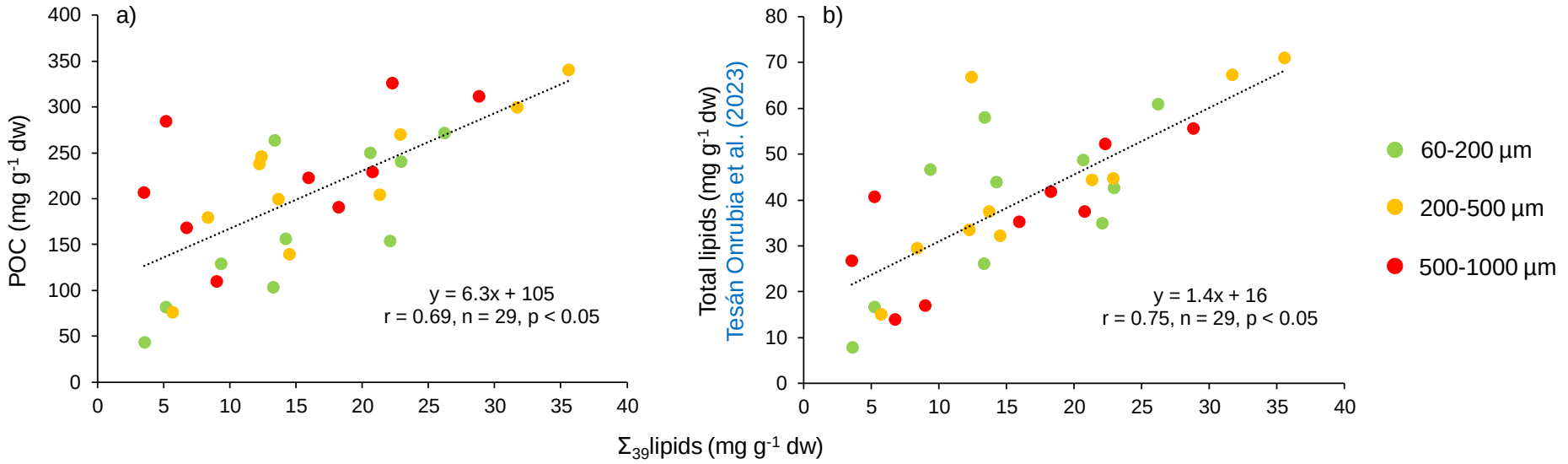


**Figure S1.** Relationships between the concentration of $\Sigma_{39}$lipids (= $\Sigma_{25}$fatty acids + $\Sigma_{8}$fatty alcohols + $\Sigma_{6}$sterols; in mg $g^{-1}$ dw) measured in the present study (horizontal axis), and **a)** the concentration of POC (in mg $g^{-1}$ dw) measured in the present study and **b)** the concentration of total lipids (in mg $g^{-1}$ dw) determined by Tésan Onrubia et al. (2023) using a global method (vertical axes), on the same planktonic size fractions (60-200, 200-500 and 500-1000 µm) recovered from the DCM at the 10 stations.

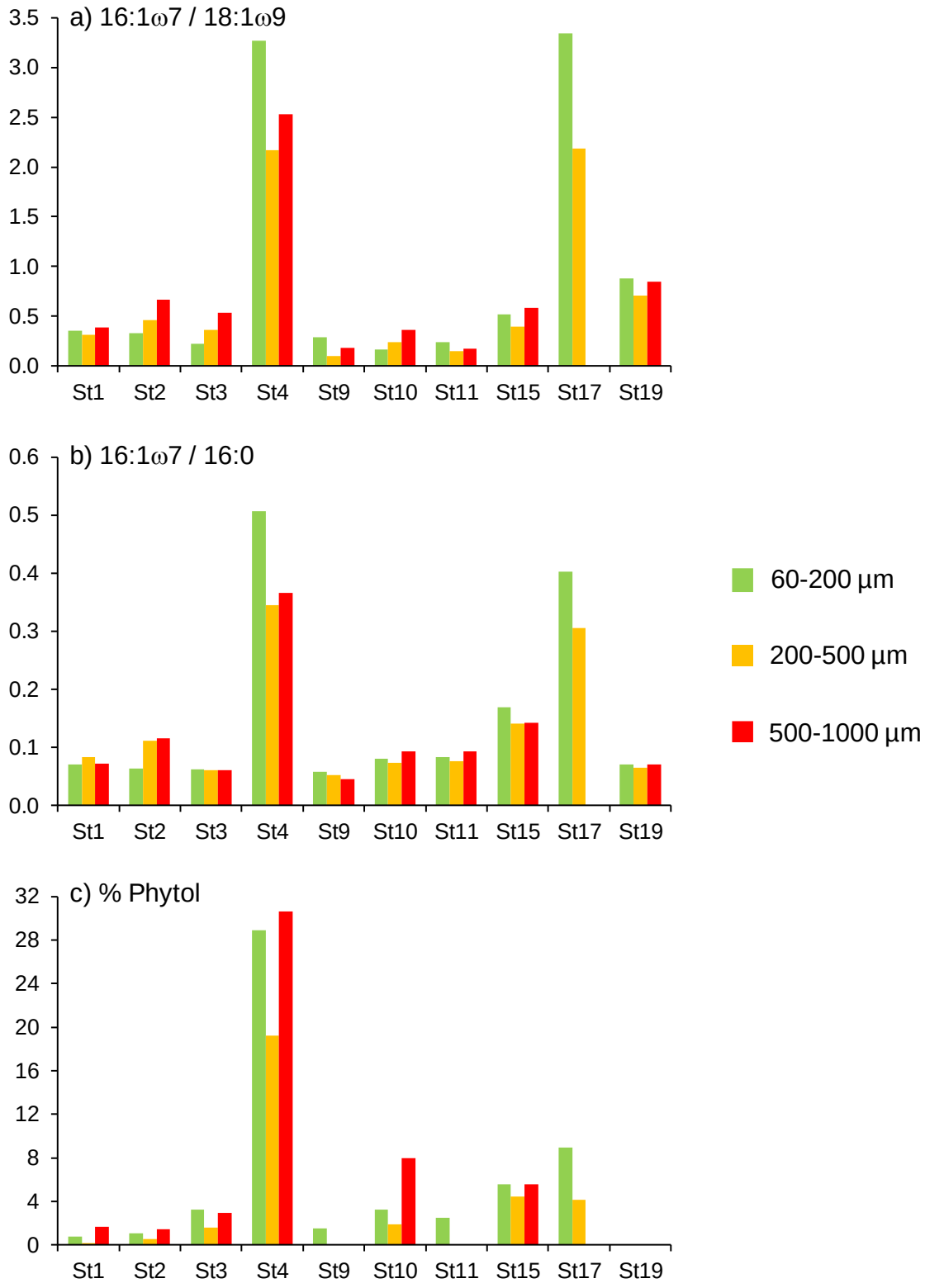


**Figure S2.** Phytoplankton biomarkers in the planktonic size fractions 60-200, 200-500 and 500-1000 µm, recovered from the DCM at the 10 stations: **a)** the ratio of fatty acids 16:1ω7/18:1ω9, **b)** the ratio of fatty acids 16:1ω7/16:0, and **c)** the relative abundance of phytol within fatty alcohols (in %).

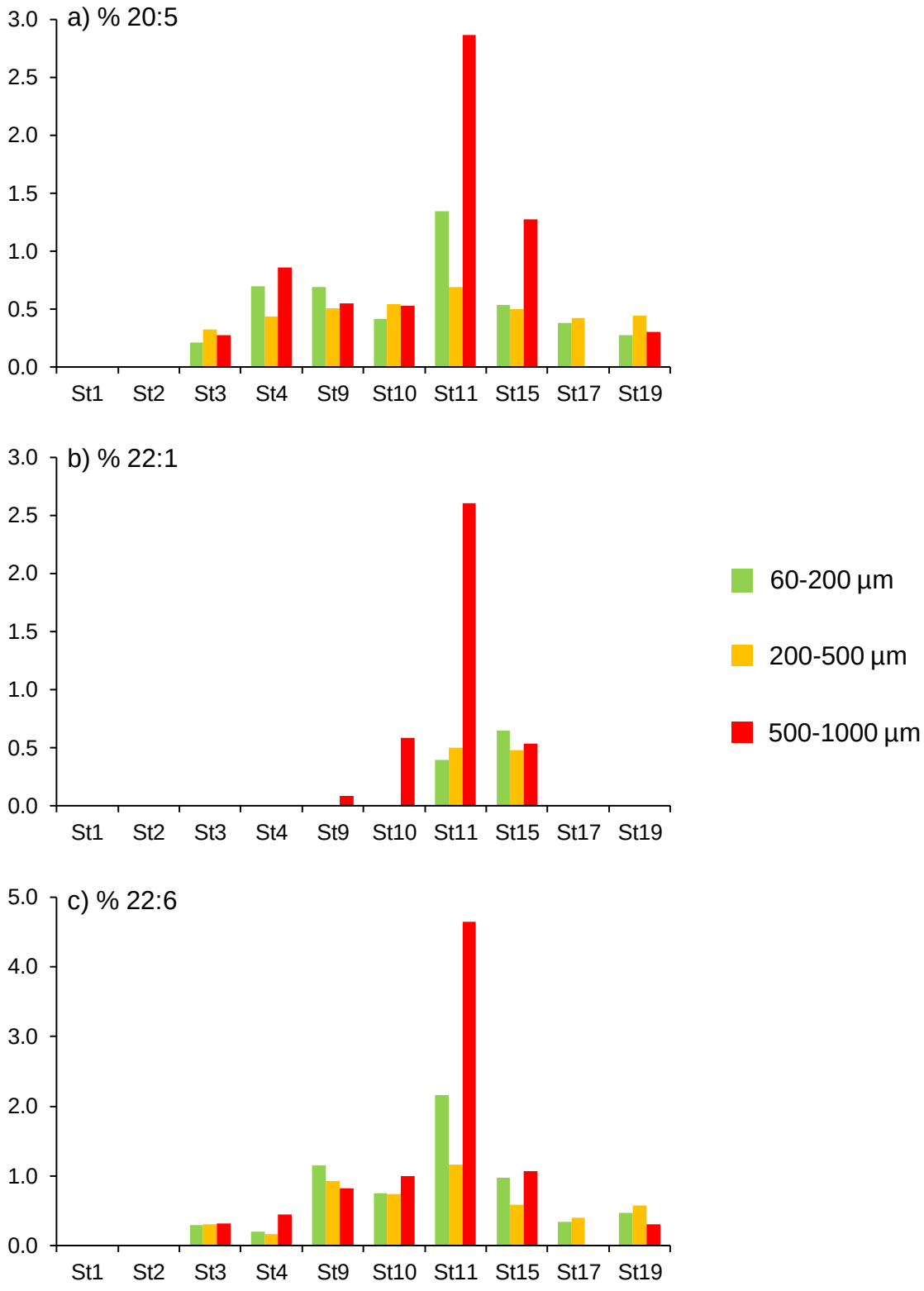


**Figure S3.** Zooplankton biomarkers in the planktonic size fractions 60-200, 200-500 and 500-1000 µm, recovered from the DCM at the 10 stations: relative abundances of **a)** 20:5, **b)** 22:1 and **c)** 22:6 within fatty acids (in %).

**Table S3.** Concentrations (in ng $L^{-1}$) of individual and total aliphatic hydrocarbons (AHs) in the dissolved phase (< 0.7 µm) of water collected at 5-20-m depth at the 10 stations.

| | **St1** | **St2** | **St3** | **St4** | **St9** | **St10** | **St11** | **St15** | **St17** | **St19** |
|---|---|---|---|---|---|---|---|---|---|---|
| *n*-$C_{15}$ | 1.3 | 1.9 | 1.5 | 1.9 | 3.0 | 1.8 | 1.1 | 1.2 | 0.8 | 0.5 |
| *n*-$C_{16}$ | *nd* | 6.2 | 4.5 | 8.3 | *nd* | 7.3 | 2.6 | 0.9 | 0.3 | 0.9 |
| *n*-$C_{17}$ | *nd* | 0.2 | 0.1 | 1.4 | 0.3 | 0.4 | *nd* | 0.7 | *nd* | 0.1 |
| Pr | *nd* | *nd* | 0.5 | 0.9 | *nd* | 0.8 | *nd* | 0.7 | *nd* | 0.8 |
| *n*-$C_{18}$ | *nd* | 1.3 | 1.3 | 2.6 | *nd* | 2.4 | 1.0 | 1.1 | 1.1 | 0.6 |
| Phy | 0.6 | *nd* | 0.8 | 0.9 | *nd* | 0.7 | *nd* | 0.6 | *nd* | 0.4 |
| *n*-$C_{19}$ | *nd* | 0.2 | *nd* | 0.9 | *nd* | 0.4 | *nd* | 0.6 | *nd* | 0.1 |
| *n*-$C_{20}$ | *nd* | 0.7 | 0.3 | 1.2 | *nd* | 0.9 | 0.4 | 0.9 | 0.1 | 0.5 |
| *n*-$C_{21}$ | 1.0 | 1.0 | 0.2 | 0.6 | *nd* | 0.3 | 0.9 | 1.2 | 0.8 | 0.7 |
| *n*-$C_{22}$ | 2.1 | 1.1 | *nd* | *nd* | *nd* | 0.2 | 1.1 | 1.6 | 1.3 | 0.9 |
| *n*-$C_{23}$ | 7.6 | 0.6 | *nd* | *nd* | 0.5 | *nd* | 1.6 | 2.5 | 3.8 | 3.6 |
| *n*-$C_{24}$ | 22 | 0.3 | 0.8 | *nd* | 5.0 | *nd* | 4.0 | 5.6 | 9.3 | 11 |
| *n*-$C_{25}$ | 51 | 1.8 | 3.5 | 1.2 | 13 | *nd* | 9.7 | 11 | 22 | 23 |
| *n*-$C_{26}$ | 73 | 2.8 | 6.7 | 1.4 | 19 | *nd* | 12 | 17 | 33 | 31 |
| *n*-$C_{27}$ | 68 | 2.8 | 8.5 | 3.2 | 24 | *nd* | 15 | 22 | 31 | 40 |
| *n*-$C_{28}$ | 67 | 4.0 | 9.2 | 2.5 | 24 | *nd* | 15 | 20 | 31 | 38 |
| *n*-$C_{29}$ | 66 | 5.6 | 9.9 | 3.3 | 23 | 0.4 | 15 | 20 | 31 | 36 |
| *n*-$C_{30}$ | 49 | 4.5 | 8.4 | 2.6 | 18 | 0.2 | 12 | 15 | 24 | 29 |
| *n*-$C_{31}$ | 37 | 4.7 | 6.8 | 2.2 | 14 | 0.7 | 10 | 12 | 19 | 21 |
| *n*-$C_{32}$ | 23 | 3.4 | 4.8 | 1.5 | 8.9 | 0.3 | 5.8 | 7.3 | 13 | 13 |
| *n*-$C_{33}$ | 13 | 2.3 | 3.1 | 1.1 | 5.7 | 0.5 | 3.7 | 4.1 | 7.4 | 7.5 |
| *n*-$C_{34}$ | 5.4 | 1.6 | 2.1 | 0.9 | 3.6 | 0.4 | 2.3 | 2.4 | 4.5 | 4.5 |
| *n*-$C_{35}$ | 2.6 | 0.9 | 1.2 | 0.6 | 1.5 | 0.3 | 0.9 | 0.8 | 1.7 | 1.4 |
| *n*-$C_{36}$ | 1.2 | 0.4 | 0.5 | 0.8 | 0.7 | *nd* | 0.4 | 0.3 | 0.8 | 0.6 |
| *n*-$C_{37}$ | *nd* | *nd* | *nd* | 0.3 | 0.7 | *nd* | *nd* | 0.1 | 0.7 | 0.3 |
| *n*-$C_{38}$ | *nd* | *nd* | *nd* | 0.6 | 0.5 | *nd* | *nd* | *nd* | *nd* | 0.3 |
| *n*-$C_{39}$ | *nd* | *nd* | *nd* | 0.5 | *nd* | *nd* | *nd* | *nd* | *nd* | *nd* |
| *n*-$C_{40}$ | *nd* | *nd* | *nd* | 0.4 | *nd* | *nd* | *nd* | *nd* | *nd* | *nd* |
| **$\Sigma_{28}$AHs** | **489** | **48** | **75** | **42** | **165** | **18** | **113** | **150** | **235** | **267** |

*nd*: not detected; Pr: pristane; Phy: phytane; $\Sigma_{28}$AHs = $\Sigma$ *n*-$C_{15}$–*n*-$C_{40}$, Pr, Phy (28 compounds).

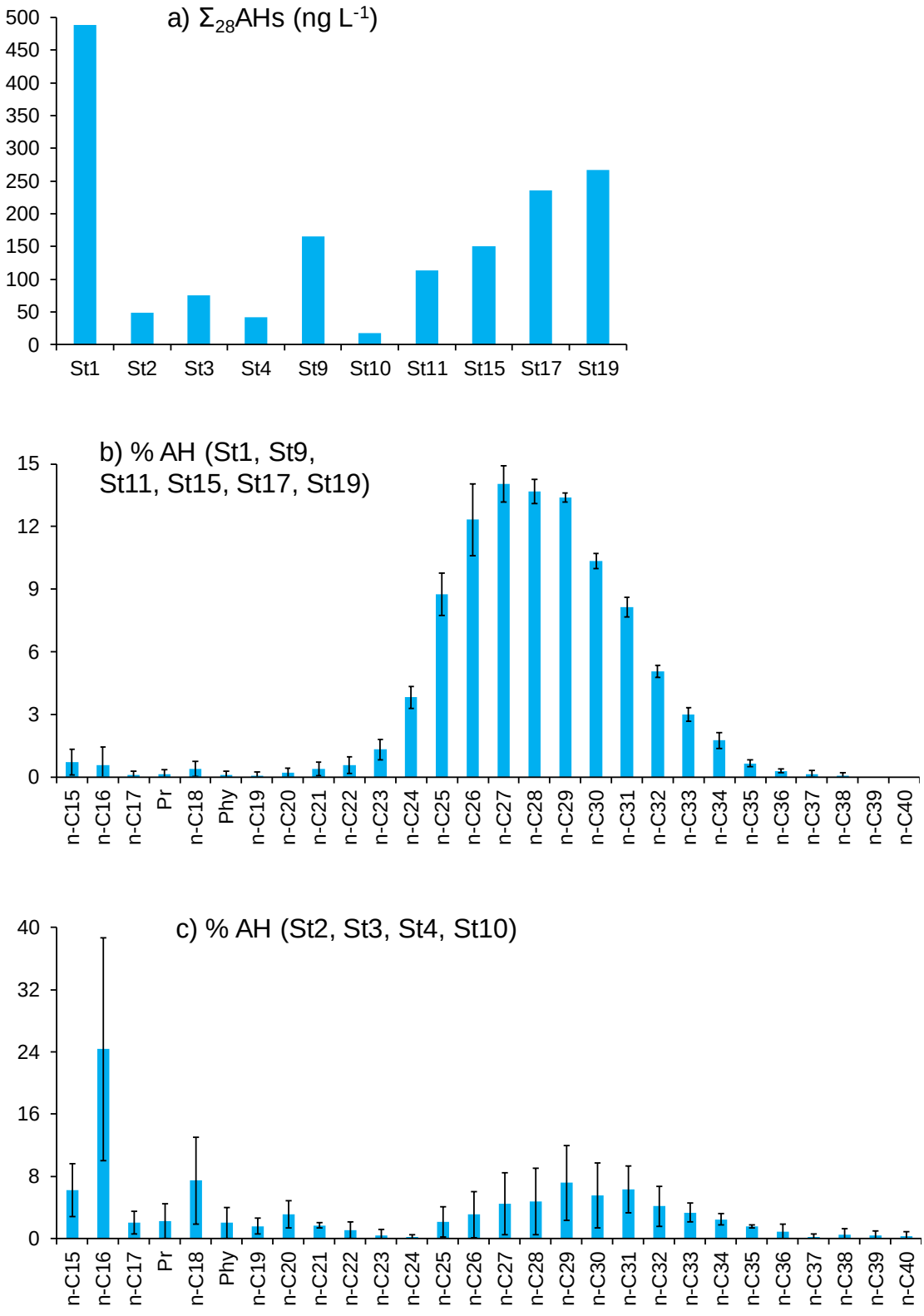


**Figure S4. a)** Concentrations of total aliphatic hydrocarbons ($\Sigma_{28}$AHs, in ng $L^{-1}$) at the 10 stations, and **b)** mean relative abundances of individual AHs (in %) for stations St1, St9, St11, St15, St17, St19 and **c)** stations St 2, St3, St4, St10, for the dissolved phase (< 0.7 µm) of water collected at 5-20-m depth. $\Sigma_{28}$AHs = Σ *n*-$C_{15}$–*n*-$C_{40}$, Pr, Phy (28 compounds).

**Table S4.** Concentrations (in µg $g^{-1}$ dw) of individual and total aliphatic hydrocarbons (AHs) in the particulate/planktonic size fractions 0.7-60, 60-200, 200-500 and 500-1000 µm recovered from the DCM at the 10 stations.

| | **St1** | | | | **St2** | | | | **St3** | | | | **St4** | | | | **St9** | | | |
|---|---|---|---|---|---|---|---|---|---|---|---|---|---|---|---|---|---|---|---|---|
| Size fraction (µm) | 0.7-60 | 60-200 | 200-500 | 500-1000 | 0.7-60 | 60-200 | 200-500 | 500-1000 | 0.7-60 | 60-200 | 200-500 | 500-1000 | 0.7-60 | 60-200 | 200-500 | 500-1000 | 0.7-60 | 60-200 | 200-500 | 500-1000 |
| *n*-$C_{15}$ | 11 | 0.7 | 1.8 | 1.2 | 16 | 1.9 | 3.2 | 5.4 | 9.2 | 1.5 | 1.9 | 1.8 | 5.0 | 0.3 | 0.5 | 0.8 | 2.1 | 0.5 | 0.2 | 0.1 |
| *n*-$C_{16}$ | 0.5 | 0.1 | 0.1 | 0.1 | 1.2 | 0.0 | 0.1 | 0.2 | 1.7 | 0.1 | 0.1 | 0.0 | 0.4 | *nd* | *nd* | *nd* | 0.3 | 0.1 | 0.1 | *nd* |
| *n*-$C_{17}$ | 1.4 | 0.4 | 0.4 | 0.4 | 4.6 | 0.4 | 0.3 | 0.7 | 7.2 | 0.4 | 0.5 | 0.1 | 2.2 | 0.3 | 0.3 | 0.1 | 0.3 | 0.2 | 0.1 | 0.1 |
| Pr | 0.2 | 0.9 | 2.5 | 2.0 | 1.6 | 3.7 | 2.6 | 3.1 | 6.9 | 2.1 | 1.5 | 0.4 | 1.1 | 1.3 | 1.5 | 1.0 | *nd* | 0.2 | 0.3 | 0.4 |
| *n*-$C_{18}$ | 0.3 | *nd* | *nd* | 0.1 | 1.9 | *nd* | *nd* | 0.1 | 8.9 | *nd* | *nd* | 1.7 | 0.6 | 0.1 | 0.1 | 0.1 | 0.1 | *nd* | *nd* | *nd* |
| Phy | *nd* | *nd* | *nd* | *nd* | 1.1 | *nd* | *nd* | *nd* | 5.5 | *nd* | *nd* | *nd* | 0.4 | *nd* | *nd* | *nd* | *nd* | *nd* | *nd* | *nd* |
| *n*-$C_{19}$ | 0.1 | 0.1 | 0.1 | 0.1 | 1.6 | *nd* | *nd* | 0.1 | 7.3 | *nd* | 0.1 | *nd* | 0.7 | 0.2 | 0.4 | 0.1 | 0.1 | 0.1 | 0.1 | *nd* |
| *n*-$C_{20}$ | *nd* | 0.1 | *nd* | 0.1 | 1.1 | 0.1 | *nd* | 0.1 | 4.6 | *nd* | *nd* | *nd* | 0.2 | 0.1 | 0.1 | 0.1 | *nd* | *nd* | *nd* | *nd* |
| *n*-$C_{21}$ | 0.1 | 0.2 | 0.2 | 0.2 | 0.6 | 0.1 | 0.1 | 0.1 | 1.8 | 0.1 | 0.1 | 0.1 | 0.4 | 0.1 | 0.2 | 0.2 | *nd* | 0.1 | 0.1 | 0.1 |
| *n*-$C_{22}$ | 0.1 | 0.1 | 0.1 | 0.1 | 0.4 | 0.1 | 0.1 | 0.2 | 0.7 | 0.1 | 0.1 | 0.1 | 0.7 | 0.1 | 0.2 | 0.2 | *nd* | 0.1 | 0.1 | *nd* |
| *n*-$C_{23}$ | 0.1 | 0.4 | 0.6 | 0.9 | 0.4 | 0.2 | 0.1 | 0.4 | 0.4 | 0.2 | 0.2 | 0.4 | 1.7 | 0.2 | 0.4 | 0.6 | *nd* | 0.3 | 0.4 | 0.2 |
| *n*-$C_{24}$ | 0.1 | *nd* | 0.1 | 0.2 | 0.5 | 0.2 | 0.1 | 0.3 | 0.7 | 0.3 | 0.2 | 0.1 | 2.0 | 0.2 | 0.2 | 0.3 | *nd* | 0.2 | 0.2 | 0.1 |
| *n*-$C_{25}$ | 0.3 | 0.8 | 1.4 | 2.6 | 0.7 | 0.2 | 0.2 | 0.6 | 1.4 | 0.5 | 0.4 | 0.4 | 2.4 | 0.5 | 0.8 | 1.3 | 0.1 | 0.9 | 1.0 | 0.6 |
| *n*-$C_{26}$ | 0.1 | 0.3 | *nd* | 0.3 | 0.8 | 0.2 | 0.1 | 0.3 | 2.3 | 0.6 | 0.4 | 0.2 | 2.3 | 0.3 | 0.6 | 0.5 | *nd* | 0.2 | 0.2 | 0.1 |
| *n*-$C_{27}$ | 0.3 | 2.8 | 2.5 | 10 | 0.8 | 0.5 | 0.5 | 1.5 | 2.5 | 1.0 | 0.9 | 0.8 | 2.4 | 1.6 | 2.5 | 4.4 | 0.1 | 2.6 | 2.4 | 2.0 |
| *n*-$C_{28}$ | 0.1 | 0.3 | *nd* | 0.5 | 0.7 | 0.2 | 0.1 | 0.3 | 2.3 | 0.6 | 0.4 | 0.3 | 1.8 | 0.7 | 0.9 | 0.6 | *nd* | 0.1 | 0.2 | 0.1 |
| *n*-$C_{29}$ | 0.4 | 3.1 | 2.6 | 10 | 0.9 | 0.4 | 0.3 | 1.0 | 2.3 | 1.0 | 0.7 | 0.9 | 2.2 | 1.5 | 2.2 | 2.3 | 0.4 | 0.3 | 2.5 | 1.8 |
| *n*-$C_{30}$ | 0.2 | 0.2 | 0.2 | 0.2 | 0.5 | 0.1 | 0.1 | 0.3 | 1.7 | 0.7 | 0.4 | 0.2 | 1.6 | 0.8 | 1.2 | 0.6 | 0.1 | 0.2 | 0.1 | 0.1 |
| *n*-$C_{31}$ | 0.3 | 1.9 | 1.6 | 4.2 | 0.7 | 0.4 | 0.2 | 0.8 | 1.6 | 0.9 | 0.5 | 0.6 | 2.1 | 1.2 | 1.8 | 1.9 | 0.1 | 1.7 | 1.6 | 0.9 |
| *n*-$C_{32}$ | 0.1 | 0.0 | 0.3 | 0.2 | 0.4 | 0.1 | 0.0 | 0.3 | 1.1 | 0.4 | 0.3 | 0.1 | 1.0 | 0.5 | 0.6 | 0.3 | *nd* | 0.1 | 0.1 | 0.1 |
| *n*-$C_{33}$ | 0.1 | 1.7 | 1.1 | 3.1 | 0.4 | 0.1 | 0.2 | 0.7 | 0.8 | 0.3 | 0.3 | 0.3 | 0.9 | 0.4 | 1.2 | 1.8 | *nd* | 0.1 | 1.6 | 0.9 |
| *n*-$C_{34}$ | *nd* | 0.1 | 0.2 | 0.1 | 0.3 | *nd* | 0.1 | 0.1 | 0.5 | 0.1 | *nd* | *nd* | 0.5 | 0.2 | 0.2 | 0.1 | *nd* | 0.1 | *nd* | *nd* |
| *n*-$C_{35}$ | *nd* | *nd* | 0.3 | 0.3 | 0.2 | *nd* | *nd* | 0.2 | 0.3 | 0.1 | *nd* | *nd* | 0.5 | 0.1 | 0.2 | 0.2 | *nd* | 0.2 | 0.2 | 0.1 |
| *n*-$C_{36}$ | *nd* | *nd* | 0.2 | *nd* | 0.2 | *nd* | *nd* | 0.0 | 0.2 | *nd* | *nd* | *nd* | 0.2 | 0.1 | 0.1 | *nd* | *nd* | *nd* | *nd* | *nd* |
| *n*-$C_{37}$ | *nd* | *nd* | 0.1 | *nd* | *nd* | *nd* | *nd* | 0.1 | 0.1 | *nd* | *nd* | *nd* | *nd* | 0.1 | 0.1 | *nd* | *nd* | *nd* | *nd* | *nd* |
| *n*-$C_{38}$ | *nd* | *nd* | 0.1 | *nd* | *nd* | *nd* | *nd* | *nd* | *nd* | *nd* | *nd* | *nd* | *nd* | *nd* | 0.1 | *nd* | *nd* | *nd* | *nd* | *nd* |
| *n*-$C_{39}$ | *nd* | *nd* | 0.1 | *nd* | *nd* | *nd* | *nd* | *nd* | *nd* | *nd* | *nd* | *nd* | *nd* | *nd* | 0.1 | *nd* | *nd* | *nd* | *nd* | *nd* |
| *n*-$C_{40}$ | *nd* | *nd* | 0.1 | *nd* | *nd* | *nd* | *nd* | *nd* | *nd* | *nd* | *nd* | *nd* | *nd* | *nd* | 0.1 | *nd* | *nd* | *nd* | *nd* | *nd* |
| **$\Sigma_{28}$AHs** | **16** | **14** | **17** | **37** | **38** | **8.9** | **8.5** | **17** | **72** | **11** | **8.9** | **8.6** | **33** | **11** | **17** | **18** | **3.9** | **8.2** | **11** | **7.7** |

| | **St10** | | | | **St11** | | | | **St15** | | | | **St17** | | | | **St19** | | | |
|---|---|---|---|---|---|---|---|---|---|---|---|---|---|---|---|---|---|---|---|---|
| Size fraction (µm) | 0.7-60 | 60-200 | 200-500 | 500-1000 | 0.7-60 | 60-200 | 200-500 | 500-1000 | 0.7-60 | 60-200 | 200-500 | 500-1000 | 0.7-60 | 60-200 | 200-500 | 500-1000 | 0.7-60 | 60-200 | 200-500 | 500-1000 |
| *n*-$C_{15}$ | 7.0 | 1.3 | 1.9 | 1.8 | 11.9 | 1.4 | 1.6 | 2.3 | 3.7 | 1.7 | 2.3 | 1.9 | 5.6 | 0.5 | 0.7 | *na* | 8.3 | 0.6 | 0.5 | 1.1 |
| *n*-$C_{16}$ | 0.5 | 0.1 | 0.2 | 0.1 | 1.7 | 0.1 | 0.1 | 0.1 | 0.3 | 0.1 | 0.1 | 0.1 | 0.2 | *nd* | *nd* | *na* | 0.3 | 0.1 | *nd* | *nd* |
| *n*-$C_{17}$ | 1.5 | 0.7 | 2.1 | 1.2 | 10.8 | 3.5 | 2.8 | 3.0 | 1.9 | 0.5 | 1.4 | 1.0 | 0.7 | 0.3 | 0.3 | *na* | 0.3 | 0.2 | 0.2 | 0.4 |
| Pr | 0.2 | 1.0 | 4.3 | 4.2 | 5.4 | 3.6 | 32.9 | 45 | 0.1 | 0.9 | 1.8 | 3.1 | 0.1 | 1.0 | 1.5 | *na* | 0.6 | 4.4 | 2.9 | 6.9 |
| *n*-$C_{18}$ | 0.3 | *nd* | 0.1 | 0.1 | 6.0 | 0.1 | *nd* | *nd* | 0.2 | *nd* | 0.1 | 0.1 | 0.1 | *nd* | *nd* | *na* | 0.2 | *nd* | 0.1 | *nd* |
| Phy | 0.1 | *nd* | *nd* | *nd* | 3.5 | *nd* | *nd* | *nd* | *nd* | *nd* | *nd* | *nd* | *nd* | *nd* | *nd* | *na* | 0.1 | *nd* | *nd* | *nd* |
| *n*-$C_{19}$ | 0.2 | 0.1 | 0.2 | 0.1 | 4.1 | 0.2 | 0.1 | 0.1 | *nd* | *nd* | *nd* | *nd* | *nd* | *nd* | *nd* | *na* | 0.2 | 0.1 | 0.1 | 0.1 |
| *n*-$C_{20}$ | 0.0 | 0.1 | 0.1 | 0.0 | 2.2 | 0.1 | *nd* | *nd* | 0.0 | 0.1 | 0.0 | 0.1 | nd | *nd* | *nd* | *na* | *nd* | *nd* | *nd* | *nd* |
| *n*-$C_{21}$ | 0.1 | 0.2 | 0.2 | 0.1 | 1.4 | 0.2 | 0.1 | 0.1 | 0.1 | 0.1 | 0.1 | 0.1 | 0.1 | *nd* | *nd* | *na* | 0.1 | 0.1 | 0.1 | 0.1 |
| *n*-$C_{22}$ | 0.1 | 0.1 | 0.1 | 0.1 | 1.0 | 0.1 | 0.1 | 0.1 | 0.2 | 0.1 | 0.1 | 0.1 | 0.1 | *nd* | *nd* | *na* | *nd* | 0.1 | 0.1 | 0.1 |
| *n*-$C_{23}$ | 0.1 | 0.4 | 0.4 | 0.4 | 2.3 | 0.2 | 0.1 | 0.1 | 0.2 | 0.2 | 0.1 | 0.2 | 0.1 | *nd* | 0.1 | *na* | 0.1 | 0.1 | 0.2 | 0.4 |
| *n*-$C_{24}$ | 0.1 | 0.2 | 0.2 | 0.2 | 3.3 | 0.2 | 0.1 | 0.1 | 0.3 | 0.1 | 0.1 | 0.1 | 0.1 | *nd* | 0.1 | *na* | 0.1 | 0.2 | 0.3 | 0.8 |
| *n*-$C_{25}$ | 0.1 | 0.8 | 0.8 | 1.0 | 6.9 | 0.4 | 0.3 | 0.3 | 0.4 | 0.4 | 0.3 | 0.3 | 0.3 | 0.1 | 0.1 | *na* | 0.1 | 0.3 | 0.6 | 1.3 |
| *n*-$C_{26}$ | 0.1 | 0.4 | 0.3 | 0.4 | 6.7 | 0.3 | 0.2 | 0.3 | 0.3 | 0.2 | 0.1 | 0.2 | 0.1 | 0.1 | 0.1 | *na* | 0.1 | 0.2 | 0.5 | 1.3 |
| *n*-$C_{27}$ | 0.2 | 2.0 | 1.8 | 2.8 | 10 | 0.7 | 0.4 | 0.5 | 0.4 | 0.7 | 0.4 | 0.3 | 0.3 | 0.1 | 0.1 | *na* | 0.1 | 0.6 | 0.8 | 1.9 |
| *n*-$C_{28}$ | 0.1 | 0.4 | 0.3 | 0.5 | 5.8 | 0.2 | 0.1 | 0.2 | 0.3 | 0.3 | 0.1 | 0.1 | 0.1 | 0.1 | 0.1 | *na* | 0.1 | 0.2 | 0.4 | 1.0 |
| *n*-$C_{29}$ | 0.3 | 4.0 | 3.0 | 4.8 | 7.3 | 1.5 | 0.8 | 0.9 | 0.4 | 1.4 | 0.7 | 0.5 | 0.3 | 0.2 | 0.2 | *na* | 0.3 | 2.0 | 1.3 | 2.9 |
| *n*-$C_{30}$ | 0.2 | 0.6 | 0.3 | 0.4 | 3.7 | 0.2 | 0.2 | 0.1 | 0.3 | 0.2 | 0.1 | 0.1 | 0.1 | 0.1 | 0.1 | *na* | 0.1 | 0.3 | 0.3 | 0.7 |
| *n*-$C_{31}$ | 0.2 | 5.1 | 3.0 | 4.2 | 5.3 | 2.3 | 1.0 | 1.0 | 0.5 | 2.2 | 0.7 | 0.4 | 0.3 | 0.3 | 0.3 | *na* | 0.3 | 3.2 | 1.8 | 3.5 |
| *n*-$C_{32}$ | 0.2 | 0.5 | 0.3 | 0.3 | 1.7 | 0.2 | 0.0 | 0.1 | 0.2 | 0.1 | 0.1 | 0.1 | 0.1 | 0.0 | 0.0 | *na* | 0.1 | 0.3 | 0.3 | 0.5 |
| *n*-$C_{33}$ | 0.2 | 1.8 | 1.0 | 1.2 | 1.6 | 0.8 | 0.3 | 0.3 | 0.1 | 0.5 | 0.2 | 0.1 | 0.1 | 0.1 | 0.1 | *na* | 0.1 | 1.1 | 0.7 | 1.1 |
| *n*-$C_{34}$ | 0.1 | 0.2 | 0.1 | 0.1 | 0.6 | 0.1 | *nd* | *nd* | *nd* | *nd* | *nd* | *nd* | *nd* | *nd* | *nd* | *na* | *nd* | 0.1 | 0.1 | 0.2 |
| *n*-$C_{35}$ | 0.1 | 0.8 | 0.7 | 0.2 | 0.4 | 0.2 | 0.1 | 0.1 | *nd* | 0.1 | 0.1 | *nd* | *nd* | *nd* | *nd* | *na* | 0.2 | 0.2 | 0.2 | 0.2 |
| *n*-$C_{36}$ | 0.1 | *nd* | *nd* | *nd* | 0.2 | *nd* | *nd* | *nd* | *nd* | *nd* | *nd* | *nd* | *nd* | *nd* | *nd* | *na* | *nd* | *nd* | 0.1 | 0.1 |
| *n*-$C_{37}$ | 0.1 | 0.1 | 0.3 | nd | 0.2 | *nd* | *nd* | *nd* | *nd* | *nd* | *nd* | *nd* | *nd* | *nd* | *nd* | *na* | *nd* | *nd* | 0.4 | 0.1 |
| *n*-$C_{38}$ | 0.1 | *nd* | 0.1 | nd | *nd* | *nd* | *nd* | *nd* | *nd* | *nd* | *nd* | *nd* | *nd* | *nd* | *nd* | *na* | *nd* | *nd* | *nd* | *nd* |
| *n*-$C_{39}$ | *nd* | *nd* | *nd* | *nd* | *nd* | *nd* | *nd* | *nd* | *nd* | *nd* | *nd* | *nd* | *nd* | *nd* | *nd* | *na* | *nd* | *nd* | *nd* | *nd* |
| *n*-$C_{40}$ | *nd* | *nd* | *nd* | *nd* | *nd* | *nd* | *nd* | *nd* | *nd* | *nd* | *nd* | *nd* | *nd* | *nd* | *nd* | *na* | *nd* | *nd* | *nd* | *nd* |
| **$\Sigma_{28}$AHs** | **12** | **21** | **22** | **24** | **104** | **17** | **41** | **55** | **10** | **10** | **9.4** | **8.8** | **8.8** | **3.4** | **4.0** | ***na*** | **12** | **14** | **12** | **25** |

*na*: not available; *nd*: not detected; Pr: pristane; Phy: phytane; $\Sigma_{28}$AHs = Σ *n*-$C_{15}$–*n*-$C_{40}$, Pr, Phy (28 compounds).

**Table S5.** Concentrations (in ng $L^{-1}$) of individual and total polycyclic aromatic hydrocarbons (PAHs) in the dissolved phase (< 0.7 µm) of water collected at 5-20-m depth at the 10 stations.

| | **St1** | **St2** | **St3** | **St4** | **St9** | **St10** | **St11** | **St15** | **St17** | **St19** |
|---|---|---|---|---|---|---|---|---|---|---|
| Nap | 0.29 | 0.69 | 0.24 | 0.93 | 0.11 | 0.44 | 0.06 | 0.34 | 0.18 | 0.41 |
| C1-Nap | *nd* | *nd* | *nd* | 3.13 | *nd* | *nd* | *nd* | *nd* | *nd* | *nd* |
| C2-Nap | *nd* | *nd* | *nd* | 7.06 | *nd* | *nd* | *nd* | *nd* | *nd* | *nd* |
| C3-Nap | *nd* | *nd* | *nd* | 2.43 | *nd* | *nd* | *nd* | *nd* | *nd* | *nd* |
| Acy | *0.01* | *nd* | *nd* | *nd* | *nd* | *nd* | *nd* | *nd* | 0.01 | 0.01 |
| Ace | 0.08 | 0.10 | 0.12 | 0.12 | 0.08 | 0.09 | 0.04 | 0.06 | 0.06 | 0.06 |
| Flu | 0.27 | 0.26 | 0.21 | 0.40 | 0.14 | 0.23 | 0.09 | 0.16 | 0.15 | 0.19 |
| DBT | 0.01 | 0.07 | 0.03 | 0.18 | 0.03 | 0.02 | 0.02 | 0.01 | 0.01 | 0.01 |
| Phe | 0.43 | 1.06 | 0.91 | 1.14 | 3.52 | 0.46 | 0.33 | 0.34 | 0.28 | 0.32 |
| Ant | 0.03 | *nd* | 0.07 | *nd* | *nd* | *nd* | *nd* | 0.05 | 0.03 | 0.06 |
| Flt | 0.17 | 0.34 | 0.82 | 0.17 | 0.13 | 0.15 | 0.13 | 0.14 | 0.15 | 0.12 |
| Pyr | 0.10 | 0.29 | 0.65 | 0.12 | 0.10 | 0.13 | 0.09 | 0.12 | 0.12 | 0.12 |
| BaA | 0.05 | 0.04 | 0.13 | 0.05 | 0.04 | 0.03 | 0.04 | 0.05 | 0.05 | 0.05 |
| Chr | 0.10 | 0.13 | 0.62 | 0.06 | 0.09 | 0.11 | 0.08 | 0.12 | 0.18 | 0.11 |
| **$\Sigma_{14}$PAHs** | **1.5** | **3.0** | **3.8** | **16** | **4.2** | **1.7** | **0.9** | **1.4** | **1.2** | **1.4** |
| **$\Sigma_{7}$PAHs** | **1.4** | **2.8** | **3.6** | **2.9** | **4.1** | **1.6** | **0.8** | **1.3** | **1.1** | **1.3** |
| LMW PAHs (%) | 73 | 73 | 42 | 97 | 92 | 74 | 61 | 69 | 59 | 73 |
| HMW PAHs (%) | 27 | 27 | 58 | 3 | 8 | 26 | 39 | 31 | 41 | 27 |

*nd*: not detected; C1: methyl; C2: di-methyl; C3: tri-methyl; $\Sigma_{14}$PAHs = Σ Nap–Chr (14 compounds); $\Sigma_{7}$PAHs = Σ Nap, Flu, Phe, Flt, Pyr, BaA, Chr; LMW: low molecular weight, i.e., 2-3 rings; HMW: high molecular weight, i.e., 4-6 rings.

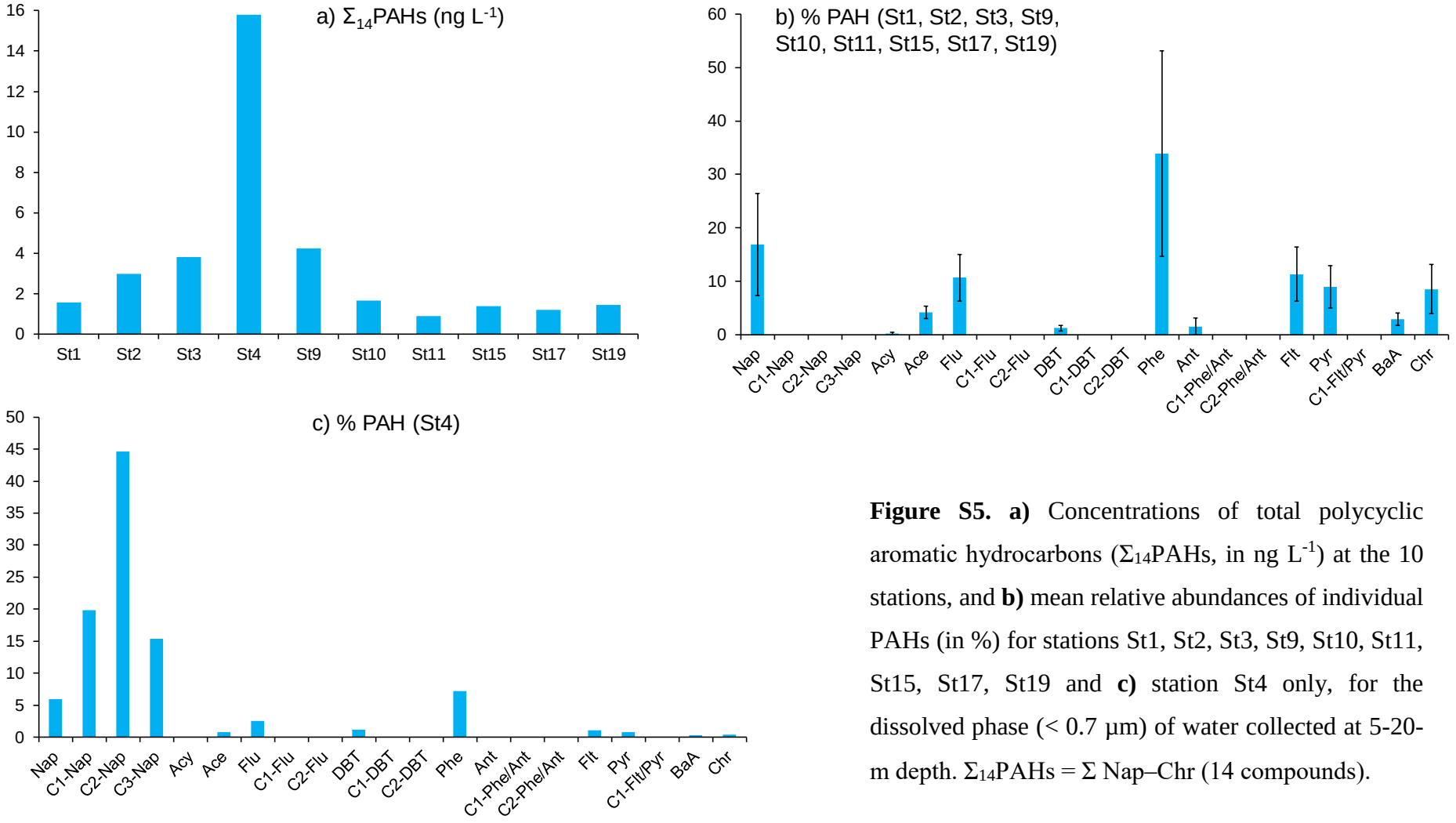


**Figure S5. a)** Concentrations of total polycyclic aromatic hydrocarbons ($\Sigma_{14}$PAHs, in ng $L^{-1}$) at the 10 stations, and **b)** mean relative abundances of individual PAHs (in %) for stations St1, St2, St3, St9, St10, St11, St15, St17, St19 and **c)** station St4 only, for the dissolved phase (< 0.7 µm) of water collected at 5-20-m depth. $\Sigma_{14}$PAHs = Σ Nap–Chr (14 compounds).

**Table S6.** Concentrations (in ng $g^{-1}$ dw) of individual and total polycyclic aromatic hydrocarbons (PAHs) in the particulate/planktonic size fractions 0.7-60, 60-200, 200-500 and 500-1000 µm recovered from the DCM at the 10 stations.

| | **St1** | | | | **St2** | | | | **St3** | | | | **St4** | | | | **St9** | | | |
|---|---|---|---|---|---|---|---|---|---|---|---|---|---|---|---|---|---|---|---|---|
| Size fraction (µm) | 0.7-60 | 60-200 | 200-500 | 500-1000 | 0.7-60 | 60-200 | 200-500 | 500-1000 | 0.7-60 | 60-200 | 200-500 | 500-1000 | 0.7-60 | 60-200 | 200-500 | 500-1000 | 0.7-60 | 60-200 | 200-500 | 500-1000 |
| Nap | 18 | 8.0 | 2.9 | 13 | 25 | 31 | 7.0 | 7.0 | 36 | 14 | 5.6 | 3.6 | 20 | 6.2 | 7.8 | 18 | 11 | 3.9 | 2.1 | 5.2 |
| C1-Nap | *nd* | 4.5 | 1.3 | 2.9 | *nd* | 8.1 | 2.1 | 1.7 | *nd* | 5.0 | 2.4 | 1.2 | *nd* | 3.9 | 5.1 | 4.7 | *nd* | 1.5 | 0.9 | 1.5 |
| C2-Nap | *nd* | 16 | 4.4 | 8.1 | *nd* | 18 | 2.0 | 5.9 | *nd* | 18 | 14 | 7.8 | *nd* | *nd* | *nd* | *nd* | *nd* | 6.4 | 4.0 | 5.9 |
| C3-Nap | *nd* | 16 | 0.2 | 6.1 | *nd* | 17 | 5.4 | 5.9 | *nd* | 16 | 12.5 | 5.8 | *nd* | 10.3 | 14 | 10 | *nd* | 6.4 | 4.0 | 5.8 |
| Acy | *nd* | 1.8 | 3.1 | 1.4 | *nd* | *nd* | *nd* | *nd* | *nd* | 0.9 | 0.4 | 0.3 | *nd* | *nd* | 1.2 | 0.8 | *nd* | 0.5 | 0.2 | *nd* |
| Ace | *nd* | *nd* | *nd* | *nd* | *nd* | *nd* | *nd* | *nd* | *nd* | *nd* | *nd* | *nd* | *nd* | *nd* | *nd* | *nd* | *nd* | 0.5 | 0.4 | *nd* |
| Flu | 14 | 4.3 | 3.4 | 7.6 | 20 | 19 | 5.5 | 6.9 | 38 | 15 | 4.9 | 2.2 | 18 | 5.5 | 14 | 11 | 9.7 | 3.1 | 2.7 | 2.3 |
| C1-Flu | *nd* | 6.8 | 3.6 | 4.0 | *nd* | 7.5 | 4.5 | 4.5 | *nd* | 7.9 | 7.8 | 4.0 | *nd* | 4.9 | 4.4 | 3.0 | *nd* | 3.6 | 2.9 | 2.1 |
| C2-Flu | *nd* | 5.7 | *nd* | *nd* | *nd* | *nd* | *nd* | *nd* | *nd* | *nd* | *nd* | *nd* | *nd* | *nd* | *nd* | *nd* | *nd* | *nd* | *nd* | *nd* |
| DBT | 0.6 | 2.1 | *nd* | 0.5 | *nd* | *nd* | *nd* | *nd* | *nd* | 1.9 | 0.8 | 0.4 | 0.5 | 0.8 | 1.1 | 0.0 | 0.2 | 0.4 | 0.1 | 0.2 |
| C1-DBT | *nd* | 1.7 | *nd* | *nd* | *nd* | *nd* | *nd* | *nd* | *nd* | *nd* | *nd* | *nd* | *nd* | *nd* | *nd* | *nd* | *nd* | *nd* | *nd* | *nd* |
| C2-DBT | *nd* | 2.4 | *nd* | *nd* | *nd* | *nd* | *nd* | *nd* | *nd* | *nd* | *nd* | *nd* | *nd* | *nd* | *nd* | *nd* | *nd* | *nd* | *nd* | *nd* |
| Phe | 16 | 39 | 16 | 17 | 21 | 71 | 20 | 24 | 51 | 79 | 29 | 14 | 19 | 32 | 26 | 25 | 5.3 | 19 | 9.1 | 6.8 |
| Ant | *nd* | 1.7 | *nd* | 1.3 | *nd* | *nd* | 7.0 | 0.0 | 10 | 3.8 | 1.1 | 0.5 | *nd* | 2.1 | 1.9 | 2.4 | *nd* | 0.7 | 0.4 | 0.3 |
| C1-Phe/Ant | *nd* | 16 | 6.0 | 8.1 | *nd* | *nd* | 2.6 | 8.7 | *nd* | 9.1 | 6.9 | 4.7 | *nd* | 17 | 14 | 0.0 | *nd* | 6.9 | 5.1 | 4.0 |
| C2-Phe/Ant | *nd* | 12 | nd | 4.0 | *nd* | *nd* | *nd* | *nd* | *nd* | 5.7 | 5.1 | 2.9 | *nd* | 9.0 | 12 | 0.0 | *nd* | 4.8 | 2.8 | 1.4 |
| Flt | 23 | 24 | 12 | 9.3 | 7.0 | 14 | 4.3 | 8.3 | 22 | 10 | 5.1 | 3.4 | 17 | 16 | 13 | 12 | 6.6 | 3.4 | 3.4 | 2.1 |
| Pyr | 31 | 21 | 12 | 8.6 | 19 | 12 | 5.2 | 7.3 | 41 | 8.4 | 3.6 | 2.4 | 14 | 13 | 11 | 12 | 13 | 2.9 | 1.6 | 1.1 |
| C1-Flt/Pyr | *nd* | 17 | 6.1 | 4.7 | *nd* | *nd* | *nd* | *nd* | *nd* | *nd* | *nd* | *nd* | *nd* | 7.8 | 5.6 | 0.0 | *nd* | 2.2 | 3.0 | 1.2 |
| BaA | 9.0 | 14 | 0.3 | 3.6 | 8.2 | 2.9 | 1.1 | 1.6 | 11 | 2.5 | 1.3 | 0.6 | 14 | 5.9 | 4.9 | 4.7 | 4.4 | 2.3 | 0.4 | 0.7 |
| Chr | 19 | 17 | 4.8 | 8.2 | 12 | 5.1 | 2.6 | 6.1 | 12 | 3.9 | 3.0 | 3.5 | 35 | 13 | 8.9 | 16 | 3.5 | 3.0 | 2.4 | 1.2 |
| BbF | *nd* | *nd* | *nd* | *nd* | *nd* | *nd* | *nd* | *nd* | *nd* | *nd* | *nd* | *nd* | *nd* | *nd* | *nd* | *nd* | *nd* | *nd* | *nd* | *nd* |
| BkF | *nd* | *nd* | *nd* | *nd* | *nd* | *nd* | *nd* | *nd* | *nd* | *nd* | *nd* | *nd* | *nd* | *nd* | *nd* | *nd* | *nd* | *nd* | *nd* | *nd* |
| BaP | *nd* | *nd* | *nd* | *nd* | *nd* | *nd* | *nd* | *nd* | *nd* | *nd* | *nd* | *nd* | *nd* | *nd* | *nd* | *nd* | *nd* | *nd* | *nd* | *nd* |
| IndP | *nd* | 8.2 | *nd* | 2.5 | *nd* | *nd* | *nd* | *nd* | *nd* | *nd* | *nd* | *nd* | *nd* | *nd* | 7.3 | 6.9 | *nd* | 2.1 | *nd* | *nd* |
| DahA | *nd* | 6.1 | *nd* | *nd* | *nd* | *nd* | *nd* | *nd* | *nd* | *nd* | *nd* | *nd* | *nd* | *nd* | 1.7 | *nd* | *nd* | *nd* | *nd* | *nd* |
| BP | *nd* | 8.6 | *nd* | 5.2 | *nd* | *nd* | *nd* | *nd* | *nd* | *nd* | *nd* | *nd* | *nd* | *nd* | 11.5 | 11 | nd | 2.4 | *nd* | *nd* |
| **$\Sigma_{27}$PAHs** | **130** | **255** | **76** | **116** | **111** | **206** | **69** | **88** | **220** | **201** | **104** | **57** | **136** | **168** | **162** | **119** | **53** | **76** | **45** | **42** |
| **$\Sigma_{7}$PAHs** | **129** | **127** | **51** | **67** | **111** | **155** | **46** | **61** | **211** | **133** | **52** | **29** | **136** | **91** | **85** | **98** | **53** | **37** | **22** | **19** |
| LMW PAHs | 37 | 55 | 54 | 64 | 59 | 83 | 81 | 73 | 61 | 88 | 83 | 81 | 41 | 55 | 62 | 63 | 48 | 76 | 76 | 85 |
| HMW PAHs | 63 | 45 | 46 | 36 | 41 | 17 | 19 | 27 | 39 | 12 | 17 | 19 | 59 | 45 | 38 | 37 | 52 | 24 | 24 | 15 |

| | **St10** | | | | **St11** | | | | **St15** | | | | **St17** | | | | **St19** | | | |
|---|---|---|---|---|---|---|---|---|---|---|---|---|---|---|---|---|---|---|---|---|
| Size fraction (µm) | 0.7-60 | 60-200 | 200-500 | 500-1000 | 0.7-60 | 60-200 | 200-500 | 500-1000 | 0.7-60 | 60-200 | 200-500 | 500-1000 | 0.7-60 | 60-200 | 200-500 | 500-1000 | 0.7-60 | 60-200 | 200-500 | 500-1000 |
| Nap | 23 | 8.9 | 3.0 | 8.2 | 64 | 5.5 | 4.0 | 3.0 | 29 | 11 | 2.9 | 4.3 | 15 | 2.7 | 3.8 | *na* | 13 | 2.9 | 2.7 | 11 |
| C1-Nap | *nd* | 2.4 | 2.0 | 1.9 | *nd* | 2.2 | 1.6 | 1.4 | *nd* | 4.1 | 2.7 | 1.4 | *nd* | 1.5 | 1.6 | *na* | *nd* | 1.1 | 0.9 | *nd* |
| C2-Nap | *nd* | 8.4 | 14 | 6.7 | *nd* | 10 | 9.1 | 7.4 | *nd* | 0.0 | 17 | 8.8 | *nd* | *nd* | *nd* | *na* | *nd* | 6.2 | 5.5 | *nd* |
| C3-Nap | *nd* | 19 | 0.0 | 6.3 | *nd* | 12 | 13 | 8.5 | *nd* | 17 | 16 | 8.6 | *nd* | 5.1 | 4.2 | *na* | *nd* | 4.0 | 4.9 | *nd* |
| Acy | *nd* | 1.2 | 0.6 | 0.7 | *nd* | 0.5 | 0.2 | 0.2 | *nd* | *nd* | 0.6 | 0.2 | *nd* | *nd* | *nd* | *na* | *nd* | *nd* | *nd* | *nd* |
| Ace | *nd* | *nd* | *nd* | *nd* | *nd* | *nd* | 1.0 | 0.9 | *nd* | *nd* | 1.8 | 1.1 | *nd* | *nd* | *nd* | *na* | *nd* | 0.6 | 0.3 | *nd* |
| Flu | 14 | 7.7 | 5.6 | 7.1 | 41 | 6.8 | 4.8 | 4.5 | 20 | 12 | 8.5 | 4.8 | 13 | 3.1 | 4.2 | *na* | 11 | 2.9 | 2.5 | 6.9 |
| C1-Flu | *nd* | 6.3 | 9.3 | 4.9 | *nd* | 7.8 | 7.8 | 7.0 | *nd* | 4.1 | 8.2 | 3.9 | *nd* | *nd* | *nd* | *na* | *nd* | *nd* | *nd* | *nd* |
| C2-Flu | *nd* | *nd* | *nd* | *nd* | *nd* | *nd* | *nd* | *nd* | *nd* | *nd* | *nd* | *nd* | *nd* | *nd* | *nd* | *na* | *nd* | *nd* | *nd* | *nd* |
| DBT | 0.2 | 0.8 | 0.7 | 0.3 | *nd* | 1.1 | 0.5 | 0.3 | 0.6 | 1.9 | 1.0 | 0.5 | *nd* | 0.4 | 0.3 | *na* | 0.2 | 0.4 | 0.3 | 0.4 |
| C1-DBT | *nd* | *nd* | *nd* | *nd* | *nd* | *nd* | *nd* | *nd* | *nd* | *nd* | *nd* | *nd* | *nd* | *nd* | *nd* | *na* | *nd* | *nd* | *nd* | *nd* |
| C2-DBT | *nd* | *nd* | *nd* | *nd* | *nd* | *nd* | *nd* | *nd* | *nd* | *nd* | *nd* | *nd* | *nd* | *nd* | *nd* | *na* | *nd* | *nd* | *nd* | *nd* |
| Phe | 9.4 | 38 | 24 | 21 | 41 | 46 | 23 | 15 | 22 | 67 | 37 | 21 | 8.7 | 15 | 14 | *na* | 8.7 | 14 | 8.6 | 17 |
| Ant | *nd* | 1.2 | 1.1 | 0.6 | *nd* | 1.4 | 0.6 | 0.4 | *nd* | *nd* | 1.3 | 0.7 | *nd* | *nd* | *nd* | *na* | *nd* | 0.3 | 0.1 | 0.0 |
| C1-Phe/Ant | *nd* | 9.9 | 10 | 6.7 | *nd* | 5.4 | 7.2 | 6.8 | *nd* | 9.3 | 9.8 | 7.0 | *nd* | 6.0 | 5.4 | *na* | *nd* | 5.7 | 3.3 | 0.0 |
| C2-Phe/Ant | *nd* | 6.0 | 5.9 | 3.1 | *nd* | 4.5 | 3.6 | 3.6 | *nd* | 0.0 | 11 | 8.6 | *nd* | 4.8 | 4.0 | *na* | *nd* | 3.5 | 2.6 | 0.0 |
| Flt | 9.1 | 7.3 | 4.8 | 4.9 | 20 | 7.2 | 2.6 | 2.3 | 24 | 5.2 | 3.6 | 3.2 | 11 | 1.4 | 1.7 | *na* | 9.0 | 1.1 | 1.0 | 2.0 |
| Pyr | 21 | 5.9 | 3.1 | 4.4 | 24 | 4.8 | 1.6 | 1.4 | 31 | 8.3 | 2.6 | 4.0 | 19 | 2.1 | 3.1 | *na* | 18 | 1.4 | 1.0 | 2.7 |
| C1-Flt/Pyr | *nd* | *nd* | *nd* | *nd* | *nd* | *nd* | *nd* | *nd* | *nd* | *nd* | *nd* | *nd* | *nd* | *nd* | *nd* | *na* | *nd* | *nd* | *nd* | *nd* |
| BaA | 7.6 | 1.3 | 0.8 | 1.0 | 18 | 1.9 | 0.6 | 0.6 | 19 | 0.0 | 1.3 | 0.9 | 7.3 | 0.3 | 0.4 | *na* | 6.9 | 0.3 | 0.3 | 1.5 |
| Chr | 9.4 | 4.1 | 2.9 | 2.7 | 11 | 4.4 | 1.6 | 1.8 | 18 | 2.1 | 2.0 | 2.0 | 15 | 0.9 | 0.9 | *na* | 4.3 | 0.5 | 0.5 | 1.0 |
| BbF | *nd* | *nd* | *nd* | *nd* | *nd* | *nd* | *nd* | *nd* | *nd* | *nd* | *nd* | *nd* | *nd* | *nd* | *nd* | *na* | *nd* | *nd* | *nd* | *nd* |
| BkF | *nd* | *nd* | *nd* | *nd* | *nd* | *nd* | *nd* | *nd* | *nd* | *nd* | *nd* | *nd* | *nd* | *nd* | *nd* | *na* | *nd* | *nd* | *nd* | *nd* |
| BaP | *nd* | *nd* | *nd* | *nd* | *nd* | *nd* | *nd* | *nd* | *nd* | *nd* | *nd* | *nd* | *nd* | *nd* | *nd* | *na* | *nd* | *nd* | *nd* | *nd* |
| IndP | *nd* | *nd* | *nd* | *nd* | *nd* | *nd* | *nd* | *nd* | *nd* | *nd* | *nd* | *nd* | *nd* | *nd* | *nd* | *na* | *nd* | *nd* | *nd* | *nd* |
| DahA | *nd* | *nd* | *nd* | *nd* | *nd* | *nd* | *nd* | *nd* | *nd* | *nd* | *nd* | *nd* | *nd* | *nd* | *nd* | *na* | *nd* | *nd* | *nd* | *nd* |
| BP | *nd* | *nd* | *nd* | *nd* | *nd* | 2.0 | *nd* | *nd* | *nd* | *nd* | *nd* | *nd* | *nd* | *nd* | *nd* | *na* | *nd* | *nd* | *nd* | *nd* |
| **$\Sigma_{27}$PAHs** | **94** | **128** | **87** | **80** | **219** | **124** | **83** | **65** | **163** | **141** | **126** | **81** | **89** | **43** | **44** | ***na*** | **71** | **45** | **35** | **43** |
| **$\Sigma_{7}$PAHs** | **94** | **73** | **44** | **49** | **219** | **76** | **38** | **28** | **163** | **105** | **58** | **40** | **89** | **25** | **28** | ***na*** | **71** | **23** | **17** | **42** |
| LMW PAHs | 50 | 85 | 87 | 84 | 66 | 84 | 92 | 90 | 43 | 89 | 92 | 87 | 41 | 89 | 86 | *na* | 47 | 93 | 92 | 83 |
| HMW PAHs | 50 | 15 | 13 | 16 | 34 | 16 | 8 | 10 | 57 | 11 | 8 | 13 | 59 | 11 | 14 | *na* | 53 | 7 | 8 | 17 |

*na*: not available; *nd*: not detected; C1: methyl; C2: di-methyl; C3: tri-methyl; $\Sigma_{27}$PAHs = Σ Nap–BP (27 compounds); $\Sigma_{7}$PAHs = Σ Nap, Flu, Phe, Flt, Pyr, BaA, Chr; LMW: low molecular weight, i.e., 2-3 rings; HMW: high molecular weight, i.e., 4-6 rings.

**Table S7.** Summary of SPM, biomass, POC and individual PAH concentration data for the particulate/planktonic size fractions 0.7-60, 60-200, 200-500, 500-1000 µm, but also 60-1000 µm, recovered from the DCM at the 10 stations.

| | **Size fractions (µm)** | **Biomass (mg dw $L^{-1}$) or SPM (mg $L^{-1}$)** | **$f_{Biomass}$** | **POC (mg $g^{-1}$ dw)** | **$f_{OC}$** | **ng $L^{-1}$ for < 0.7 µm, ng $g^{-1}$ dw for other fractions** | | | | | | |
|---|---|---|---|---|---|---|---|---|---|---|---|---|
| | | | | | | **Nap** | **Flu** | **Phe** | **Flt** | **Pyr** | **BaA** | **Chr** |
| **St1** | < 0.7 | *na* | *na* | *na* | *na* | 0.29 | 0.27 | 0.43 | 0.17 | 0.10 | 0.05 | 0.10 |
| | 0.7-60 | 0.347 | *na* | 134.5 | 0.135 | 18.0 | 13.6 | 16.1 | 22.8 | 31.2 | 9.0 | 18.7 |
| | 60-200 | 0.020 | 0.3 | 263.4 | 0.263 | 8.0 | 4.3 | 39.1 | 23.8 | 20.5 | 13.7 | 17.4 |
| | 200-500 | 0.037 | 0.6 | 246.4 | 0.246 | 2.9 | 3.4 | 16.3 | 12.0 | 11.9 | 0.3 | 4.8 |
| | 500-1000 | 0.005 | 0.1 | 284.9 | 0.285 | 13.3 | 7.6 | 16.5 | 9.3 | 8.6 | 3.6 | 8.2 |
| | 60-1000 | 0.062 | 1.0 | 254.8 | 0.255 | 5.3 | 4.0 | 23.6 | 15.6 | 14.4 | 4.8 | 9.1 |
| **St2** | < 0.7 | *na* | *na* | *na* | *na* | 0.69 | 0.26 | 1.06 | 0.34 | 0.29 | 0.04 | 0.13 |
| | 0.7-60 | 0.320 | *na* | 67.3 | 0.067 | 25.3 | 19.6 | 20.7 | 7.0 | 18.5 | 8.2 | 12.2 |
| | 60-200 | 0.007 | 0.3 | 129.4 | 0.129 | 31.2 | 19.0 | 71.2 | 13.9 | 12.1 | 2.9 | 5.1 |
| | 200-500 | 0.007 | 0.3 | 238.0 | 0.238 | 7.0 | 5.5 | 20.1 | 4.3 | 5.2 | 1.1 | 2.6 |
| | 500-1000 | 0.007 | 0.3 | 207.1 | 0.207 | 7.0 | 6.9 | 23.9 | 8.3 | 7.3 | 1.6 | 6.1 |
| | 60-1000 | 0.021 | 1.0 | 190.7 | 0.191 | 15.3 | 10.6 | 38.9 | 8.9 | 8.3 | 1.9 | 4.6 |
| **St3** | < 0.7 | *na* | *na* | *na* | *na* | 0.24 | 0.21 | 0.91 | 0.82 | 0.65 | 0.13 | 0.62 |
| | 0.7-60 | 0.210 | *na* | 78.3 | 0.078 | 36.3 | 38.1 | 50.8 | 22.2 | 40.6 | 11.2 | 11.6 |
| | 60-200 | 0.002 | 0.2 | 81.9 | 0.082 | 14.0 | 15.4 | 78.5 | 10.2 | 8.4 | 2.5 | 3.9 |
| | 200-500 | 0.002 | 0.3 | 179.6 | 0.180 | 5.6 | 4.9 | 28.5 | 5.1 | 3.6 | 1.3 | 3.0 |
| | 500-1000 | 0.004 | 0.5 | 168.5 | 0.169 | 3.6 | 2.2 | 13.5 | 3.4 | 2.4 | 0.6 | 3.5 |
| | 60-1000 | 0.008 | 1.0 | 152.0 | 0.152 | 6.5 | 5.9 | 32.5 | 5.4 | 4.1 | 1.2 | 3.4 |
| **St4** | < 0.7 | *na* | *na* | *na* | *na* | 0.93 | 0.4 | 1.14 | 0.17 | 0.12 | 0.05 | 0.06 |
| | 0.7-60 | 0.220 | *na* | 159.5 | 0.159 | 19.7 | 17.5 | 18.8 | 16.5 | 14.4 | 14.0 | 34.9 |
| | 60-200 | 0.068 | 0.7 | 103.5 | 0.104 | 6.2 | 5.5 | 31.7 | 16.4 | 13.2 | 5.9 | 12.6 |
| | 200-500 | 0.028 | 0.3 | 139.4 | 0.139 | 7.8 | 13.5 | 26.4 | 12.5 | 10.9 | 4.9 | 8.9 |
| | 500-1000 | 0.007 | 0.1 | 109.7 | 0.110 | 18.2 | 11.4 | 24.6 | 12.0 | 11.6 | 4.7 | 15.5 |
| | 60-1000 | 0.104 | 1.0 | 113.8 | 0.114 | 7.4 | 8.1 | 29.8 | 15.0 | 12.5 | 5.5 | 11.8 |
| **St9** | < 0.7 | *na* | *na* | *na* | *na* | 0.11 | 0.14 | 3.52 | 0.13 | 0.1 | 0.04 | 0.09 |
| | 0.7-60 | 0.670 | *na* | 261.8 | 0.262 | 10.5 | 9.7 | 5.3 | 6.6 | 13.2 | 4.4 | 3.5 |
| | 60-200 | 0.017 | 0.4 | 249.8 | 0.250 | 3.9 | 3.1 | 18.7 | 3.4 | 2.9 | 2.3 | 3.0 |
| | 200-500 | 0.023 | 0.5 | 341.0 | 0.341 | 2.1 | 2.7 | 9.1 | 3.4 | 1.6 | 0.4 | 2.4 |
| | 500-1000 | 0.004 | 0.1 | 326.2 | 0.326 | 5.2 | 2.3 | 6.8 | 2.1 | 1.1 | 0.7 | 1.2 |
| | 60-1000 | 0.044 | 1.0 | 304.2 | 0.304 | 3.1 | 2.8 | 12.7 | 3.3 | 2.1 | 1.2 | 2.6 |
| **St10** | < 0.7 | *na* | *na* | *na* | *na* | 0.44 | 0.23 | 0.46 | 0.15 | 0.13 | 0.03 | 0.11 |
| | 0.7-60 | 0.250 | *na* | 118.6 | 0.119 | 23.1 | 14.3 | 9.4 | 9.1 | 20.5 | 7.6 | 9.4 |
| | 60-200 | 0.003 | 0.4 | 240.3 | 0.240 | 8.9 | 7.7 | 37.9 | 7.3 | 5.9 | 1.3 | 4.1 |
| | 200-500 | 0.004 | 0.4 | 269.8 | 0.270 | 3.0 | 5.6 | 24.0 | 4.8 | 3.1 | 0.8 | 2.9 |
| | 500-1000 | 0.002 | 0.2 | 222.8 | 0.223 | 8.2 | 7.1 | 20.5 | 4.9 | 4.4 | 1.0 | 2.7 |
| | 60-1000 | 0.010 | 1.0 | 249.1 | 0.249 | 6.3 | 6.7 | 28.3 | 5.7 | 4.4 | 1.0 | 3.3 |
| **St11** | < 0.7 | *na* | *na* | *na* | *na* | 0.06 | 0.09 | 0.33 | 0.13 | 0.09 | 0.04 | 0.08 |
| | 0.7-60 | 0.150 | *na* | 121.7 | 0.122 | 64.2 | 40.5 | 40.7 | 20.4 | 24.3 | 17.6 | 11.3 |
| | 60-200 | 0.004 | 0.2 | 271.5 | 0.271 | 5.5 | 6.8 | 45.9 | 7.2 | 4.8 | 1.9 | 4.4 |
| | 200-500 | 0.005 | 0.3 | 299.9 | 0.300 | 4.0 | 4.8 | 22.8 | 2.6 | 1.6 | 0.6 | 1.6 |

| | | | | | | | | | | | | |
|---|---|---|---|---|---|---|---|---|---|---|---|---|
| | 500-1000 | 0.009 | 0.5 | 311.4 | 0.311 | 3.0 | 4.5 | 14.5 | 2.3 | 1.4 | 0.6 | 1.8 |
| | 60-1000 | 0.018 | 1.0 | 299.1 | 0.299 | 3.9 | 5.1 | 23.9 | 3.5 | 2.2 | 0.9 | 2.4 |
| **St15** | < 0.7 | *na* | *na* | *na* | *na* | 0.34 | 0.16 | 0.34 | 0.14 | 0.12 | 0.05 | 0.12 |
| | 0.7-60 | 0.120 | *na* | 120.6 | 0.121 | 28.6 | 19.7 | 22.0 | 24.0 | 31.0 | 18.8 | 18.4 |
| | 60-200 | 0.006 | 0.3 | 153.7 | 0.154 | 10.5 | 12.0 | 66.9 | 5.2 | 8.3 | *na* | 2.1 |
| | 200-500 | 0.010 | 0.4 | 199.6 | 0.200 | 2.9 | 8.5 | 37.0 | 3.6 | 2.6 | 1.3 | 2.0 |
| | 500-1000 | 0.009 | 0.3 | 228.9 | 0.229 | 4.3 | 4.8 | 20.6 | 3.2 | 4.0 | 0.9 | 2.0 |
| | 60-1000 | 0.025 | 1.0 | 198.1 | 0.198 | 5.3 | 8.1 | 38.9 | 3.9 | 4.5 | 0.8 | 2.0 |
| **St17** | < 0.7 | *na* | *na* | *na* | *na* | 0.18 | 0.15 | 0.28 | 0.15 | 0.12 | 0.05 | 0.18 |
| | 0.7-60 | 0.290 | *na* | 80.9 | 0.081 | 15.0 | 13.1 | 8.7 | 10.7 | 18.9 | 7.3 | 15.1 |
| | 60-200 | 0.083 | 0.5 | 43.5 | 0.044 | 2.7 | 3.1 | 14.5 | 1.4 | 2.1 | 0.3 | 0.9 |
| | 200-500 | 0.072 | 0.5 | 75.9 | 0.076 | 3.8 | 4.2 | 14.0 | 1.7 | 3.1 | 0.4 | 0.9 |
| | 500-1000 | 0.002 | 0.0 | *na* | 0.000 | *na* | *na* | *na* | *na* | *na* | *na* | *na* |
| | 60-1000 | 0.157 | 1.0 | 57.7 | 0.058 | 3.2 | 3.6 | 14.1 | 1.5 | 2.6 | 0.4 | 0.9 |
| **St19** | < 0.7 | *na* | *na* | *na* | *na* | 0.41 | 0.19 | 0.32 | 0.12 | 0.12 | 0.05 | 0.11 |
| | 0.7-60 | 0.340 | *na* | 141.9 | 0.142 | 13.4 | 10.7 | 8.7 | 9.0 | 17.6 | 6.9 | 4.3 |
| | 60-200 | 0.029 | 0.4 | 156.0 | 0.156 | 2.9 | 2.9 | 14.0 | 1.1 | 1.4 | 0.3 | 0.5 |
| | 200-500 | 0.038 | 0.5 | 204.7 | 0.205 | 2.7 | 2.5 | 8.6 | 1.0 | 1.0 | 0.3 | 0.5 |
| | 500-1000 | 0.011 | 0.1 | 190.5 | 0.191 | 10.8 | 6.9 | 17.3 | 2.0 | 2.7 | 1.5 | 1.0 |
| | 60-1000 | 0.078 | 1.0 | 184.9 | 0.185 | 3.9 | 3.3 | 11.8 | 1.2 | 1.4 | 0.5 | 0.6 |

*na*: not available.

$f_{Biomass}$: contribution of the biomass of a given size fraction to the total biomass of the fraction 60-1000 µm (i.e., $f_{Biomass}$ *x* = biomass fraction *x* / biomass 60-1000 µm), with biomass 60-1000 µm = biomass 60-200 µm + biomass 200-500 µm + biomass 500-1000 µm.

$f_{OC}$: contribution of the OC mass (in g) to the total matter mass (in g) for a given size fraction (i.e., $f_{OC}$ = POC in mg $g^{-1}$ dw / 1000).

Concentrations of POC and individual PAHs in the size fraction 60-1000 µm were calculated by summing the concentrations of POC/PAH in the fractions 60-200, 200-500 and 500-1000 µm, each of these concentrations being weighted (multiplied) by the corresponding $f_{Biomass}$ value.

**Table S8.** Partition coefficient between particulate matter and water ($K_D$ in L $kg^{-1}$) and Log $K_D$ for the 7 individual PAHs in each particulate/ planktonic size fraction (0.7-60, 60-200, 200-500, 500-1000 and 60-1000 µm) and station.

| | **Size fractions (µm)** | **$K_D$ (L $kg^{-1}$)** | | | | | | | **Log $K_D$** | | | | | | |
|---|---|---|---|---|---|---|---|---|---|---|---|---|---|---|---|
| | | **Nap** | **Flu** | **Phe** | **Flt** | **Pyr** | **BaA** | **Chr** | **Nap** | **Flu** | **Phe** | **Flt** | **Pyr** | **BaA** | **Chr** |
| **St1** | 0.7-60 | 61968 | 50402 | 37546 | 133838 | 311743 | 180191 | 186903 | 4.79 | 4.70 | 4.57 | 5.13 | 5.49 | 5.26 | 5.27 |
| | 60-200 | 27589 | 16089 | 90814 | 140275 | 205392 | 274689 | 173735 | 4.44 | 4.21 | 4.96 | 5.15 | 5.31 | 5.44 | 5.24 |
| | 200-500 | 9828 | 12537 | 37820 | 70311 | 118644 | 5214 | 48387 | 3.99 | 4.10 | 4.58 | 4.85 | 5.07 | 3.72 | 4.68 |
| | 500-1000 | 45902 | 28186 | 38282 | 54476 | 86145 | 71473 | 82200 | 4.66 | 4.45 | 4.58 | 4.74 | 4.94 | 4.85 | 4.91 |
| | 60-1000 | 18260 | 14858 | 54904 | 91627 | 144104 | 96901 | 91261 | 4.26 | 4.17 | 4.74 | 4.96 | 5.16 | 4.99 | 4.96 |
| **St2** | 0.7-60 | 36609 | 75278 | 19529 | 20684 | 63624 | 204506 | 93689 | 4.56 | 4.88 | 4.29 | 4.32 | 4.80 | 5.31 | 4.97 |
| | 60-200 | 45212 | 73198 | 67132 | 40743 | 41854 | 72886 | 39568 | 4.66 | 4.86 | 4.83 | 4.61 | 4.62 | 4.86 | 4.60 |
| | 200-500 | 10146 | 21025 | 18963 | 12569 | 17848 | 27888 | 19819 | 4.01 | 4.32 | 4.28 | 4.10 | 4.25 | 4.45 | 4.30 |
| | 500-1000 | 10112 | 26496 | 22549 | 24554 | 25330 | 39204 | 46882 | 4.00 | 4.42 | 4.35 | 4.39 | 4.40 | 4.59 | 4.67 |
| | 60-1000 | 22158 | 40704 | 36652 | 26149 | 28527 | 47018 | 35442 | 4.35 | 4.61 | 4.56 | 4.42 | 4.46 | 4.67 | 4.55 |
| **St3** | 0.7-60 | 151402 | 181259 | 55817 | 27024 | 62409 | 86410 | 18700 | 5.18 | 5.26 | 4.75 | 4.43 | 4.80 | 4.94 | 4.27 |
| | 60-200 | 58158 | 73373 | 86227 | 12394 | 12911 | 19161 | 6264 | 4.76 | 4.87 | 4.94 | 4.09 | 4.11 | 4.28 | 3.80 |
| | 200-500 | 23466 | 23460 | 31367 | 6262 | 5549 | 10291 | 4771 | 4.37 | 4.37 | 4.50 | 3.80 | 3.74 | 4.01 | 3.68 |
| | 500-1000 | 14877 | 10256 | 14874 | 4152 | 3625 | 4582 | 5674 | 4.17 | 4.01 | 4.17 | 3.62 | 3.56 | 3.66 | 3.75 |
| | 60-1000 | 27090 | 28257 | 35665 | 6611 | 6268 | 9488 | 5553 | 4.43 | 4.45 | 4.55 | 3.82 | 3.80 | 3.98 | 3.74 |
| **St4** | 0.7-60 | 21168 | 43669 | 16528 | 96979 | 120318 | 279300 | 582278 | 4.33 | 4.64 | 4.22 | 4.99 | 5.08 | 5.45 | 5.77 |
| | 60-200 | 6636 | 13871 | 27774 | 96459 | 109872 | 117408 | 210352 | 3.82 | 4.14 | 4.44 | 4.98 | 5.04 | 5.07 | 5.32 |
| | 200-500 | 8399 | 33723 | 23161 | 73713 | 90808 | 98657 | 148349 | 3.92 | 4.53 | 4.36 | 4.87 | 4.96 | 4.99 | 5.17 |
| | 500-1000 | 19537 | 28604 | 21574 | 70335 | 96549 | 94223 | 259076 | 4.29 | 4.46 | 4.33 | 4.85 | 4.98 | 4.97 | 5.41 |
| | 60-1000 | 7969 | 20296 | 26098 | 88489 | 103755 | 110729 | 196512 | 3.90 | 4.31 | 4.42 | 4.95 | 5.02 | 5.04 | 5.29 |
| **St9** | 0.7-60 | 95270 | 68960 | 1493 | 50734 | 132374 | 110649 | 39342 | 4.98 | 4.84 | 3.17 | 4.71 | 5.12 | 5.04 | 4.59 |
| | 60-200 | 35853 | 21900 | 5322 | 25968 | 28505 | 57125 | 33596 | 4.55 | 4.34 | 3.73 | 4.41 | 4.45 | 4.76 | 4.53 |
| | 200-500 | 19084 | 19166 | 2576 | 26267 | 16184 | 10828 | 26720 | 4.28 | 4.28 | 3.41 | 4.42 | 4.21 | 4.03 | 4.43 |
| | 500-1000 | 47133 | 16105 | 1925 | 16116 | 10509 | 17476 | 13828 | 4.67 | 4.21 | 3.28 | 4.21 | 4.02 | 4.24 | 4.14 |
| | 60-1000 | 27946 | 19982 | 3595 | 25313 | 20528 | 29460 | 28343 | 4.45 | 4.30 | 3.56 | 4.40 | 4.31 | 4.47 | 4.45 |

| | | | | | | | | | | | | | | | |
|---|---|---|---|---|---|---|---|---|---|---|---|---|---|---|---|
| **St10** | 0.7-60 | 52540 | 62279 | 20510 | 60652 | 157676 | 254108 | 85776 | 4.72 | 4.79 | 4.31 | 4.78 | 5.20 | 5.41 | 4.93 |
| | 60-200 | 20289 | 33631 | 82380 | 48585 | 45451 | 44561 | 37710 | 4.31 | 4.53 | 4.92 | 4.69 | 4.66 | 4.65 | 4.58 |
| | 200-500 | 6842 | 24396 | 52248 | 31807 | 23638 | 26642 | 26065 | 3.84 | 4.39 | 4.72 | 4.50 | 4.37 | 4.43 | 4.42 |
| | 500-1000 | 18656 | 30738 | 44642 | 32334 | 33982 | 32109 | 24520 | 4.27 | 4.49 | 4.65 | 4.51 | 4.53 | 4.51 | 4.39 |
| | 60-1000 | 14207 | 29077 | 61501 | 37973 | 33709 | 34270 | 29938 | 4.15 | 4.46 | 4.79 | 4.58 | 4.53 | 4.53 | 4.48 |
| **St11** | 0.7-60 | 1069630 | 450076 | 123387 | 157163 | 269475 | 438959 | 141026 | 6.03 | 5.65 | 5.09 | 5.20 | 5.43 | 5.64 | 5.15 |
| | 60-200 | 92396 | 75597 | 138982 | 55169 | 52831 | 46976 | 55423 | 4.97 | 4.88 | 5.14 | 4.74 | 4.72 | 4.67 | 4.74 |
| | 200-500 | 66860 | 53573 | 69056 | 19705 | 17609 | 14275 | 20606 | 4.83 | 4.73 | 4.84 | 4.29 | 4.25 | 4.15 | 4.31 |
| | 500-1000 | 49587 | 49642 | 44022 | 17633 | 15897 | 14987 | 22986 | 4.70 | 4.70 | 4.64 | 4.25 | 4.20 | 4.18 | 4.36 |
| | 60-1000 | 64228 | 56554 | 72511 | 26545 | 24568 | 21838 | 29436 | 4.81 | 4.75 | 4.86 | 4.42 | 4.39 | 4.34 | 4.47 |
| **St15** | 0.7-60 | 84002 | 123336 | 64712 | 171305 | 258611 | 376558 | 153414 | 4.92 | 5.09 | 4.81 | 5.23 | 5.41 | 5.58 | 5.19 |
| | 60-200 | 30812 | 74703 | 196819 | 37477 | 68844 | *na* | 17260 | 4.49 | 4.87 | 5.29 | 4.57 | 4.84 | *na* | 4.24 |
| | 200-500 | 8393 | 53192 | 108873 | 25889 | 21841 | 25581 | 16829 | 3.92 | 4.73 | 5.04 | 4.41 | 4.34 | 4.41 | 4.23 |
| | 500-1000 | 12633 | 29775 | 60603 | 23024 | 33464 | 17750 | 16592 | 4.10 | 4.47 | 4.78 | 4.36 | 4.52 | 4.25 | 4.22 |
| | 60-1000 | 15576 | 50540 | 114513 | 27846 | 37849 | 16346 | 16856 | 4.19 | 4.70 | 5.06 | 4.44 | 4.58 | 4.21 | 4.23 |
| **St17** | 0.7-60 | 83560 | 87018 | 31093 | 71024 | 157840 | 146655 | 83961 | 4.92 | 4.94 | 4.49 | 4.85 | 5.20 | 5.17 | 4.92 |
| | 60-200 | 14794 | 20698 | 51923 | 9088 | 17663 | 6351 | 4730 | 4.17 | 4.32 | 4.72 | 3.96 | 4.25 | 3.80 | 3.67 |
| | 200-500 | 21283 | 27846 | 49855 | 11467 | 26234 | 8756 | 5032 | 4.33 | 4.44 | 4.70 | 4.06 | 4.42 | 3.94 | 3.70 |
| | 500-1000 | *na* | *na* | *na* | *na* | *na* | *na* | *na* | *na* | *na* | *na* | *na* | *na* | *na* | *na* |
| | 60-1000 | 17559 | 23683 | 50268 | 10051 | 21340 | 7364 | 4804 | 4.24 | 4.37 | 4.70 | 4.00 | 4.33 | 3.87 | 3.68 |
| **St19** | 0.7-60 | 32747 | 56337 | 27095 | 75145 | 146679 | 138735 | 39072 | 4.52 | 4.75 | 4.43 | 4.88 | 5.17 | 5.14 | 4.59 |
| | 60-200 | 7098 | 15390 | 43658 | 9115 | 11776 | 6363 | 4416 | 3.85 | 4.19 | 4.64 | 3.96 | 4.07 | 3.80 | 3.65 |
| | 200-500 | 6464 | 13385 | 26780 | 8743 | 8199 | 6837 | 4486 | 3.81 | 4.13 | 4.43 | 3.94 | 3.91 | 3.83 | 3.65 |
| | 500-1000 | 26428 | 36095 | 54197 | 17081 | 22413 | 29267 | 8729 | 4.42 | 4.56 | 4.73 | 4.23 | 4.35 | 4.47 | 3.94 |
| | 60-1000 | 9560 | 17377 | 36894 | 10076 | 11548 | 9881 | 5069 | 3.98 | 4.24 | 4.57 | 4.00 | 4.06 | 3.99 | 3.70 |

*na*: not available.

$K_D$ in a given size fraction (in L $kg^{-1}$) was calculated as ($C_P$ / $C_W$) × 1000 where $C_P$ is the concentration in the given size fraction (0.7-60, 60-200, 200-500, 500-1000 or 60-1000 µm) in ng $g^{-1}$ dw, and $C_w$ is the concentration in the dissolved phase (size fraction < 0.7 µm) in ng $L^{-1}$ (see concentration values in Table S7).

**Table S9.** Partition coefficient between particulate organic carbon and water ($K_{OC}$ in L $kg^{-1}$) and Log $K_{oc}$ for the 7 individual PAHs in each particulate/planktonic size fraction (0.7-60, 60-200, 200-500, 500-1000 and 60-1000 µm) and station.

| | **Size fractions (µm)** | **$K_{OC}$ (L $kg^{-1}$)** | | | | | | | **Log $K_{OC}$** | | | | | | |
|---|---|---|---|---|---|---|---|---|---|---|---|---|---|---|---|
| | | **Nap** | **Flu** | **Phe** | **Flt** | **Pyr** | **BaA** | **Chr** | **Nap** | **Flu** | **Phe** | **Flt** | **Pyr** | **BaA** | **Chr** |
| **St1** | 0.7-60 | 460668 | 374689 | 279118 | 994947 | 2317478 | 1339528 | 1389425 | 5.66 | 5.57 | 5.45 | 6.00 | 6.37 | 6.13 | 6.14 |
| | 60-200 | 104753 | 61088 | 344818 | 532618 | 779864 | 1042985 | 659666 | 5.02 | 4.79 | 5.54 | 5.73 | 5.89 | 6.02 | 5.82 |
| | 200-500 | 39882 | 50870 | 153465 | 285307 | 481430 | 21158 | 196344 | 4.60 | 4.71 | 5.19 | 5.46 | 5.68 | 4.33 | 5.29 |
| | 500-1000 | 161111 | 98931 | 134364 | 191204 | 302359 | 250863 | 288511 | 5.21 | 5.00 | 5.13 | 5.28 | 5.48 | 5.40 | 5.46 |
| | 60-1000 | 71668 | 58317 | 215492 | 359625 | 565591 | 380325 | 358190 | 4.86 | 4.77 | 5.33 | 5.56 | 5.75 | 5.58 | 5.55 |
| **St2** | 0.7-60 | 544172 | 1118977 | 290285 | 307460 | 945751 | 3039907 | 1392659 | 5.74 | 6.05 | 5.46 | 5.49 | 5.98 | 6.48 | 6.14 |
| | 60-200 | 349441 | 565739 | 518858 | 314903 | 323486 | 563330 | 305815 | 5.54 | 5.75 | 5.72 | 5.50 | 5.51 | 5.75 | 5.49 |
| | 200-500 | 42629 | 88340 | 79678 | 52811 | 74993 | 117177 | 83274 | 4.63 | 4.95 | 4.90 | 4.72 | 4.88 | 5.07 | 4.92 |
| | 500-1000 | 48817 | 127917 | 108860 | 118539 | 122289 | 189270 | 226335 | 4.69 | 5.11 | 5.04 | 5.07 | 5.09 | 5.28 | 5.35 |
| | 60-1000 | 116218 | 213486 | 192237 | 137151 | 149619 | 246607 | 185889 | 5.07 | 5.33 | 5.28 | 5.14 | 5.17 | 5.39 | 5.27 |
| **St3** | 0.7-60 | 1932978 | 2314155 | 712623 | 345014 | 796789 | 1103212 | 238747 | 6.29 | 6.36 | 5.85 | 5.54 | 5.90 | 6.04 | 5.38 |
| | 60-200 | 710302 | 896119 | 1053109 | 151376 | 157686 | 234022 | 76500 | 5.85 | 5.95 | 6.02 | 5.18 | 5.20 | 5.37 | 4.88 |
| | 200-500 | 130691 | 130660 | 174696 | 34874 | 30906 | 57318 | 26572 | 5.12 | 5.12 | 5.24 | 4.54 | 4.49 | 4.76 | 4.42 |
| | 500-1000 | 88273 | 60852 | 88254 | 24633 | 21508 | 27187 | 33664 | 4.95 | 4.78 | 4.95 | 4.39 | 4.33 | 4.43 | 4.53 |
| | 60-1000 | 178195 | 185871 | 234598 | 43486 | 41231 | 62414 | 36528 | 5.25 | 5.27 | 5.37 | 4.64 | 4.62 | 4.80 | 4.56 |
| **St4** | 0.7-60 | 132741 | 273843 | 103643 | 608138 | 754497 | 1751447 | 3651377 | 5.12 | 5.44 | 5.02 | 5.78 | 5.88 | 6.24 | 6.56 |
| | 60-200 | 64104 | 133993 | 268299 | 931804 | 1061367 | 1134174 | 2032019 | 4.81 | 5.13 | 5.43 | 5.97 | 6.03 | 6.05 | 6.31 |
| | 200-500 | 60238 | 241861 | 166114 | 528673 | 651276 | 707567 | 1063960 | 4.78 | 5.38 | 5.22 | 5.72 | 5.81 | 5.85 | 6.03 |
| | 500-1000 | 178166 | 260857 | 196749 | 641429 | 880487 | 859272 | 2362657 | 5.25 | 5.42 | 5.29 | 5.81 | 5.94 | 5.93 | 6.37 |
| | 60-1000 | 70029 | 178362 | 229349 | 777627 | 911784 | 973070 | 1726916 | 4.85 | 5.25 | 5.36 | 5.89 | 5.96 | 5.99 | 6.24 |
| **St9** | 0.7-60 | 363924 | 263421 | 5701 | 193802 | 505661 | 422670 | 150284 | 5.56 | 5.42 | 3.76 | 5.29 | 5.70 | 5.63 | 5.18 |
| | 60-200 | 143511 | 87660 | 21304 | 103943 | 114097 | 228659 | 134477 | 5.16 | 4.94 | 4.33 | 5.02 | 5.06 | 5.36 | 5.13 |
| | 200-500 | 55964 | 56205 | 7553 | 77028 | 47460 | 31755 | 78358 | 4.75 | 4.75 | 3.88 | 4.89 | 4.68 | 4.50 | 4.89 |
| | 500-1000 | 144472 | 49366 | 5900 | 49400 | 32212 | 53567 | 42386 | 5.16 | 4.69 | 3.77 | 4.69 | 4.51 | 4.73 | 4.63 |
| | 60-1000 | 91876 | 65691 | 11818 | 83219 | 67489 | 96851 | 93180 | 4.96 | 4.82 | 4.07 | 4.92 | 4.83 | 4.99 | 4.97 |

| | | | | | | | | | | | | | | | |
|---|---|---|---|---|---|---|---|---|---|---|---|---|---|---|---|
| **St10** | 0.7-60 | 443056 | 525175 | 172952 | 511461 | 1329629 | 2142808 | 723320 | 5.65 | 5.72 | 5.24 | 5.71 | 6.12 | 6.33 | 5.86 |
| | 60-200 | 84431 | 139949 | 342812 | 202181 | 189140 | 185436 | 156926 | 4.93 | 5.15 | 5.54 | 5.31 | 5.28 | 5.27 | 5.20 |
| | 200-500 | 25363 | 90433 | 193676 | 117905 | 87623 | 98759 | 96619 | 4.40 | 4.96 | 5.29 | 5.07 | 4.94 | 4.99 | 4.99 |
| | 500-1000 | 83737 | 137966 | 200373 | 145130 | 152524 | 144120 | 110055 | 4.92 | 5.14 | 5.30 | 5.16 | 5.18 | 5.16 | 5.04 |
| | 60-1000 | 57025 | 116708 | 246848 | 152412 | 135298 | 137552 | 120162 | 4.76 | 5.07 | 5.39 | 5.18 | 5.13 | 5.14 | 5.08 |
| **St11** | 0.7-60 | 8790529 | 3698855 | 1014031 | 1291613 | 2214626 | 3607490 | 1158992 | 6.94 | 6.57 | 6.01 | 6.11 | 6.35 | 6.56 | 6.06 |
| | 60-200 | 340341 | 278463 | 511941 | 203214 | 194604 | 173037 | 204152 | 5.53 | 5.44 | 5.71 | 5.31 | 5.29 | 5.24 | 5.31 |
| | 200-500 | 222956 | 178647 | 230279 | 65711 | 58719 | 47601 | 68714 | 5.35 | 5.25 | 5.36 | 4.82 | 4.77 | 4.68 | 4.84 |
| | 500-1000 | 159212 | 159389 | 141344 | 56615 | 51042 | 48120 | 73804 | 5.20 | 5.20 | 5.15 | 4.75 | 4.71 | 4.68 | 4.87 |
| | 60-1000 | 214702 | 189051 | 242391 | 88736 | 82127 | 73001 | 98398 | 5.33 | 5.28 | 5.38 | 4.95 | 4.91 | 4.86 | 4.99 |
| **St15** | 0.7-60 | 696518 | 1022653 | 536565 | 1420401 | 2144309 | 3122278 | 1272055 | 5.84 | 6.01 | 5.73 | 6.15 | 6.33 | 6.49 | 6.10 |
| | 60-200 | 200476 | 486051 | 1280589 | 243839 | 447930 | *na* | 112302 | 5.30 | 5.69 | 6.11 | 5.39 | 5.65 | *na* | 5.05 |
| | 200-500 | 42054 | 266527 | 545532 | 129722 | 109436 | 128180 | 84325 | 4.62 | 5.43 | 5.74 | 5.11 | 5.04 | 5.11 | 4.93 |
| | 500-1000 | 55199 | 130105 | 264806 | 100604 | 146222 | 77560 | 72498 | 4.74 | 5.11 | 5.42 | 5.00 | 5.17 | 4.89 | 4.86 |
| | 60-1000 | 78642 | 255181 | 578188 | 140595 | 191104 | 82533 | 85109 | 4.90 | 5.41 | 5.76 | 5.15 | 5.28 | 4.92 | 4.93 |
| **St17** | 0.7-60 | 1032441 | 1075161 | 384173 | 877555 | 1950225 | 1812018 | 1037395 | 6.01 | 6.03 | 5.58 | 5.94 | 6.29 | 6.26 | 6.02 |
| | 60-200 | 339793 | 475388 | 1192589 | 208734 | 405686 | 145862 | 108647 | 5.53 | 5.68 | 6.08 | 5.32 | 5.61 | 5.16 | 5.04 |
| | 200-500 | 280379 | 366838 | 656778 | 151058 | 345594 | 115350 | 66296 | 5.45 | 5.56 | 5.82 | 5.18 | 5.54 | 5.06 | 4.82 |
| | 500-1000 | *na* | *na* | *na* | *na* | *na* | *na* | *na* | *na* | *na* | *na* | *na* | *na* | *na* | *na* |
| | 60-1000 | 304082 | 410144 | 870539 | 174068 | 369568 | 127522 | 83192 | 5.48 | 5.61 | 5.94 | 5.24 | 5.57 | 5.11 | 4.92 |
| **St19** | 0.7-60 | 230824 | 397097 | 190980 | 529667 | 1033887 | 977889 | 275405 | 5.36 | 5.60 | 5.28 | 5.72 | 6.01 | 5.99 | 5.44 |
| | 60-200 | 45495 | 98644 | 279833 | 58425 | 75483 | 40786 | 28306 | 4.66 | 4.99 | 5.45 | 4.77 | 4.88 | 4.61 | 4.45 |
| | 200-500 | 31570 | 65375 | 130801 | 42704 | 40044 | 33392 | 21910 | 4.50 | 4.82 | 5.12 | 4.63 | 4.60 | 4.52 | 4.34 |
| | 500-1000 | 138704 | 189442 | 284452 | 89649 | 117631 | 153609 | 45814 | 5.14 | 5.28 | 5.45 | 4.95 | 5.07 | 5.19 | 4.66 |
| | 60-1000 | 51715 | 94001 | 199576 | 54504 | 62468 | 53453 | 27421 | 4.71 | 4.97 | 5.30 | 4.74 | 4.80 | 4.73 | 4.44 |

*na*: not available.

$K_{OC}$ in a given size fraction (in L $kg^{-1}$) was calculated as $K_D$ / $f_{OC}$ in the corresponding fraction (0.7-60, 60-200, 200-500, 500-1000 or 60-1000 µm) (see values of $K_D$ in Table S8 and values of $f_{OC}$ in Table S7).

**Table S10.** Nonlinear regression parameters (power function) between SPM (in mg $L^{-1}$) or biomass (in mg dw $L^{-1}$; horizontal axis) and PAH concentration ($C_p$ in ng $g^{-1}$ dw; vertical axis) for each particulate/planktonic size fraction (0.7-60, 60-200, 200-500, 500-1000 and 60-1000 µm) and individual PAH; The power functions are of the form: $y = ax^{-m}$ (i.e., $C_p = aSPM^{-m}$ or $aBiomass^{-m}$). The number of samples n correspond to the stations. Power functions for Phe are shown Fig. 8.

| | Size fractions (µm) | Constant (a) | Slope (-m) | Coefficient of correlation (r) | Number of samples (n) | Probability (p) |
|---|---|---|---|---|---|---|
| **Nap** | 0.7-60 | 6.98 | 0.863 | - 0.79 | 10 | < 0.05 |
| | 60-200 | 1.44 | 0.362 | - 0.62 | 10 | < 0.05 |
| | 200-500 | 2.42 | 0.106 | - 0.27 | 10 | > 0.05 |
| | 500-1000 | 6.61 | 0.008 | - 0.01 | 9 | > 0.05 |
| | 60-1000 | 2.91 | 0.181 | - 0.38 | 10 | > 0.05 |
| **Flu** | 0.7-60 | 6.65 | 0.723 | - 0.72 | 10 | < 0.05 |
| | 60-200 | 1.18 | 0.384 | - 0.72 | 10 | < 0.05 |
| | 200-500 | 3.05 | 0.111 | - 0.25 | 10 | > 0.05 |
| | 500-1000 | 19.10 | - 0.249 | 0.24 | 9 | > 0.05 |
| | 60-1000 | 2.77 | 0.195 | - 0.44 | 10 | > 0.05 |
| **Phe** | 0.7-60 | 3.70 | 1.091 | - 0.73 | 10 | < 0.05 |
| | 60-200 | 6.81 | 0.373 | - 0.75 | 10 | < 0.05 |
| | 200-500 | 6.11 | 0.261 | - 0.62 | 10 | < 0.05 |
| | 500-1000 | 46.86 | - 0.200 | 0.27 | 9 | > 0.05 |
| | 60-1000 | 9.75 | 0.260 | - 0.58 | 10 | < 0.05 |
| **Flt** | 0.7-60 | 4.72 | 0.769 | - 0.72 | 10 | < 0.05 |
| | 60-200 | 1.93 | 0.262 | - 0.33 | 10 | > 0.05 |
| | 200-500 | 2.56 | 0.100 | - 0.15 | 10 | > 0.05 |
| | 500-1000 | 1.50 | 0.202 | - 0.16 | 9 | > 0.05 |
| | 60-1000 | 2.74 | 0.160 | - 0.19 | 10 | > 0.05 |
| **Pyr** | 0.7-60 | 12.29 | 0.423 | - 0.57 | 10 | < 0.05 |
| | 60-200 | 2.85 | 0.166 | - 0.25 | 10 | > 0.05 |
| | 200-500 | 4.48 | - 0.071 | 0.10 | 10 | > 0.05 |
| | 500-1000 | 4.86 | - 0.054 | 0.23 | 9 | > 0.05 |
| | 60-1000 | 4.46 | - 0.014 | 0.12 | 10 | > 0.05 |
| **BaA** | 0.7-60 | 2.92 | 0.886 | - 0.94 | 10 | < 0.05 |
| | 60-200 | 0.97 | 0.157 | - 0.17 | 9 | > 0.05 |
| | 200-500 | 0.26 | 0.254 | - 0.33 | 10 | > 0.05 |
| | 500-1000 | 4.09 | - 0.226 | 0.16 | 9 | > 0.05 |
| | 60-1000 | 1.37 | - 0.026 | 0.03 | 10 | > 0.05 |
| **Chr** | 0.7-60 | 3.84 | 0.821 | - 0.58 | 10 | < 0.05 |
| | 60-200 | 1.88 | 0.134 | - 0.16 | 10 | > 0.05 |
| | 200-500 | 1.17 | 0.154 | - 0.22 | 10 | > 0.05 |
| | 500-1000 | 1.07 | 0.209 | - 0.12 | 9 | > 0.05 |
| | 60-1000 | 1.69 | 0.153 | - 0.16 | 10 | > 0.05 |

**Table S11.** Mean values of Log $K_D$ and Log $K_{OC}$, and slope (-m) of the power function between SPM or biomass and PAH concentration for each particulate/planktonic size fraction (0.7-60, 60-200, 200-500, 500-1000 and 60-1000 µm) and individual PAHs. Mean Log $K_D$ and Log $K_{OC}$ were determined over the 10 stations from Log $K_D$ and Log $K_{OC}$ values reported in Tables S8 and S9, respectively. Slope values are also reported Table S10.

| | **Size fractions (µm)** | **Mean Log $K_D$** | **Mean Log $K_{OC}$** | **Slope (-m)** |
|---|---|---|---|---|
| **Nap** | 0.7-60 | 4.895 | 5.818 | 0.863 |
| | 60-200 | 4.402 | 5.233 | 0.362 |
| | 200-500 | 4.130 | 4.820 | 0.106 |
| | 500-1000 | 4.366 | 5.029 | 0.008 |
| | 60-1000 | 4.277 | 5.016 | 0.181 |
| **Flu** | 0.7-60 | 4.955 | 5.877 | 0.723 |
| | 60-200 | 4.520 | 5.351 | 0.384 |
| | 200-500 | 4.402 | 5.092 | 0.111 |
| | 500-1000 | 4.418 | 5.081 | - 0.249 |
| | 60-1000 | 4.437 | 5.177 | 0.195 |
| **Phe** | 0.7-60 | 4.414 | 5.337 | 1.091 |
| | 60-200 | 4.760 | 5.591 | 0.373 |
| | 200-500 | 4.485 | 5.175 | 0.261 |
| | 500-1000 | 4.393 | 5.056 | - 0.200 |
| | 60-1000 | 4.580 | 5.320 | 0.260 |
| **Flt** | 0.7-60 | 4.851 | 5.773 | 0.769 |
| | 60-200 | 4.517 | 5.348 | 0.262 |
| | 200-500 | 4.324 | 5.014 | 0.100 |
| | 500-1000 | 4.350 | 5.013 | 0.202 |
| | 60-1000 | 4.400 | 5.140 | 0.160 |
| **Pyr** | 0.7-60 | 5.170 | 6.093 | 0.423 |
| | 60-200 | 4.608 | 5.439 | 0.166 |
| | 200-500 | 4.353 | 5.043 | - 0.071 |
| | 500-1000 | 4.390 | 5.053 | - 0.054 |
| | 60-1000 | 4.463 | 5.202 | - 0.014 |
| **BaA** | 0.7-60 | 5.292 | 6.215 | 0.886 |
| | 60-200 | 4.593 | 5.426 | 0.157 |
| | 200-500 | 4.197 | 4.887 | 0.254 |
| | 500-1000 | 4.414 | 5.077 | - 0.226 |
| | 60-1000 | 4.410 | 5.149 | - 0.026 |
| **Chr** | 0.7-60 | 4.966 | 5.889 | 0.821 |
| | 60-200 | 4.436 | 5.267 | 0.134 |
| | 200-500 | 4.257 | 4.947 | 0.154 |
| | 500-1000 | 4.423 | 5.086 | 0.209 |
| | 60-1000 | 4.356 | 5.095 | 0.153 |

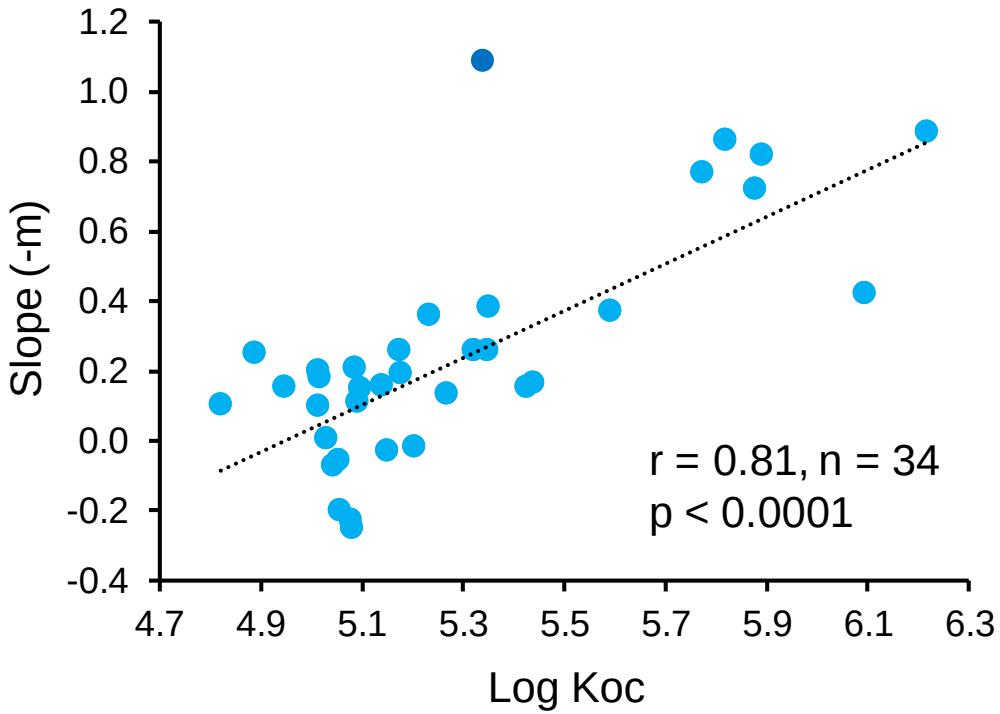


**Figure S6.** Linear relationship between the mean Log $K_{OC}$ and slope (-m) values (reported in Table S11) for all the particulate/planktonic size fractions, i.e., 0.7-60, 60-200, 200-500, 500-1000 and 60-1000 µm, and the 7 PAHs (Nap, Flu, Phe, Flt, Pyr, BaA, Chr). The darker blue dot is not taken into account in the linear regression.

## References cited

Fierro-González, P., Pagano, M., Guilloux, L., Makhlouf Belkahia, N., Tedetti, M., Carlotti, F., 2023. Zooplankton biomass, size structure, and associated metabolic fluxes with focus on its roles at the chlorophyll maximum layer during the plankton-contaminant MERITE-HIPPOCAMPE cruise. Marine Pollution Bulletin, 193, 115056.
doi: 10.1016/j.marpolbul.2023.115056.

González-Gaya, B., Martínez-Varela, A., Vila-Costa, M., Casal, P., Cerro-Gálvez, E., Berrojalbiz, N., Lundin, D., Vidal, M., Mompean, C., Bode, A., Jiménez, B., Dachs, J., 2019. Biodegradation as an important sink of aromatic hydrocarbons in the oceans. Nature Geosciences, 12, 119–125. doi: 10.1038/s41561-018-0285-3

Tesán-Onrubia, J.A., Tedetti, M., Carlotti, F., Tenaille, M., Guilloux, L., Pagano, M., Lebreton, B., Guillou, G., Fierro-González, P., Guigue, C., Chifflet, S., Garcia, T., Boudriga, I., Belhassen, M., Bellaaj-Zouari, M., Bănaru, D., 2023a. Spatial variations of biochemical content and stable

isotope ratios of size-fractionated plankton in the Mediterranean Sea (MERITE-HIPPOCAMPE campaign). Marine Pollution Bulletin, 189, 114787. doi: 10.1016/j.marpolbul.2023.114787